

Activation and Transformation of C-F and C-H Bonds Through Late Transition Metal Binding

By

Benjamin Richard Joseph Mueller

Dissertation

Submitted to the Faculty of the
Graduate School of Vanderbilt University
in partial fulfillment of the requirements

for the degree of

DOCTOR OF PHILOSOPHY

in

Chemistry

May 14, 2021

Nashville, Tennessee

Approved:

Nathan D. Schley, Ph.D.

Timothy P. Hanusa, Ph.D.

David W. Wright, Ph.D.

Sean B. Seymore, Ph.D.

Copyright © 2021 by Benjamin Richard Joseph Mueller.
All Rights Reserved.

Dedicated to my grandparents, Richard, Joseph, Norma, and Margaret,

and other family who have left us too early.

“You’ve never arrived, you’re always becoming.”

-JJ Redick

Acknowledgments

It takes a village to raise a Ph.D. and there are so many people without whom I would not have been able to finish this journey. First and foremost, I want to thank my advisor, Prof. Nathan Schley, for his mentorship over the last five and a half years. His office was always open to us to troubleshoot our problems, even as the size of the group and his responsibilities increased, and for that I am so grateful. I also want to thank my committee members, Prof. Tim Hanusa, Prof. David Wright, and Prof. Sean Seymore for their support and for pushing me to be a better scientist.

In addition to support I received from faculty members, I would not be where I am without my fellow group members. First, I want to thank Dr. Yuanyuan Zhang, who co-authored the published work on iridium carbene chemistry in Chapter III. She imparted many lessons on me in terms of the chemistry we were doing, as well as a lot of techniques and tricks for air-free and glovebox chemistry. Dr. Scott Chapp and I joined the lab together as first years in a brand-new lab, and his presence has helped to form me as a scientist and as a person. Other group members who I grew close to include Dr. Caleb Jones, Maggie Jones and Caleb Fast, and I want to thank them for helpful insights, fun conversations, and generally keeping good company in the lab. Finally, I would like to acknowledge Janna Berman and Xiaoyu (Dan) Tong for their contributions to this research while working in our lab as undergraduate researchers.

There are a number of experiments described in this dissertation that required specialized equipment not found in our laboratory space, and I want to thank those who helped me access and learn to use this instrumentation. Don Stec and Markus Voehler were immensely helpful in not just keeping the NMR spectrometers working but also helping me set up unique experiments for some of the more unusual metal complexes. The Townsend lab provided access to their LC-MS, microwave reactor, and UV lamp, in addition to helpful discussions with many members of the

lab, particularly Eric Huseman. The Hanusa lab also provided numerous chemicals and technical advice over the years, and I would specifically like to recognize the contributions of Ross Koby. Finally, the Analytical Chemistry Laboratory gave us access to GC-MS and GC-FID instruments. I particularly want to thank Andrzej Balinski for helping me understand not only how to run samples on these instruments, but also how to maintain and troubleshoot them.

Outside of the lab, I also want to thank and recognize the people who have made up my personal support system. Graduate school can be hard, requiring one to maintain a laser focus on detail-oriented problems in chemistry, and having friends with outside interests can really help to reset one's mind. Some days, this took the form of talking about sports with John Terrell or Drew Kellum. Other times, it came in the form of shooting the breeze at Tuesday Wing Night with Louie Thal, Dan Jeffries, and Quinn Bumpers. At times, the solution to mental fatigue is to replace it with physical fatigue, and I would like to thank Eric Roll for always making time to throw a football in Centennial Park. To all these people, and many others, I want to thank you from the bottom of my heart.

I also want to thank my family, who have supported and encouraged me throughout my life to pursue a career in science. My parents recognized from a young age my interest in science and always fostered the necessary curiosity. Throughout my education I have also had teachers and professors who served as mentors in getting me to where I am, and I would like to highlight the contributions of Edward Constantine at Enloe High School and Prof. Steven Mansoorabadi at Auburn University.

Finally, I want to thank my girlfriend, Jenna, for being my rock through this experience. The stresses of preparing this dissertation and defending it have been massive, not to mention the process of running the experiments described, and I truly cannot imagine surviving it without her.

Table of Contents

	Page
Dedication	iii
Acknowledgments.....	v
List of Figures	x
List of Schemes	xii
List of Tables.....	xiii
List of Abbreviations.....	xiv
Chapter	
I. Introduction to C-F and C-H Bond Activation by Transition Metal Complexes	1
Transition metal arene complexes	1
Reactivity of fluoroarenes	3
Metal carbenes.....	3
Directed C-H activation.....	5
Lactate racemase model complexes	5
II. Nucleophilic Aromatic Substitution through π -Arene Catalysis	7
Introduction.....	7
Results and Discussion.....	9
Catalyst resting state and the role of additives	10
S _N Ar kinetics and arene binding thermodynamics	13
Role of phosphine ligands	16

Role of acid additives	18
Arene binding in 2.2 vs. 2.3	19
Dimerization	20
Fluoride generation.....	21
Trifluoromethylation	23
Other nucleophiles.....	26
Functional group tolerance of fluoroarenes.....	27
Conclusion.....	29
Future Directions.....	29
Experimental Section	32
III. Formation of a Delocalized Iridium Benzyldiene with Azaquinone Methide Character via Alkoxy-carbene Cleavage	39
Introduction.....	39
Results and Discussion.....	40
Synthesis of cationic alkoxy-carbenes via ether dehydrogenation	40
Base-induced C-O bond cleavage.....	42
Formation of a neutral iridium alkoxy-carbene	46
Ethylene insertion into iridium benzyldiene.....	47
Stoichiometric reactions of iridium alkoxy-carbenes	49
Ether-directed alkoxy-carbenes	50

Catalytic reactions	52
Conclusion.....	53
Future Directions.....	54
Experimental Section	56
IV. Synthesis of SCS-Pincer Ligands for a Lactate Racemase Model Complex.....	63
Background and Introduction.....	63
Lactate racemase in <i>Lactobacillus plantarum</i>	63
Lactate racemase active site	64
Synthesis of a Lactate Racemase Model Complex	67
Ligand synthesis	67
Second-generation ligand synthesis.....	70
Metalation of second generation ligand.....	72
Third-generation ligand synthesis	73
Metalation of third generation ligand	75
Conclusion.....	76
Experimental Section	79
V. References.....	83
VI. Appendix A – Supplemental Information for Chapter II.....	87
VII. Appendix B – Supplemental Information for Chapter III.....	91
VIII. Appendix C – Supplemental Information for Chapter IV	93

List of Figures

Figure	Page
2.1 ORTEPs of complexes 2.1 and 2.2	9
2.2 ORTEP of complex 2.3	11
2.3 Stoichiometric S _N Ar reaction of complex 2.1	13
2.4 Predicted fraction of fluoroarene complex 2.1	14
2.5 ORTEP of complex 2.4-OTf	18
2.6 ORTEP of complex 2.5	20
2.7 ¹⁹ F{ ¹ H}NMR	22
2.8 ORTEP of butylamine adduct.....	27
3.1 ORTEP of complex 3.3	41
3.2 Proposed structure of 3.3 adduct with acetonitrile.....	41
3.3 ORTEP of complex 3.4	43
3.4 Depiction of the HOMO of 3.4	43
3.5 ORTEPs of complexes 3.5 and 3.6	47
3.6 ORTEP of complex 3.9	51
4.1 Active site of lactate racemase.....	64
4.2 Structure of reduced and oxidized form of lactate racemase cofactor.....	65
4.3 Proposed model complex of lactate racemase (4.9).....	66

4.4 Published model complexes of lactate racemase	66
4.5 Proposed mechanism of unsymmetric hydrolysis of 4.12	68
4.6 Plausible products of thionation of 4.24	75

List of Schemes

Scheme	Page
2.1 Reported catalysts for π -arene S_NAr	8
3.1 Proposal for formation of 3.4	45
3.2 Proposed mechanism for formation of 3.6	47
4.1 Proposed synthesis of model complex 4.9	67
4.2 Progress towards the synthesis of model complex 4.9	70
4.3 Proposed synthesis of model complex 4.20	71
4.4 Progress towards the synthesis of model complex 4.20	73
4.5 Proposed synthesis of model complex 4.26	74
4.6 Progress towards the synthesis of model complex 4.26	76

List of Tables

Table	Page
2.1 Effect of precatalyst and additives on reaction yield.....	10
2.2 Effect of added product on reaction yield.....	15
2.3 Rate of product arene exchange in 2.2	16
2.4 Effect of phosphine ligand on reaction yield.....	17
2.5 Effect of acid and base additives on reaction yield.....	19
2.6 Effect of added glass on reaction yield.....	23
2.7 Effect of arene substitution on reaction yield.....	28
2.8 Calculated ΔG	30
3.1 Selected bond lengths.....	42

List of Abbreviations

Å – angstrom

atm – atmospheres

BAr_4^{F} – tetrakis[3,5-bis(trifluoromethyl)phenyl]borate

cod – 1,5-cyclooctadiene

d – days

D-Ala – D-alanine

DCC – *N,N'*-dicyclohexylcarbodiimide

DCM – dichloromethane

DFT – density functional theory

D-Lac – D-lactate

DPPent – 1,5-bis(diphenylphosphino)pentane

EDC – 1-ethyl-3-(3-dimethylaminopropyl)carbodiimide

eq. – equation

equiv. – equivalents

GC-FID – gas chromatography flame ionization detector

GC-MS – gas chromatography mass spectrometry

HATU – 1-[bis(dimethylamino)methylene]-1H-1,2,3-triazolo[4,5-b]pyridinium 3-oxide hexafluorophosphate

hr – hours

K_{eq} – equilibrium constant

k_{obs} – observed rate constant

M – molar

min – minutes

mol% – mole percent

NMR – nuclear magnetic resonance

OTf – triflate

Ph – phenyl

Py – pyridine

s – seconds

S_NAr – nucleophilic aromatic substitution

THF – tetrahydrofuran

TON – turnover number

I. INTRODUCTION TO C-F AND C-H BOND ACTIVATION BY TRANSITION METAL COMPLEXES

The transformation of bonds which are traditionally considered to be inert lies at the heart of organometallic chemistry. Bonds that organic chemistry once held as immutable, such as C-F and C-H bonds, are able to be routinely manipulated through the use of metal complexes. The unique bonding properties of transition metals, which make use of d-orbitals, allow them to react in ways that are inaccessible to traditional organic chemistry. This dissertation will focus on systems that activate C-F and C-H bonds and the subsequent transformations of the resulting organometallic intermediates. The next three chapters will describe a ruthenium system that enables facile amination of fluoroarenes, an iridium system that converts ethers to the corresponding alkoxy-carbenes, and a nickel system that racemizes both enantiomeric forms of lactate.

Transition metal arene complexes

In Chapter II, a mechanistic study is undertaken of a ruthenium catalyst which activates fluoroarenes towards nucleophilic aromatic substitution (S_NAr). This catalyst activates arenes by binding them in an η^6 coordination mode, meaning that the entire $6e^- \pi$ system is engaged in bonding with the metal center. The π coordination of arenes to transition metal centers imparts a strong electron withdrawing effect on the bound arene. The resulting stabilization of negative charge can increase the acidity of C-H bonds both on the ring and at benzylic positions. The electrophilicity of benzylic carbonyls is increased, and the electrophilicity of the ring is increased for S_NAr reactions.¹ In essence, metal binding can be thought of as introducing a large electron-

withdrawing group, with an effect analogous to between one and three nitro groups,² depending on the specific metal fragment chosen.

The most commonly-used metal fragment for π -arene coordination in organic chemistry, $\text{Cr}(\text{CO})_3$, activates arenes towards an impressive array of stoichiometric reactions.³ However, the removal of the chromium auxiliary is often accomplished oxidatively with 2,3-dichloro-5,6-dicyano-1,4-benzoquinone (DDQ), requiring an additional step.⁴ Among organometallic chemists, there is often interest in the translation of existing reactivity to a catalytic manifold. The reasons for this interest can include the high cost of some metal reagents, the toxicity of those reagents and their byproducts, and access to molecules that are otherwise difficult or impossible to synthesize. Furthermore, organometallic catalysts can reduce the temperature required for reactions⁵ and improve both regioselectivity and enantioselectivity.⁶

To this end, a limited number of examples of catalytic reactions have been developed which make use of π -arene intermediates.¹ Work from the Hartwig group on the cleavage of diaryl ethers with $\text{Ni}(\text{cod})_2$ showed that the catalyst resting state is a π -arene nickel complex, which helps to facilitate rate-limiting oxidative addition.^{7,8} In other work from the Hartwig group, coordination of styrene as a π -arene ligand to a ruthenium fragment was shown to promote anti-Markovnikov hydroamination of the olefin.^{9,10} This reaction nicely demonstrates the ability of π -arene complexes to stabilize a benzylic anion by delocalization of charge into the arene ring. The Matsuzaka group has reported a catalytic condensation reaction in which aryl aldehydes condense with toluene and xylene to form stilbene derivatives.¹¹ The increased acidity of the benzylic positions conferred by η^6 binding in these arenes is paramount to this reactivity. The most frequent use of π -arene intermediates in catalysis has been with the $\text{S}_{\text{N}}\text{Ar}$ reaction, a brief review of which can be found in Chapter II.

Reactivity of fluoroarenes

The chemistry of fluoroarenes is unique with respect to other haloarenes. They are generally much less prone to oxidative addition.¹² In fact, the calculated bond enthalpy of the C(sp²)-F bond in fluorobenzene is about 14 kcal mol⁻¹ greater than that of a C(sp²)-H bond in benzene,¹³ in contrast to the other haloarenes. As such, many of the reactions that are available to functionalize haloarenes are not effective on fluoroarenes.

One of the more common reactions that is performed on fluoroarenes is nucleophilic aromatic substitution. While alkyl fluorides typically react more slowly than chlorides, bromides, and iodides in S_N2 and S_N1 pathways, aryl fluorides are the most amenable to S_NAr due to their relatively small size and electron withdrawing properties, which generate a strongly electrophilic ipso position.¹² However, further activation of the arene, in the form of electron withdrawal from the π system, is often required.¹⁴ This generally comes in the form of covalent electron-withdrawing groups, such as nitro groups or other halogens. Chapter II of this dissertation describes a system which accomplishes the activation of unactivated fluoroarenes via catalytic complexation as η^6 arene complexes.

Metal carbenes

Chapter III of this dissertation focuses on the synthesis and reactivity of iridium alkoxycarbene complexes. Metal carbene complexes contain a formal metal-carbon double bond and are broadly subdivided into two types: Fischer carbenes and Schrock carbenes. Each type of complex can be considered a metal-stabilized version of a free carbene. Schrock carbenes are stabilized triplet carbenes and as such are counted as two 1e⁻ donating ligands. They are typically ligands to metals in high oxidation states, often in the early transition block.⁵ Meanwhile, Fischer carbenes are stabilized singlet carbenes which are counted as neutral 2e⁻ donors. They generally

bind to low oxidation state, late transition metals. They contain an empty p orbital on carbon, which is stabilized by π -backbonding from the metal and π donation from an α -heteroatom. As a result, the M-C bond is polarized towards the metal center, due to incomplete backbonding.⁵ This renders Fischer carbenes electrophilic at carbon, while Schrock carbenes display nucleophilic behavior at carbon due to the electronegativity difference between carbon and the metal.

Metal alkoxy-carbenes refer to metal complexes containing a Fischer carbene which have an alkoxy group at the α position to the carbene. The oxygen lone pair is able to donate electron density into the carbene p orbital, providing the stabilization associated with Fischer carbenes. One of the most straightforward routes to obtain these complexes is the original route employed by Fischer – metal carbonyls can be sequentially treated with an organolithium reagent to form the metal acyl lithiate, followed by treatment with an alkyl electrophile to afford the alkoxy-carbene.¹⁵ Alternatively, the synthesis of alkoxy-carbenes can be accomplished by the addition of oxygen nucleophiles to metal vinylidenes.^{16,17}

While these routes work well to generate metal alkoxy-carbenes, our research group has been interested in the synthesis of alkoxy-carbene complexes from ethers via double C-H activation. This term is used to describe the consecutive oxidative addition of a metal across the α C-H bond of an ether and α -hydride elimination.¹⁸ This sequence produces an alkoxy-carbene without the requirement for highly reactive organolithium reagents or the intermediacy of a metal vinylidene. There are only a limited number of alkoxy-carbenes that have been derived from ethers in the literature.¹⁸⁻²²

The resulting alkoxy-carbenes are much more reactive than the parent ethers. As such, we envision this interconversion as a strategy for performing chemical transformations on the relatively inert ether group. The electrophilicity of the carbene carbon allows these complexes to

behave in ways that are analogous to carbonyl groups. Reactions typical of carbonyls such as acyl substitution^{23,24}, Michael additions²⁵, and aldol chemistry²⁶ have been reported. A more complete review of Fischer carbene reactivity has been written by Dötz and Stendel.¹⁵ Chapter III of this dissertation describes the synthesis of an iridium alkoxycarbene and the reactivity thereof.

Directed C-H activation

The activation of carbon-hydrogen bonds which are generally considered to be inert has been a subject of intense interest for decades.²⁷ The use of organometallic catalysts to effect the conversion of these bonds into other functional groups is one of the fastest ways to build complexity into a molecule. One of the most challenging aspects of this type of transformation is the issue of selectivity – a catalyst that is able to react directly with an otherwise unactivated C-H bond is unlikely to do so with high selectivity.⁶

One strategy that has been used effectively is substrate directing groups. The directing group is employed in a way that brings the desired bond in close proximity to the metal center, resulting in a kinetic advantage for the activation of a single bond. This strategy was pioneered by the Murai group in the 1990s.²⁸ The assistance of a directing group in double C-H activation of ethers is critical to the work described in Chapter III.

Lactate racemase model complexes

Nature has designed systems that allow for exquisitely selective transformations of otherwise unactivated bonds, and has done so in large part without the aid of organometallic chemistry. Chapter IV describes the synthesis of ligands for a model complex of the active site of the enzyme lactate racemase, a newly discovered enzyme possessing a transition metal-carbon bond in its active site. Although the carbinol C-H bond of lactate is sufficiently activated that transition metal activation is not necessarily required for its cleavage, the choice by nature to use

an organometallic active site for this transformation leaves many questions unanswered. The underlying principles regarding selective C-H activation discussed previously also apply to this system. The proposed mechanism invokes a metal hydride intermediate and the proposed synthesis of the model complex is formed by oxidative addition into a C(sp²)-H bond. While this is not a traditional C-H activation, there are certainly elements that overlap established organometallic chemistry in this area. The development of a suitable functional and structural model of the lactate racemase active site therefore offers an opportunity to understand how nature addresses many of the same challenges as synthetic organometallic chemists, including perhaps why it chose an organometallic complex to do so.

II. NUCLEOPHILIC AROMATIC SUBSTITUTION THROUGH π -ARENE CATALYSIS

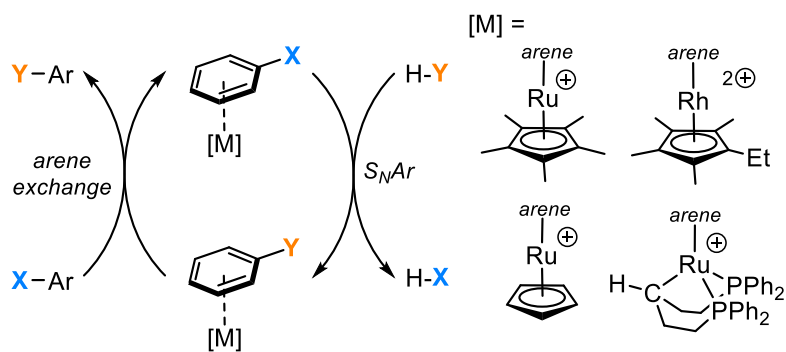
Portions of this chapter were reprinted with permission from Mueller, B. R. J.; Schley, N. D. Product Inhibition in Nucleophilic Aromatic Substitution through DPPent-Supported π -Arene Catalysis. *Dalton Trans.* **2020**, 49 (29), 10114–10119. Copyright 2020 Royal Society of Chemistry.

Introduction

Nucleophilic aromatic substitution (S_NAr) of haloarenes is a powerful synthetic tool that finds wide use in organic chemistry. A major limitation of this reaction, however, is the requirement for electron deficient arene electrophiles. One strategy for the activation of otherwise unactivated arenes is through η^6 binding to a metal center, which gives π arene complexes with significantly enhanced electrophilicity^{3,29–33}. S_NAr reactions of η^6 haloarenes often proceed at room temperature even for substrates like chlorobenzene^{34–36} which is largely inert absent metal-ion activation. In principle, catalytic turnover can be achieved by product arene exchange for the starting material haloarene as depicted in Scheme 1. However, in most cases the strong binding of the arene to the metal requires photolytic or oxidative conditions to liberate the product,² which has largely precluded catalytic applications with rare exceptions.

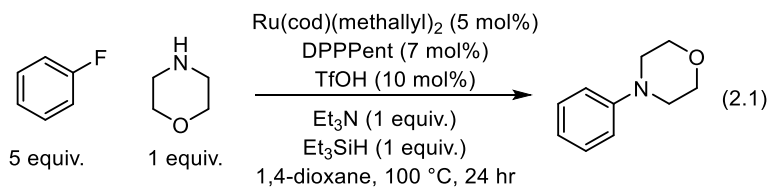
All existing examples of catalytic S_NAr reactions involving η^6 -arene coordination are limited to 2nd row transition metal catalysts. A rhodium(III) example³⁷ and a limited number of ruthenium(II) complexes – two containing cyclopentadienyl derivatives and three containing phosphine ligands, have been shown to serve as catalysts for S_NAr of haloarenes by fluoride³⁸ and amines^{39–42} at temperatures ranging from 100 °C to 180 °C. Among these, the phosphine-supported ruthenium(II) catalysts have been more successful for the S_NAr of fluoroarenes by amines.^{39–41} In all cases, the reaction is speculated to follow a general mechanism proposed by Semmelhack et al.⁴³ (Scheme 2.1) wherein arene exchange allows for catalytic turnover after S_NAr . Electron-

deficient arenes have poorer arene binding thermodynamics while electron-rich arenes have poor arene exchange kinetics.⁴⁴ This ensures that product inhibition is an intrinsic challenge in all cases where the product arene is more electron rich than the haloarene starting material, though to our knowledge this has never been quantified in a catalytic system.



Scheme 2.1. Reported catalysts for π -arene S_NAr .

The potential complementarity of catalytic S_NAr to better developed cross-coupling methods has encouraged our research group to examine this class of transformations in more detail. We chose to begin with a mechanistic study of a 1,5-bis(diphenylphosphino)pentane (DPPent)-supported Ru catalyst for S_NAr reported by the Shibata group (eqn 2.1).⁴¹ This catalytic system is closely related to one applied in the catalytic anti-Markovnikov hydroamination of styrene by the Hartwig group.¹⁰ In that study Hartwig was able to show that DPPent undergoes cyclometalation to give a facial, tridentate ligand-supported ruthenium complex that binds η^6 arenes.¹⁰



When applied to S_NAr catalysis, DPPent gave a complex (generated in situ) that displayed the highest turnover numbers and mildest reaction conditions of any intermolecular π -arene S_NAr reaction at the time.⁴¹ Their preliminary mass spectrometry and $^{31}\text{P}\{^1\text{H}\}$ NMR experiments

suggest that ruthenium arene complexes analogous to those characterized by Hartwig may be formed in situ, which represented an ideal starting point for further study.

Results and Discussion

On the basis of mass spectrometric data, Shibata proposed π -arene intermediates⁴¹ supported by a cyclometalated κ^3 DPPPent ligand analogous to the one observed by Hartwig.¹⁰ We undertook the synthesis of two arene derivatives bearing a κ^3 DPPPent ligand in an effort to study their properties in π -arene S_NAr catalysis. Complexes **2.1** and **2.2** were synthesized in a single step from Ru(cod)(methallyl)₂ using variations on a reported procedure (eqn 2.2 and 2.3).¹⁰ Both complexes were characterized by ¹H and ³¹P{¹H} NMR and combustion analysis, and their structures were confirmed by single crystal X-ray diffraction (Figure 2.1).

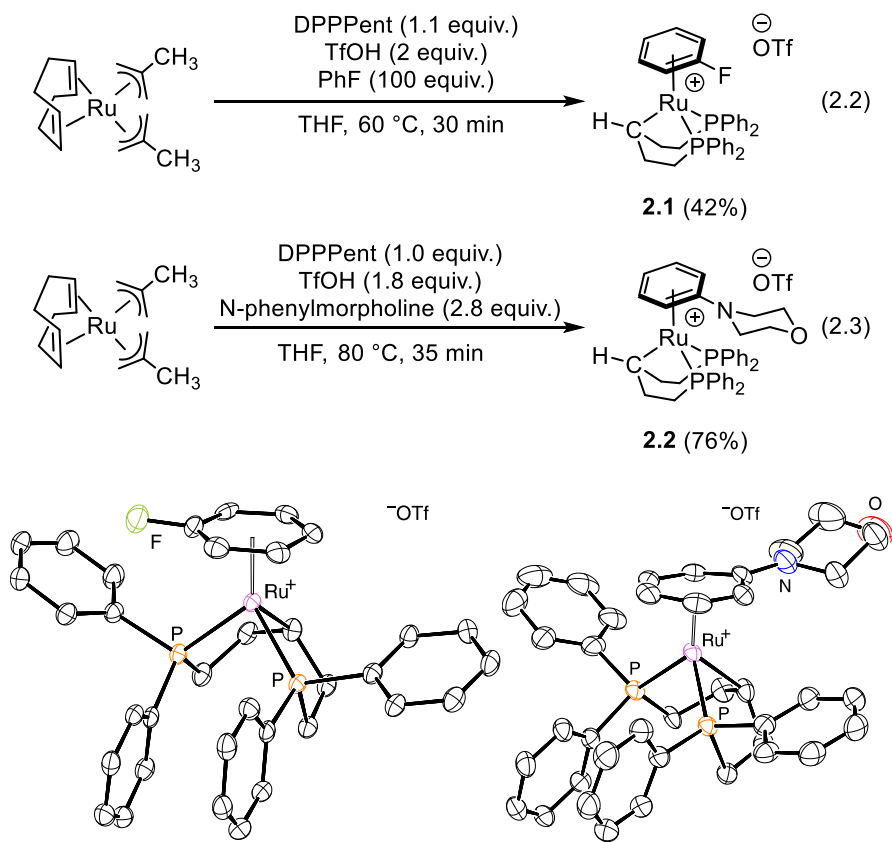
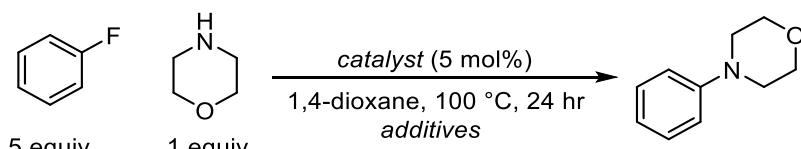


Figure 2.1. ORTEP of complexes **2.1** (left) and **2.2** (right). Ellipsoids are shown at 50% probability.

Catalyst resting state and the role of additives

Under the previously reported catalytic conditions, both **2.1** and **2.2** catalyze the reaction between fluorobenzene and morpholine in similar yields to the catalyst generated in situ from Ru(cod)(methallyl)₂ (Table 2.1). The optimized conditions reported by Shibata include triethylamine and triethylsilane additives in stoichiometric amounts which they show are required for high yields. This observation is born out in our own studies; in the absence of additives the product is still formed but in reduced yield (46% vs. 93% with additives). To address the possibility that reaction additives might influence catalyst speciation, the identity of the catalyst resting state was investigated by ³¹P{¹H} NMR both in the presence and absence of silane and amine additives.

Table 2.1. Effect of precatalyst and additives on reaction yield.



Entry	Catalyst	Additives ^a	% Yield ^b
1	<i>in situ</i> ^c	Et ₃ N, Et ₃ SiH	93
2	2.1	Et ₃ N, Et ₃ SiH	98
3	2.2	Et ₃ N, Et ₃ SiH	92 ^d
4	2.3	Et ₃ N, Et ₃ SiH	> 99 ^d
5	<i>in situ</i> ^c	None	46
6	2.1	None	57
7	2.2	None	47 ^d
8	2.3	None	> 99 ^d

^a 1 equiv. of each additive. ^b Yield by GC-FID ^c 5 mol% Ru(cod)(methallyl)₂, 7 mol% DPPent, 10 mol% TfOH. ^d **2.2** and **2.3** contribute 5% to total yield

Based on the proposed mechanism put forth by Semmelhack⁴³ and our own arene binding measurements (*vide infra*), the bound phenylmorpholine compound (**2.2**) would be the expected resting state. Indeed, **2.2** is observed as the catalyst resting state by ³¹P{¹H} NMR in the absence of triethylsilane and triethylamine, confirming that it represents a relevant system for mechanistic

experiments (vide infra). However, in the presence of these additives (the reported optimized catalytic conditions), **2.2** is observed only at very short reaction times. Instead a second, previously unknown species **2.3** is observed as the major species during productive catalysis. Initial attempts to characterize **2.3** revealed that triethylsilane is necessary for its formation and that **2.3** possesses a metal hydride which resonates upfield at -9.5 ppm. Analysis of a single-crystal of **2.3** obtained by careful isolation from a variation of a catalytic reaction (eqn 2.4) revealed that **2.3** is a bis(phosphine)ruthenium hydride lacking the alkyl ligand resulting from backbone cyclometalation in **2.2** (Figure 2.2). In separate experiments we found that **2.3** can be formed by treatment of **2.2** with 20 equiv. of triethylsilane, suggesting a route for the conversion of κ^3 cyclometalated complexes to the κ^2 form observed in **2.3**.

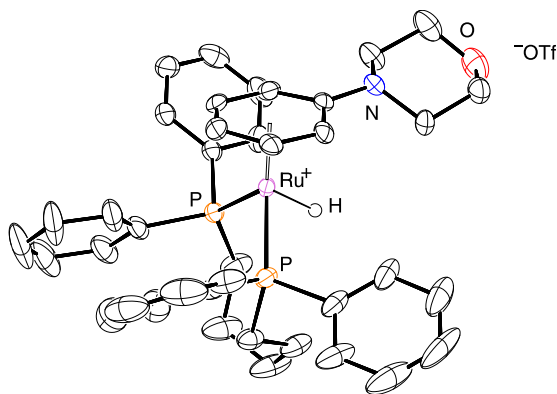
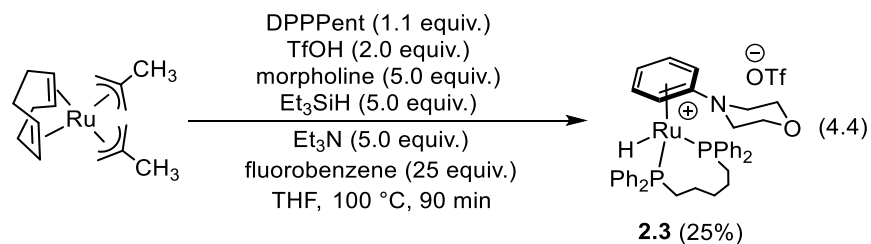


Figure 2.2. ORTEP of complex **2.3**. Ellipsoids are shown at 50% probability.

When complex **2.3** is used as a precatalyst under Shibata's optimized conditions, the N-phenylmorpholine product is obtained in quantitative yield (Table 2.1, entry 4). This observation argues that ligand cyclometalation observed in **2.1** and **2.2** is not necessary for reactivity. Unlike in the case of complex **2.2**, the performance of complex **2.3** does not suffer in the absence of Et₃SiH and Et₃N additives (Table 2.1, entry 8). The Shibata group has previously hypothesized that the inclusion of triethylsilane and triethylamine is necessary to sequester hydrofluoric acid generated as a byproduct of fluoroarene S_NAr. The observation that silane is not required when **2.3** is used as a precatalyst argues against this hypothesis for the primary function of silane in the productive catalytic reaction. Instead its most significant function appears to be the switch in ligand binding mode and thus the catalyst resting state from **2.2** to **2.3**.

Catalytic reactions conducted without additives (Table 2.1 entries 5–7, Table 2.2 entries 4–6) tended to give lower yields and were observed to deposit a yellow precipitate within the first several hours of the reaction except when **2.3** was used as a catalyst. Filtration and analysis of this precipitate after reaction completion showed that complex **2.2** precipitates in 85% yield with respect to the ruthenium precursor. Precipitation was not observed in the presence of additives, a result which argues that the change in catalyst resting state from **2.2** to **2.3** is accompanied by increased catalyst solubility.

Having determined that the presence of triethylsilane and triethylamine additives results in a switch in catalyst resting state from **2.2** to **2.3**, we attempted to investigate the corresponding fluorobenzene adduct. Unfortunately, efforts to prepare a fluoroarene complex analogous to **2.3** by treatment of **2.1** with triethylsilane gave complex mixtures of products without evidence for fluoroarene binding by NMR spectroscopy.

S_NAr kinetics and arene binding thermodynamics

Despite our inability to prepare the fluoroarene partner to complex **2.3**, the observation that **2.2** serves as the catalyst resting state in the absence of additives and leads to a productive catalytic reaction led us to pursue mechanistic studies on the **2.1/2.2** pair. In particular, the isolation of complex **2.1** affords us a unique opportunity to directly measure the rate of S_NAr on a π -arene in a system with catalytic relevance. Under pseudo-first order conditions, **2.1** reacts rapidly with morpholine to give **2.2** within 10 minutes at 23 °C, corresponding to a k_{obs} of $3.8 \times 10^{-3} \text{ s}^{-1}$ (Figure 2.3). The reactivity of complex **2.1** with morpholine at room temperature stands in contrast to the metal-free reaction of morpholine with even very highly-activated nitrofluorobenzenes. 2-Nitrofluorobenzene has been reported to undergo amination by morpholine at 40 °C,⁴⁵ while 3-nitrofluorobenzene requires heating to 100 °C for 60 hours.⁴⁶

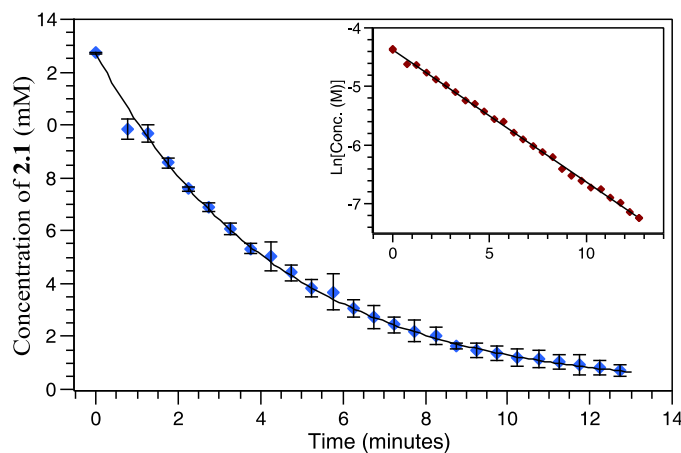


Figure 2.3. Stoichiometric S_NAr reaction of complex **2.1** with morpholine at 23 °C under pseudo-first order conditions. Inset: Ln[**2.1**] vs time. Conditions: 0.0127 M **2.1**, 0.127 M morpholine in 4:1 dioxane/DMF. See Appendix for additional details.

The high rate of conversion of **2.1** to **2.2** observed at 23 °C suggests that this step is unlikely to be the primary determinant of the overall reaction rate under the reported catalytic conditions (5 mol% Ru, 24 h, 100 °C). Thus we next examined the arene exchange step in Scheme 2.1.

Efficient displacement of product from the metal center is believed to be the most challenging aspect in the development of catalytic S_NAr reactions of π -arenes. Hartwig has previously examined the rate of displacement of N-phenethylmorpholine by styrene on the same ruthenium system.¹⁰

When complex **2.1** is treated with free N-phenylmorpholine (2 equiv.) in neat fluorobenzene at 23 °C, no arene exchange is observed. On heating to 100 °C, a stable equilibrium between **2.1** and **2.2** is obtained that allows for the determination of an equilibrium constant $K_{eq} = 2 \times 10^3$ at 100 °C. Using this experimental equilibrium constant we can predict the ratio of complexes **2.2** and **2.1** during catalysis. After a single turnover, the ratio of **2.2** to **2.1** is predicted to be 4 : 1, a value that rises rapidly to >200 : 1 after 10 turnovers (50% conversion). The predicted fraction of complex **2.1** as a function of turnover number is shown in Figure 2.4 and demonstrates the dramatic influence of strong product binding on the predicted catalyst resting state. Thus, even under idealized conditions, the proportion of catalyst in the fluoroarene form is predicted to fall by two orders of magnitude by the time the reaction yield has reached 25%.

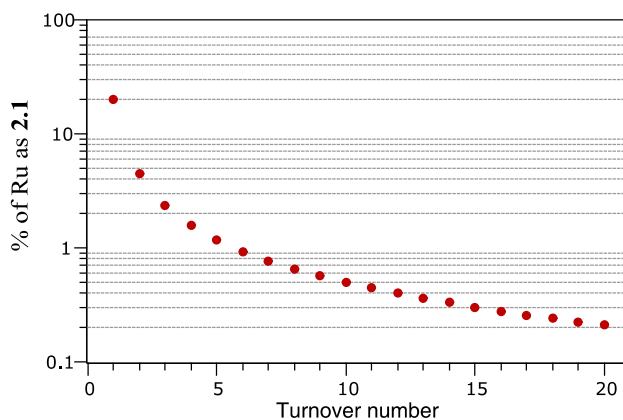
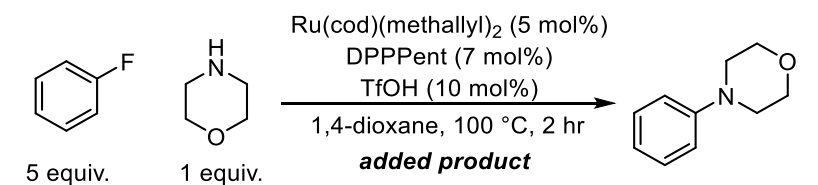


Figure 2.4. Predicted fraction of fluoroarene complex **2.1** as a function of turnover number; estimated from K_{eq} .

Indeed, product added at the beginning of the reaction has a strong inhibitory effect on catalytic turnover both in the presence and absence of additives (**2.3** and **2.2** as resting state respectively). The addition of 0.5 equiv. of N-phenylmorpholine leads to poor catalyst performance over 2 hours, while addition of a full equivalent of product inhibits catalysis even more dramatically (Table 2.2). The additive-free case appears to be affected to a larger extent, which may stem from the low apparent solubility of **2.2** (vide supra).

Table 2.2. Effect of added product on reaction yield after 2 hours.



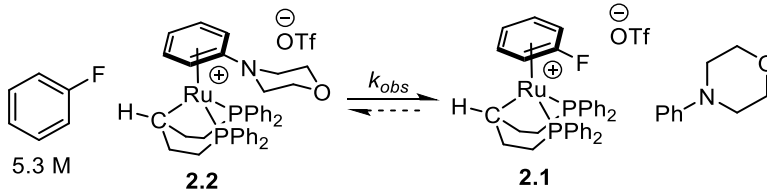
Entry	Additives ^a	Time	N-phenylmorpholine	% Yield ^b
1	Et ₃ N, Et ₃ SiH	2 hr	0 equiv.	32
2	Et ₃ N, Et ₃ SiH	2 hr	0.5 equiv.	10
3	Et ₃ N, Et ₃ SiH	2 hr	1.0 equiv.	2
4	None	2 hr	0 equiv.	15
5	None	2 hr	0.5 equiv.	1
6	None	2 hr	1.0 equiv.	2

^a 1 equiv. Et₃N, 1 equiv. Et₃SiH. ^b Yield by GC-FID.

While the thermodynamics of product binding can be expected to decrease the fraction in the active form at equilibrium, the rate of arene exchange should determine whether equilibrium concentrations are achieved under catalytic conditions. To that end, we examined the rate of displacement of N-phenylmorpholine by a large excess of fluorobenzene (conversion of **2.2** to **2.1**). Initial rate constants for the conversion of **2.2** to **2.1** via arene exchange are shown as a function of temperature in Table 2.3. Under these conditions, product displacement at 65 °C is found to be two orders of magnitude slower than S_NAr measured at 23 °C. From these data the activation energy of arene exchange is calculated to be 34 kcal mol⁻¹. The precise mechanism of

arene exchange can be complex and conditions dependent,^{44,47-51} but these values provide some insight into the lability of the product arene in **2.2**.

Table 2.3. Rate of product arene exchange in **2.2**.



Entry	Temperature	Rate constant 2.2 → 2.1 (k_{obs})
1	65 °C	$5.6 \times 10^{-5} \text{ s}^{-1}$
2	70 °C	$1.3 \times 10^{-4} \text{ s}^{-1}$
3	75 °C	$2.4 \times 10^{-4} \text{ s}^{-1}$
4	80 °C	$4.8 \times 10^{-4} \text{ s}^{-1}$
5	85 °C	$1.1 \times 10^{-3} \text{ s}^{-1}$

Together our rate and equilibrium measurements on this system demonstrate two important features of this reaction: (1) the N-phenylmorpholine product arene binds with roughly 2000 times greater affinity than fluorobenzene, leading to strong product inhibition and (2) that the requirement for elevated reaction temperatures is likely dictated largely by the kinetics of arene exchange and the requirement for S_NAr on the minute fraction of catalyst present as **2.1**.¹ While comparable studies have not been performed on related catalysts, all catalytic π -arene alkoxylation and amination systems appear to achieve no more than ca. 20 TON under reported conditions.^{37,39,40}

Role of phosphine ligands

Further evidence for the suggestion that cyclometalation is not necessary for the reactivity of the DPPent system can be obtained through the substitution of other phosphine ligands. A number of bidentate phosphines are found to give modest catalytic activity (Table 2.4). For instance, while 2,2'-bis(diphenylphosphino)diphenyl ether (DPEPhos) can coordinate through the biarylether moiety, it cannot cyclometalate to give an anionic alkyl donor, but still gives

comparable yields to DPPent (Table 2.4).⁹ Other phosphines give reduced but still appreciable yields. The results of our phosphine comparison when taken together with evidence showing a silane-controlled resting state of the catalytic reaction suggest that ligand cyclometalation is not a defining feature of S_NAr catalysis by the DPPent system.

Table 2.4. Effect of phosphine ligand on reaction yield.

Phosphine	Yield ^a	Phosphine	Yield ^a
PPh ₃	49% ^b	PAr ^F ₃	19% ^b
	93%		23%
	50%		66%
	81%		

^aYield by GC-FID ^b14 mol% phosphine used.

Both the bis(phosphine) monohydride ligand set in **2.3** and the κ^3 -phosphine in **2.2** provide monoanionic 5-electron donor environments, a motif that is conserved in pentamethylcyclopentadienyl and cyclopentadienyl catalysts reported by Grushin³⁸ and Williams⁴² respectively. Among published systems for π -arene catalyzed S_NAr, only a recent report from Shi diverges from this pattern by employing a dicationic ruthenium bis(phosphine) complex.³⁹ This observation inspired the preparation of complex **2.4-OTf** (eqn 2.5 and Figure 2.5), which conserves the hydrido bis-phosphino motif found in **2.3**. Like **2.3**, **2.4-OTf** catalyzes the amination of fluorobenzene by morpholine in good, albeit not quantitative yield in the absence of additives (Table 2.5, entry 1). **2.4-OTf** does outperform in situ-generated conditions for PPh₃ (Table 2.5

entry 1 versus Table 2.4). Thus **2.4-OTf** offers a convenient, single-component precatalyst that can be prepared in a single step from a commercially-available ruthenium source.

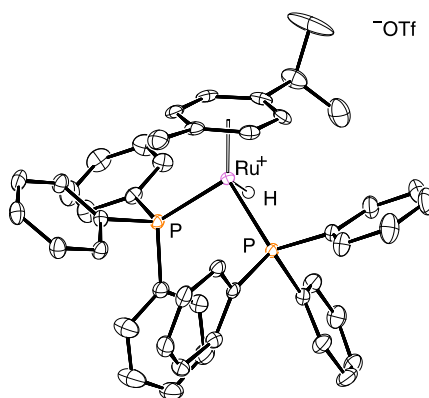
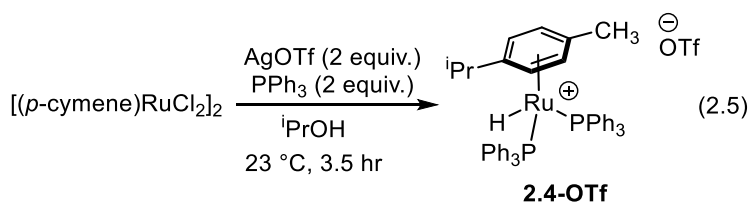


Figure 2.5. ORTEP of complex **2.4-OTf**. Ellipsoids are shown at 50% probability.

Role of acid additives

Having identified that **2.4-OTf** is an accessible, single-component catalyst with some room for improvement versus **2.3**, we examined the role of added Brønsted acid and/or metal triflates with both **2.4-OTf** and the triflate-free **2.4-PF₆** complex. In theory, protonation of the aniline product could decrease product inhibition, though any potential improvement would be counterbalanced by competing protonation of the more-basic morpholine nucleophile. In practice, addition of triflic acid with or without added triethylamine leads to reductions in yield (Table 2.5). Small amounts of triflate ion appear to be beneficial⁴⁷ (entries 1 vs. 5 and 5 vs. 6), though larger quantities of lithium triflate led to poorer results. Thus it would appear that alternative approaches are still necessary to address product inhibition if higher TONs are desired.

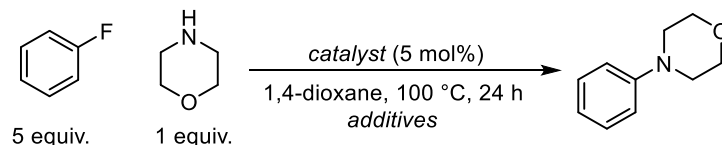


Table 2.5. Effect of acid and base additives on reaction yield.

Entry	Cat.	Additives	% Yield ^a
1	2.4-OTf	None	72
2	2.4-OTf	1 equiv. TfOH	3
3	2.4-OTf	1 equiv. TfOH, 1 equiv. Et ₃ N	41
4	2.4-OTf	0.1 equiv. TfOH, 1 equiv. Et ₃ N	71
5	2.4-PF₆	None	51
6	2.4-PF₆	0.1 equiv LiOTf	60
7	2.4-PF₆	0.2 equiv LiOTf	53
8	2.4-PF₆	1.0 equiv LiOTf	30

^a Yield by GC-FID

Arene binding in **2.2** vs. **2.3**

Owing to our inability to isolate the fluorobenzene analogue of **2.3**, the reactivity of this putative intermediate can only be inferred by comparison to complex **2.1**. We undertook a computational comparison of arene binding thermodynamics using our experimentally-determined energies for the complex **2.1/2.2** pair as a benchmark. DFT calculations (M06L/def2-SVP(CNHOF)/TZVP(RuP)) indicate that N-phenylmorpholine binding by **2.1** is exergonic by $-8.3 \text{ kcal mol}^{-1}$ at 100 °C, which is in good agreement with our experimentally determined value of $-5.3 \text{ kcal mol}^{-1}$ derived from the equilibrium constant at 100 °C. N-Phenylmorpholine displacement of fluorobenzene in the ruthenium hydride version of the catalyst to give **2.3** is computed to be exergonic by $-9.6 \text{ kcal mol}^{-1}$. Thus the small difference in affinity for the N-phenylmorpholine and fluorobenzene arene pair, computed for **2.2** and **2.3**, ($\Delta\Delta G_{\text{calc}} = 1.3 \text{ kcal mol}^{-1}$) predicts that the decyclometalated and cyclometalated forms of the catalyst are subject to comparably strong product arene binding.

Dimerization

When **2.1** is held in solution at elevated temperatures, ($>80\text{ }^{\circ}\text{C}$) it was observed that small quantities of a new product slowly appeared in the ^{31}P NMR spectrum. This compound resonates as a series of 3 to 4 overlapping doublets between 60 and 75 ppm. During one attempt to crystallize **2.1**, crystals of this previously unidentified compound, **2.5**, were inadvertently obtained instead, revealing it to be a dimer of Ru(PCP) units (Figure 2.6). In place of an exogenous arene, each metal center is bound to one of the arenes of a diphenylphosphino group coordinated through phosphorus to the other metal center.

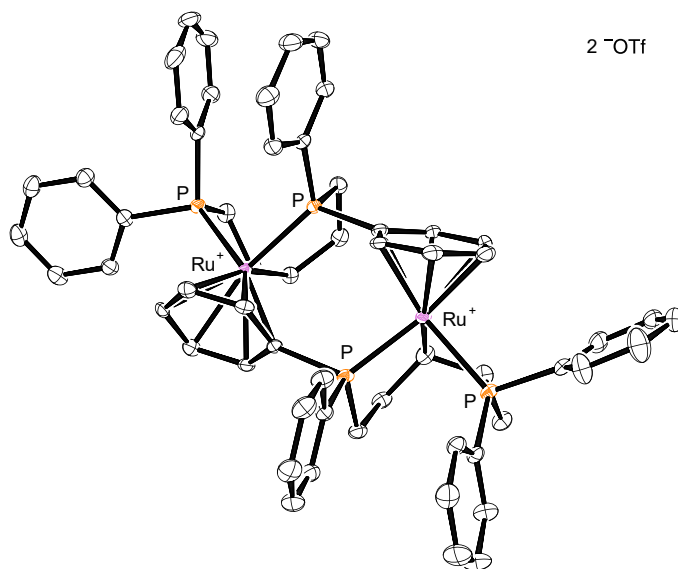


Figure 2.6. ORTEP of complex **2.5**. Ellipsoids are shown at 50% probability.

Unfortunately, the dimeric product **2.5** was difficult to isolate and exceptionally insoluble in common NMR solvents, further frustrating efforts to study its properties. It was noted that this impurity appears in the synthesis of **2.1** but not of **2.2**, leading to speculation that its formation is preferred in the absence of a sufficiently electron rich arene. This observation led us to hypothesize that this dimer is an off-path species that likely precipitates from catalytic reactions, particularly during early stages of the reaction when the concentration of electron rich product arene is low.

Fluoride generation

The Shibata group originally posited that the inclusion of triethylamine and triethylsilane additives served to sequester HF generated as a byproduct of this reaction. We were able to show that the primary role of the additives was to effect a switch in the resting state of the catalyst (*vide supra*). However, this finding leaves unaddressed the fate of the fluoride ion released during this reaction.

^{19}F NMR experiments show that in catalytic reactions that contain triethylsilane, triethylsilylfluoride is generated over the course of the reaction. However, quantitation of this byproduct by ^{19}F NMR show that only roughly 40% of the fluoride released is captured as Et_3SiF (Figure 2.7). The remainder was unaccounted for, as was the entirety of the fluoride released during additive-free reactions. Hydrofluoric acid is known to etch glass readily, so it was hypothesized that the remainder of the liberated HF might be lost to the glass sides of the reaction vessel, a common outcome when $\text{S}_{\text{N}}\text{Ar}$ reactions are conducted in glass-lined reactors process.⁵²⁻⁵⁴ We set out to provide evidence for this hypothesis by (1) quantifying an increase in detected Et_3SiF when a glass-free reaction vessel was used and (2) showing that some improvement of yield can be effected by addition of glass as a fluoride sequestrant.

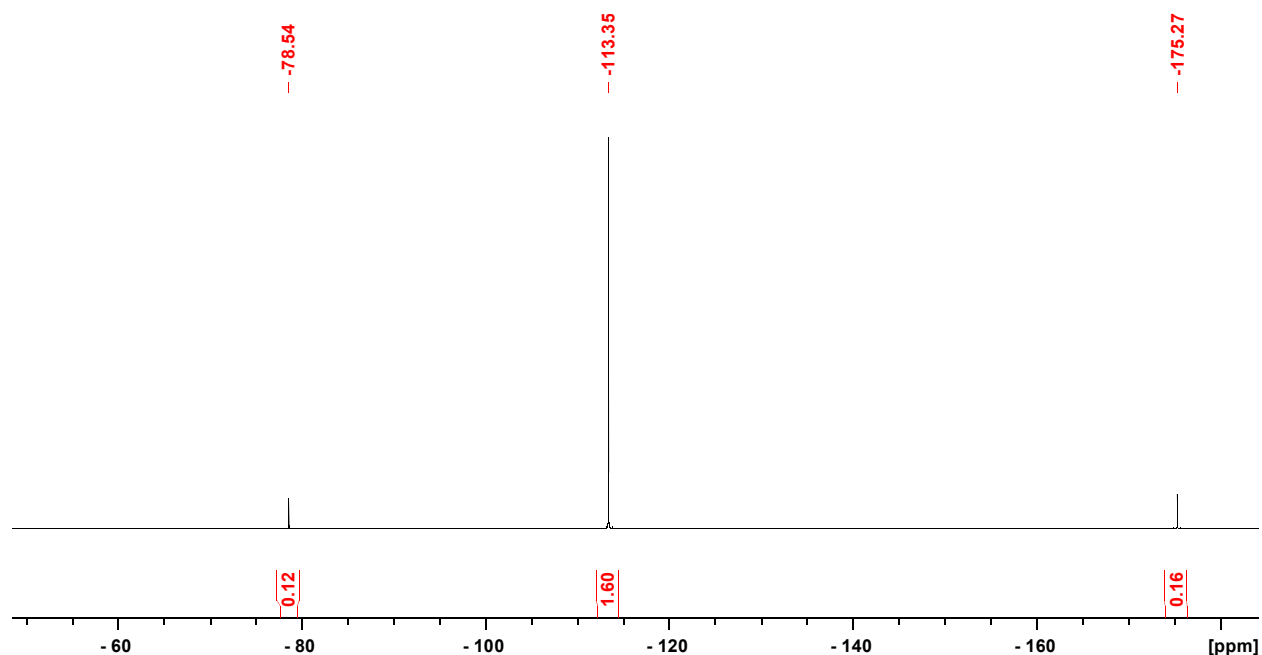
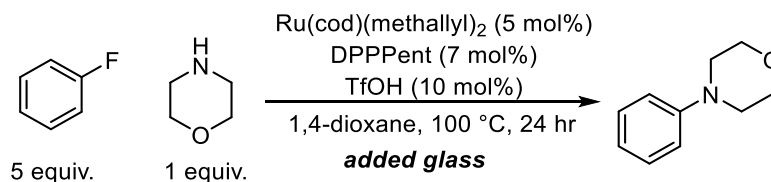


Figure 2.7. $^{19}\text{F}\{^1\text{H}\}$ NMR showing (a) triflate ion (-79 ppm) (b) fluorobenzene (-113 ppm) (c) Et_3SiF (-175 ppm). Integrations represent mmol of each product, standardized to triflate (0.12 mmol).

Using conditions for catalyst generated in situ, the reaction between fluorobenzene and morpholine was conducted in a commercial PTFE vial. These reaction vessels were difficult to seal against the elevated reaction pressures, and ^{19}F NMR analyses continued to show only about 40% conversion of triethylsilane to triethylsilyl fluoride. Moreover, reactions conducted in PTFE vials routinely showed an amount of fluorobenzene being consumed that was greater than the amount of morpholine employed. These observations persisted even when a custom PTFE reactor was employed, leading to concerns that fluorobenzene was leaching into the walls of the fluoropolymeric reactor. As such, efforts to account for the fate of all fluoride ion during these reactions were not able to provide any strong conclusions.

Table 2.6. Effect of added glass on reaction yield.



Entry	Cat.	Added glass (mg)	% Yield ^a
1	<i>in situ</i>	0	46
2	<i>in situ</i>	100	46
3	<i>in situ</i>	200	54
4	<i>in situ</i>	300	51

^a Yield by GC-FID

While exploring alternate fluoride scavengers, it was observed that the addition of trimethylborane in place of triethylsilane improved the reaction yield from 46% to 63%. It was hypothesized then that the addition of more glass to reaction vessels might similarly improve the yield of the reaction by increasing the surface area of the proposed fluoride sequestrant in the additive-free reaction. When finely-ground glass was added, a slight improvement of reaction yield was observed (Table 2.6), but the trend was not strong enough to make definitive statements about the role that the additional glass played. At this point, our hypothesis that glass is acting to sequester HF is still operative, but further evidence is required to support that assertion.

Trifluoromethylation

Perhaps the most elegant solution to the problem of product inhibition is to devise a reaction in which the product arene is more electron deficient than the starting material. Unfortunately, this solution only applies to a very limited number of transformations- the incoming group must be sufficiently electron rich to act as a nucleophile, but the subsequent product arene must somehow be more electron deficient than the fluoroarene. This requirement eliminates most heteroatom nucleophiles from consideration, due to their electron-donating resonance effects, as

well as most carbon nucleophiles. One carbon nucleophile that meets both qualifications is the trifluoromethyl group; the CF_3^- anion is nucleophilic, but the resulting benzotrifluoride should be comparable in electron richness to the fluoroarene.

Initial catalytic reactions focused on the reaction between fluoroarenes and trifluoromethyltrimethylsilane, also known as the Ruppert-Prakash reagent.⁵⁵ Using the original Shibata conditions, no product was observed by ^{19}F NMR. Activation of the Ruppert-Prakash reagent typically requires stoichiometric fluoride (although in this system the fluoride would perhaps only need to be catalytic due to its release from the arene). To this end, a series of fluorides were employed to activate the trifluoromethyl group. Potassium fluoride, sodium fluoride, and potassium bifluoride showed only trace reactivity, with significant quantities of the Ruppert-Prakash reagent remaining after heating at $100\text{ }^\circ\text{C}$ in 1,4-dioxane. Anhydrous tetramethylammonium fluoride, which is considered a “naked” fluoride (meaning that it behaves in solution as an uncoordinated F^- ion), also yielded only a trace amount of product. Critically, the ^{19}F NMR showed production of trimethylsilyl fluoride, indicating the activation of the nucleophile had occurred.

Other changes to the reaction parameters did not generate meaningful increases in yield. 4-methoxyfluorobenzene showed no conversion at all, while 4-chlorofluorobenzene also generated only trace product. Neither lowering the temperature nor varying the phosphine to triphenylphosphine, triisopropylphosphine or 1,4-(diisopropylphosphino)butane had any effect. It was noted that in ethereal solvents (1,4-dioxane and tetrahydrofuran), the appearance of a signal attributed to arene complex **2.1** was observed, in contrast to reactions run in acetonitrile.

The simultaneous presence of **2.1** and Me_3SiF in NMR spectra indicated that the nucleophilic attack step was not occurring as expected and prompted us to study this reaction

stoichiometrically. The reaction between **2.1**, Ruppert-Prakash reagent, and KF in THF at 80 °C showed degradation to dimer **2.5**. Because of the poor solubility of **2.1** in THF, the reactivity of **2.1** with Me₃SiCF₃ was also examined in DMF. This change in solvent was accompanied by the appearance of a new signal in the ³¹P NMR spectrum, which was eventually attributed to the displacement of the arene with at least one equivalent of DMF.

In addition to the Ruppert-Prakash reagent, an additional trifluoromethylation reagent was explored. Potassium (trifluoromethyl) trimethylborate is a commercially available reagent used as a stable source of CF₃⁻ anion.⁵⁶ Among the benefits of this reagent are its nucleophilicity in the absence of activators, and its compatibility with DMF.^{57,58} Unfortunately, stoichiometric reactions between this reagent and **2.1** also gave the putative DMF adduct. Catalytic reactions using Shibata's conditions in THF, 1,4-dioxane, and 1,2-dimethoxyethane did not show any product formation either.

In sum, no examples of trifluoromethylation were observed under any of the described conditions. The observation that **2.5** can be formed from the heating of **2.1** presents the largest challenge to this work. The formation of a product arene that is more electron poor than fluorobenzene will not facilitate the stabilization of the Ru(PCP) monomer, leading to dimerization. It is possible that ruthenium bis(phosphine) hydrides show a lower propensity to dimerize, or do so reversibly, as the arene complexes seem to show greater solubility. Furthermore, the use of alkyl phosphines will prevent arene binding to the ligand. Finally, there is evidence in a related ruthenium cyclopentadienyl system that the CF₃⁻ anion can attack the position ortho to the leaving group, generating an isolable Meisenheimer complex.⁵⁹ Though we have not observed this behavior in this system, it should be noted as a potential issue if nucleophilic attack is able to occur.

Other nucleophiles

Throughout the process of exploring the parameters of this system, there was a concerted effort to expand the scope of nucleophiles that are compatible with this catalytic system. The original report showed that robust reactivity is limited to secondary cyclic amines (55-75% yield), while linear secondary amines and primary amines showed more modest activity (20-44% yield). To this end, we sought to explore the scope of nucleophiles beyond amines in the hope of identifying additional reaction participants.

With the successful synthesis of the single-source precatalyst **2.4-OTf**, we were able to explore whether the poor yields of previously-unsuccessful amines resulted from intrinsically poor reactivity or simply an incompatibility with the catalyst activation step when the catalyst was generated in situ. When **2.4-OTf** was heated at 100 °C in 1,4 dioxane for 24 hours, (N-methyl)benzylamine was coupled with fluorobenzene in 24% yield (vs. 20% reported). Likewise, cyclohexylamine was coupled in just 5% yield (vs. 22% reported). These results demonstrated that the use of an isolated bis(phosphine) ruthenium hydride complex alone is not sufficient to increase the yield with challenging amine substrates. A follow-up stoichiometric experiment showed that the S_NAr reaction between **2.1** and butylamine cleanly formed the bound aniline at room temperature (Figure 2.8), suggesting that the problem in catalytic amination of a broader subset of amines is in the arene exchange.

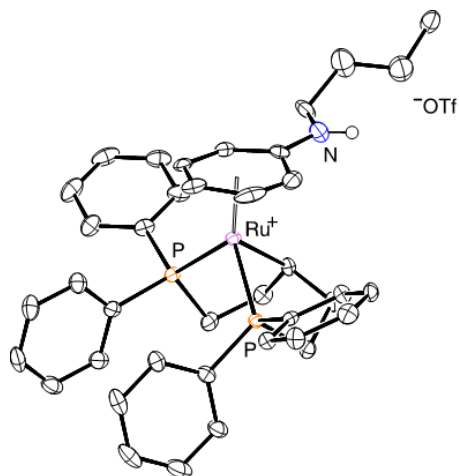


Figure 2.8. ORTEP of butylamine adduct. Ellipsoids are shown at 50% probability.

Oxygen nucleophiles in the form of lithium methoxide and methanol showed no catalytic reactivity towards fluorobenzene in the presence of **2.4-OTf**. Furthermore, lithium methoxide did not show any activity towards **2.1** in stoichiometric reactions. The triethylsilyl enol ether derivatives of cyclopentanone and acetaldehyde similarly showed no reactivity towards fluorobenzene. Nitroalkanes were tested for activity towards fluorobenzene with the in situ-generated catalyst in the presence of a variety of bases, but the only reaction observed was a dimerization of (4-trifluoromethylphenyl)nitromethane. In summary, the only nucleophiles that work reliably with this system continue to be secondary, cyclic amines. This is potentially due to their combination of strong nucleophilicity and their cyclic structure, which leaves the attacking lone pair relatively unhindered.

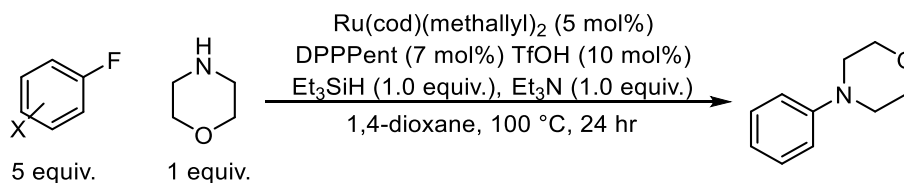
Functional group tolerance of fluoroarenes

An exciting aspect of a catalytic system based on transition metal activation of fluoroarenes for S_NAr is the potential complementarity with other cross-coupling reactions. Many traditional cross-coupling reactions rely on haloarenes that undergo oxidative addition. Reactivity trends in oxidative addition favor the heavier halogens which are more prone to oxidative addition than

fluoroarenes. However, these heavier halogens are also less active in S_NAr reactions, opening the door to orthogonal reactivity that would allow one to append separate groups to bromofluoroarenes, for example.

Preliminary experiments from the Shibata group showed that the in situ-generated catalyst, which can aminate fluorotoluene, has only trace activity towards chlorotoluene and no activity towards bromotoluene and iodotoluene. This observation encouraged an investigation of the reactivity of halofluoroarenes (Table 2.7). When 4-chlorofluorobenzene was used as the arene, the yield dropped appreciably from the unsubstituted fluorobenzene – from 93% to 11% of the observed N-(4-chlorophenyl)-morpholine (Entries 1 and 2). The corresponding bromide and triflate compounds did not show any product formation (Entries 3 and 4). Furthermore, changing the position of the bromide on the arene did not lead to any change in reactivity (Entries 5 and 6).

Table 2.7. Effect of arene substitution on reaction yield.



Entry	-X	% Yield ^a
1	H	93
2	4-Cl	11
3	4-Br	0
4	4-OTf	0
5	3-Br	0
6	2-Br	0

^a Yield by GC-FID

The decreasing activity from chloride to bromide, coupled with the high reactivity of fluoride, was attributed to an increasing propensity to undergo oxidative addition. While this

system does show a lack of S_NAr activity towards chloroarenes and bromoarenes, these groups cannot be considered inert in this context. This will be a major hurdle in the development of orthogonal S_NAr /cross-coupling reactivity.

Conclusion

In summary, our examination of the Ru-catalyzed S_NAr of fluoroarenes has revealed new details that shed light on a very rare example of catalytic nucleophilic aromatic substitution at a π -arene. We have demonstrated an additive-dependent switch in the identity of the resting state of the catalyst resulting from the ligand's ability to bind in either a κ^2 or cyclometalated κ^3 forms. Isolation of both catalytic intermediates in the cyclometalated form has allowed us to estimate the difference in the free energy of product N-phenylmorpholine binding vs. fluorobenzene binding – a key consideration in the arene exchange step necessary for catalytic turnover. These experimental results are contextualized with DFT calculations showing comparable binding affinities for the κ^2 form of the catalyst observed in the presence of silane additives. Experimental measurements and predictions of binding enthalpies quantify the severity of product inhibition encountered in this example of π -arene S_NAr amination. We show that ligand cyclometalation is not a determining factor in the ability of this class of cationic ruthenium complexes to serve as catalysts for S_NAr . The silane additive previously hypothesized to function to sequester fluoride ion appears to contribute to productive catalysis primarily through its ability to modulate ligand cyclometalation, an observation which has allowed us to employ a simple, single-component precatalyst for fluorobenzene amination.

Future Directions

The quantification of product inhibition in this system will be among the most important implications of this work. Until this thermodynamic issue can be overcome, this and related

systems will likely continue to rely on high temperatures and long reaction times. Intramolecular Lewis bases can be used to increase the kinetic exchange of arenes,³⁹ but this strategy does not address the underlying thermodynamics discussed herein.

Further DFT calculations (M06/def2svp,def2tzvp(Ru,P)) from our research group have shed some light on the types of ligands that may reduce the magnitude of product inhibition. When comparing a series of complexes of the general formula [(arene)RuH(PR₃)₂]OTf, a pattern emerges (Table 2.8). Very electron poor phosphines (Entry 3) show highly exergonic binding of N-phenylmorpholine relative to fluorobenzene, while less electron poor phosphines show reduced differences in computed binding enthalpy (Entry 1). Relatively electron rich aryl phosphines (Entries 2,4) further reduce the magnitude of this number. When triethylphosphine is used (Entry 5), the calculated ΔG is reduced to -6.08 kcal mol⁻¹. This value still represents significant product inhibition but hints that electron-rich metal arene complexes are likely to bind arenes less discriminately than electron-poor complexes. This will likely come at the expense of decreasing the kinetic lability of the bound arene, but nonetheless outlines a possible solution for observed product inhibition.

Table 2.8. Calculated ΔG for the displacement of fluorobenzene by N-phenylmorpholine in [(arene)RuH(PR₃)₂]OTf.

Entry	R =	ΔG (kcal mol ⁻¹)
1	phenyl	-8.35
2	3,5-dimethylphenyl	-6.15
3	3,5-bis(trifluoromethyl)phenyl	-12.17
4	3,5-dimethyl-4-methoxyphenyl	-7.84
5	ethyl	-6.08

One possible solution that has not been fully explored is the idea of artificially holding the catalyst in conditions that replicate the initial distribution of arenes. For the coupling of small organic molecules, such as morpholine and fluorobenzene, the boiling point of both substituents

is significantly lower than the resulting product. As such, a Soxhlet-style apparatus could be employed, in which starting materials are distilled up to a reservoir of catalyst, in which they react to form product before being returned to the collection flask. The challenge to this approach is that Soxhlet extraction is most often used to extract compounds which are only marginally soluble in the chosen solvent; the catalyst reservoir in this case needs to be completely insoluble.

To immobilize the catalyst, a triphenyl phosphine derivative which is covalently linked to styrene beads was employed. These beads are insoluble in organic solvent, and large enough to be trapped by filter paper. It was envisioned that heating **2.4-OTf** with these beads would induce phosphine exchange, appending the complex to the insoluble beads. Alternatively, attempts were made to replace all or half of the triphenylphosphine used in the synthesis of **2.4-OTf** with the phosphines of the beads. Since the beads are large and insoluble, traditional characterization techniques such as NMR and GC-MS were not suitable to ascertain the successful coupling of the complex to the beads. Nevertheless, the beads were tested as a catalyst in the presence of morpholine and fluorobenzene, showing no activity. Continued efforts to synthesize and characterize bead-immobilized catalysts may yet provide a strategy to overcome the unfavorable thermodynamics of arene binding that lead to product inhibition in this system.

Experimental Section

General Considerations. All syntheses and manipulations were carried out using standard vacuum, Schlenk, cannula, or glovebox techniques under N₂ unless otherwise specified. Tetrahydrofuran, dichloromethane, and pentane were degassed with argon and dried over activated alumina using a solvent purification system. Fluorobenzene and morpholine were degassed with nitrogen and stored over activated 4 Å molecular sieves. The following chemicals were purchased from commercial vendors and used as received: 1,5-bis(diphenylphosphino)pentane, bis[4-(trifluoromethyl)phenyl]chlorophosphine, Ru(cod)(methallyl)₂, trifluoromethanesulfonic acid, and N-phenylmorpholine.

Spectroscopy. ¹H, ¹³C{¹H}, and ³¹P{¹H} NMR spectra were recorded on Bruker NMR spectrometers at ambient temperature unless otherwise noted. ¹H and ¹³C chemical shifts are referenced to residual solvent signals; ³¹P chemical shifts are referenced to an external H₃PO₄ standard. ¹³C assignments were made with the assistance of 2D methods.

Elemental Analysis. Elemental analyses of complexes **2.1-2.3** are of the bulk samples for which yields are reported. No additional purification operations are carried out prior to packaging for analysis, but samples are dried under vacuum for *ca.* 2 days to remove residual or co-crystallized solvent. Elemental analyses were performed at the University of Rochester CENTC Elemental Analysis Facility or by Midwest Microlab.

Preparation of [(κ³-bis(diphenylphosphino)pentane)(η⁶-fluorobenzene)ruthenium]trifluoromethanesulfonate (2.1). In an inert-atmosphere glovebox a 40 mL glass vial was charged with Ru(cod)(methallyl)₂ (0.064 g, 0.20 mmol) and 1,5-bis(diphenylphosphino)pentane (0.097 g, 0.22 mmol, 1.1 equiv.) in 6 mL THF. While stirring, trifluoromethanesulfonic acid (35 μL, 0.40 mmol) was added via microsyringe, followed by fluorobenzene (1.87 mL, 20.0 mmol, 100 equiv.).

The solution was heated at 60 °C for 30 minutes after which it was cooled to room temperature and evaporated to dryness. The resulting residue was suspended in 1 mL THF, then was filtered and washed with two 1 mL portions of THF after which it was dried under vacuum. The resulting solid was dissolved in 3 mL of dichloromethane and filtered through a 0.45 µm PTFE syringe filter which was rinsed with an additional 3 mL of dichloromethane. The combined filtrate was dried under vacuum to give the solid product. Yield: 0.065 g (42%). Single crystals were obtained by vapor diffusion of pentane into a solution of THF at room temperature. Elemental Analysis for C₃₆H₃₄F₄O₃P₂RuS: C, 55.03; H, 4.36. Found C, 52.12; H, 3.86.

¹H NMR (400 MHz, 23 °C, CDCl₃): δ 2.00-2.20 (m, 4H, CH₂ of DPPent), 2.29-2.39 (m, 2H, CH₂ of DPPent), 2.43-2.50 (m, 2H, CH₂ of DPPent), 5.03 (t, ²J_{HP} = 6.8 Hz, 1H, C-H of DPPent), 5.29 (dd, ³J_{HH} = 5.6 Hz, ⁴J_{HH} = 4.8 Hz, 2H, o-C-H of arene), 5.46 (apparent q, ³J_{HH} = 3.7 Hz, 2H, m-C-H of arene), 6.32 (td, ³J_{HH} = 5.9 Hz, ⁴J_{HH} = 2.6 Hz, 1H, p-C-H of arene), 7.11-7.21 (m, 12H, C-H of PPh₂), 7.29-7.35 (m, 8H, C-H of PPh₂).

¹⁹F{¹H} NMR (376 MHz, 23 °C, CDCl₃): δ -132.72 (s, C-F), -78.00 (s, S-CF₃).

³¹P{¹H} NMR (202 MHz, 23 °C, CDCl₃): δ 65.45 (s).

¹³C{¹H,³¹P} NMR (126 MHz, 23 °C, CD₂Cl₂): δ 33.2 (CH₂ of DPPent), 40.2 (CH₂ of DPPent), 46.2 (CH of DPPent), 79.8 (d, ²J_{CF} = 20.0 Hz, o-C-H of arene), 88.1 (p-C-H of arene), 98.6 (d, ³J_{CF} = 6.7 Hz, m-C-H of arene), 129.1 (m-C-H of PPh₂), 129.2 (m-C-H of PPh₂), 130.8 (o-C-H of PPh₂), 130.9 (o-C-H of PPh₂), 131.0 (o-C-H of PPh₂), 132.2 (p-C-H of PPh₂), 138.5 (C of DPPent), 143.2 (d, ¹J_{CF} = 278.3, C-F of arene).

*Triflate carbon was observed only by ¹³C{¹H} NMR at δ 121.6 (q, ¹J_{CF} = 321.4 Hz).

Preparation of $[(\kappa^3\text{-bis(diphenylphosphino)pentane})(\eta^6\text{-N-phenylmorpholine})\text{ruthenium}]\text{trifluoromethanesulfonate (2.2)}$. In an inert-atmosphere glove box a 40 mL glass vial was charged with Ru(cod)(methallyl)₂ (0.070 g, 0.22 mmol, 1.0 equiv.) and 1,5-bis(diphenylphosphino)pentane (0.097 g, 0.22 mmol, 1.0 equiv.) in 6 mL THF. While stirring, trifluoromethanesulfonic acid (35 μL , 0.40 mmol, 1.8 equiv.) was added via microsyringe, followed by N-phenylmorpholine (0.100 g, 0.605 mmol, 2.8 equiv.). The solution was heated at 80 $^{\circ}\text{C}$ for 35 minutes. After cooling to room temperature, the volume was reduced to approximately 3 mL under vacuum. The resulting suspension was filtered and washed with three 1 mL portions of THF. The filtered solid was dried under vacuum to give the product as a yellow solid. Yield: 0.129 g (76%). Single crystals were obtained by vapor diffusion of pentane into a solution of dichloromethane at room temperature. Elemental Analysis for C₄₀H₄₂F₃NO₄P₂RuS: C, 56.33; H, 4.96; N, 1.64. Found C, 55.81; H, 4.82; N 1.59.

¹H NMR (500 MHz, 23 $^{\circ}\text{C}$, CD₂Cl₂): δ 2.02-2.21 (m, 4H, CH₂ of DPPPent), 2.29-2.38 (m, 2H, CH₂ of DPPPent), 2.47-2.51 (m, 2H, CH₂ of DPPPent), 3.42 (t, ³J_{HH} = 4.9 Hz, 4H, N-CH₂ of morpholine), 3.81 (t, ³J_{HH} = 4.9 Hz, 4H, O-CH₂ of morpholine), 4.68 (d, ³J_{HH} = 6.5 Hz, 2H, *o*-C-H of arene), 4.68 (bs, 1H, C-H of DPPPent), 5.01 (apparent t, ³J_{HH} = 5.0 Hz, 2H, *m*-C-H of arene), 5.87 (t, ³J_{HH} = 5.5 Hz, 1H, *p*-C-H of arene), 7.08-7.12 (m, 12H, C-H of PPh₂), 7.29-7.35 (m, 8H, C-H of PPh₂).

³¹P{¹H} NMR (202 MHz, 23 $^{\circ}\text{C}$, CD₂Cl₂): δ 67.65 (s).

¹³C{¹H, ³¹P} NMR (126 MHz, 23 $^{\circ}\text{C}$, CD₂Cl₂): δ 34.0 (CH₂ of DPPPent), 41.1 (CH₂ of DPPPent), 46.3 (N-CH₂ of morpholine), 47.0 (C-H of DPPPent), 66.8 (O-CH₂ of morpholine), 70.0 (*o*-C-H of arene), 82.0 (*p*-C-H of arene), 98.6 (*m*-C-H of arene), 128.8 (*m*-C-H of PPh₂), 128.9 (*m*-C-H of

PPh₂), 130.3 (*o*-C-H of PPh₂), 130.6 (*o*-C-H of PPh₂), 132.2 (*p*-C-H of PPh₂), 139.5 (C of arene), 139.7 (C of PPh₂).

*Triflate carbon was observed only by ¹³C{¹H} NMR at δ 121.5 (q, ¹J_{CF} = 320.0 Hz).

Preparation of [(κ²-bis(diphenylphosphino)pentane)(η⁶-(N-phenylmorpholine))hydridoruthenium]trifluoromethanesulfonate (2.3). In an inert-atmosphere glove box a 20 mL glass vial was charged with Ru(cod)(methallyl)₂ (0.190 g, 0.595 mmol, 1.0 equiv.) and 1,5-bis(diphenylphosphino)pentane (0.288 g, 0.654 mmol, 1.1 equiv.) in 5.0 mL THF. While stirring, the following reagents were added in order: trifluoromethanesulfonic acid (105 μL, 1.19 mmol, 2.0 equiv.), fluorobenzene (1,395 μL, 14.86 mmol, 25.0 equiv.), morpholine (257 μL, 2.98 mmol, 5.0 equiv.), triethylamine (415 μL, 2.98 mmol, 5.0 equiv.), and triethylsilane (475 μL, 2.98 mmol, 5.0 equiv.). The reaction mixture was heated at 100 °C for 90 minutes, then allowed to cool to room temperature before being filtered through a 0.45 μm PTFE syringe filter. Crystallization of the separated filtrate was accomplished by vapor diffusion of pentane at room temperature overnight. The crude product obtained by crystallization was separated by decanting off the mother liquor and the resulting crystals were washed with 5 mL of pentane. The crystals were then dried under vacuum. The crystals were treated with 5.5 mL THF and the resulting suspension was stirred for 15 minutes, filtered, and washed with THF (3 x 1 mL). The resulting solid was dried under vacuum to give the product as an off-white solid. Yield: 0.150 g (25%). Single crystals were obtained by vapor diffusion of pentane into a solution of THF at room temperature. Elemental Analysis for C₄₀H₄₄F₃NO₄P₂RuS: C, 56.20; H, 5.19; N, 1.64. Found C, 55.90; H, 5.48; N 1.52.

¹H NMR (500 MHz, 23 °C, acetone-*d*₆): δ -9.53 (t, ²J_{HP} = 39.0 Hz, 1H, Ru-*H*), 1.03-1.09 (m, 1H, CH₂ of DPPPent), 1.28-1.33 (m, 1H, CH₂ of DPPPent), 1.37-1.45 (m, 2H, CH₂ of DPPPent), 1.74-1.85 (m, 2H, CH₂ of DPPPent), 2.52 (t, ³J_{HH} = 4.8 Hz, 4H, N-CH₂ of morpholine), 2.64-2.72 (m,

2H, CH₂ of DPPPent), 2.97-3.04 (m, 2H, CH₂ of DPPPent), 3.65 (t, ³J_{HH} = 4.8 Hz, 4H, O-CH₂ of morpholine), 3.73 (d, ³J_{HH} = 6.5 Hz, 2H, *o*-C-H of arene), 5.64 (t, ³J_{HH} = 5.5 Hz, 2H, *m*-C-H of arene), 6.60 (t, ²J_{Hh} = 5.6 Hz, 1H, *p*-C-H of arene), 7.33-7.96 (m, 20H, C-H of PPh₂).

³¹P{¹H} NMR (202 MHz, 23 °C, acetone-*d*₆): δ 44.74 (s).

¹³C{¹H,³¹P} NMR (151 MHz, 23 °C, acetone-*d*₆): δ 24.2 (CH₂ of DPPPent), 24.9 (CH₂ of DPPPent), 32.6 (CH₂ of DPPPent), 48.4 (N-CH₂ of morpholine), 66.1 (O-CH₂ of morpholine), 73.9 (*o*-C-H of arene), 88.9 (*p*-C-H of arene), 98.9 (*m*-C-H of arene), 129.2 (*m*-C-H of PPh₂), 129.6 (*m*-C-H of PPh₂), 130.3 (*o*-C-H of PPh₂), 132.0 (*o*-C-H of PPh₂), 134.0 (C of PPh₂), 135.2 (*p*-C-H of PPh₂), 137.6 (C of arene), 145.0 (C of PPh₂).

*Triflate carbon was observed only by ¹³C{¹H} NMR at δ 122.7 (q, ¹J_{CF} = 321.7 Hz).

Preparation of 1,5-bis(bis(4'-(trifluoromethyl)phenyl)phosphino)pentane (CF₃DPPPent). A flame-dried 100 mL three neck flask equipped with a reflux condenser was charged with magnesium turnings (0.157 g, 6.46 mmol, 2.3 equiv.) and a few small crystals of iodine, followed by 10 mL of dry THF under nitrogen. 1,5-dibromopentane (0.645 g, 2.80 mmol, 1.0 equiv.) was added slowly while heating to 80 °C. Once initiation had occurred, the addition rate was controlled to maintain the reaction at reflux. After addition, the reaction was heated in an 80 °C oil bath for 1.5 hours, at which point little residual magnesium was observed. Upon cooling to room temperature, the resulting cloudy solution was added dropwise by syringe to a solution of bis(4-trifluoromethylphenyl)chlorophosphine (2.02 g, 5.66 mmol, 2.02 equiv.) in 6 mL of dry THF. The solution was allowed to stir for 5 days, during which time a white precipitate slowly appeared, followed by removal of the solvent under vacuum. The resulting white solid was extracted with 10 mL of diethyl ether, which was removed under vacuum to yield a clear oil. The

oil solidified upon standing overnight. This white solid was washed with pentane (6 x 5 mL) and dried under vacuum to give a white solid. This material was dissolved in 6 mL of 1,4-dioxane, flushed through a short plug of silica, and eluted with CH₂Cl₂. The resulting solution was dried under vacuum at 50 °C to give the solid product. Yield: 0.286 g (14%) HRMS (ESI) m/z [M-H]⁺ Calcd for C₃₃H₂₆F₁₂P₂H⁺: 713.1391, Found: 713.1375

¹H NMR (500 MHz, 23 °C, CDCl₃): δ 1.39-1.47 (m, 4H, CH₂ of DPPent), 1.56-1.62 (m, 2H, CH₂ of DPPent), 2.01-2.09 (m, 4H, CH₂ of DPPent), 7.44-7.51 (m, 8H, C-H of P-Ar), 7.55-7.61 (m, 8H, C-H of P-Ar).

¹⁹F{¹H} NMR (471 MHz, 23 °C, CDCl₃): δ -61.19 (s).

³¹P{¹H} NMR (202 MHz, 23 °C, CDCl₃): δ -14.60 (s).

¹³C{¹H} NMR (126 MHz, 23 °C, CDCl₃): δ 25.5 (d, ²J_{CP} = 15.9 Hz, CH₂ of DPPent), 27.6 (d, ¹J_{CP} = 12.3 Hz, CH₂ of DPPent), 32.5 (t, ³J_{CP} = 12.9 Hz, CH₂ of DPPent), 124.1 (q, ¹J_{CF} = 272.4 Hz, CF₃), 125.4 (m, C-H of P-Ar), 131.1 (q, ²J_{CF} = 32.7 Hz, C-CF₃), 133.1 (d, ²J_{CP} = 18.5 Hz, C-H of P-Ar), 143.2 (d, ¹J_{CP} = 16.7 Hz, C of P-Ar).

Preparation of [bis(triphenylphosphino)(η⁶-(1-isopropyl-4-methylbenzene))hydridoruthenium] trifluoromethanesulfonate (2.4-PF₆). Compound **2.4-PF₆** was synthesized according a reported procedure⁶⁰ from [(*p*-cymene)RuCl₂]₂.⁶¹

Preparation of [bis(triphenylphosphino)(η⁶-(1-isopropyl-4-methylbenzene))hydridoruthenium] trifluoromethanesulfonate (2.4-OTf). Compound **2.4-OTf** was prepared by a variant of the procedure for **2.4-PF₆**. AgOTf was substituted for AgPF₆, two molar equivalents of PPh₃ were used per ruthenium, and isopropanol was substituted for methanol. Single crystals were obtained by storage of a concentrated Et₂O/methanol solution of **2.4-OTf** at -35 °C.

^1H NMR (500 MHz, 23 °C, CDCl_3): δ -9.69 (t, $^2J_{\text{HP}} = 37.8$ Hz, 1H, Ru-*H*), 1.38 (d, $^3J_{\text{HH}} = 6.9$ Hz, 6 H, CH-(CH_3)₂), 2.30 (s, 3 H, CH_3), 2.85 (quint, $^3J_{\text{HH}} = 6.9$ Hz, 1H, CH-(CH_3)₂), 4.50 (d, $^3J_{\text{HH}} = 5.9$ Hz, 2H, C-H of arene), 4.88 (d, $^3J_{\text{HH}} = 5.9$ Hz, 2H, C-H of arene), 7.17-7.43 (m, 30H, C-*H* of PPh_3).

$^{31}\text{P}\{^1\text{H}\}$ NMR (202 MHz, 23 °C, CD_2Cl_2): δ 52.6 (s).

III. FORMATION OF A DELOCALIZED IRIDIUM BENZYLIDENE WITH AZAQUINONE METHIDE CHARACTER VIA ALKOXYCARBENE CLEAVAGE

Portions of this chapter were reprinted with permission from Zhang, Y.; Mueller, B. R. J.; Schley, N. D. Formation of a Delocalized Iridium Benzylidene with Azaquinone Methide Character via Alkoxy-carbene Cleavage. *Organometallics* **2018**, 37 (12), 1825–1828. Copyright 2018 American Chemical Society.

Introduction

The ubiquitous role of alkyl ethers as solvents stems from their low cost and relative inertness to oxidation, cleavage, or functionalization. As a result, selective catalytic methods for the functionalization of ethers are somewhat limited. The in situ conversion of ethers to their corresponding alkoxy-carbenes via α,α -dehydrogenation at a late transition metal center is one promising avenue for ether activation; however, existing systems for this transformation largely rely on ether activation at electron-rich, neutral iridium complexes which give iridium alkoxy-carbenes with low intrinsic reactivity.^{62–65}

Our research group has been exploring ether dehydrogenation at cationic metal centers with the aim of developing systems capable of ether conversion to reactive, electrophilic alkoxy-carbenes in a catalytic manifold. Our approach has led us to examine cationic bis(phosphine)iridium complexes, which we have shown engage in reversible α -hydride insertion/elimination to interconvert α -alkoxyalkyl and alkoxy-carbene functionalities.^{22,66}

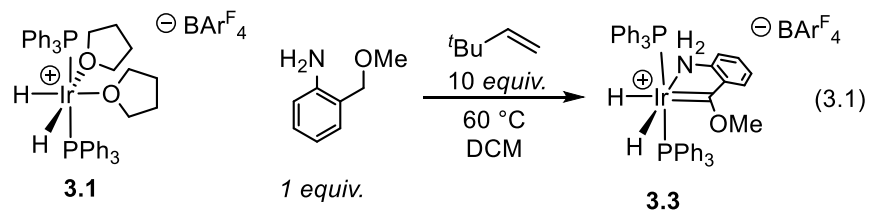
We now find that alkoxy-carbene formation can be extended to an intermolecular example via a Lewis base directed approach. In this case, reversible α -hydride insertion into the resulting alkoxy-carbene enables C–O cleavage in the formation of an iridium benzylidene with significant azaquinone methide character. Delocalized benzylidenes of this type have recently been explored

in the context of a search for an iron olefin metathesis catalyst.⁶⁷ Our findings demonstrate that these highly delocalized carbenes can participate in C–C bond forming reactions reminiscent of electrophilic metal carbenes.

Results and Discussion

Synthesis of cationic alkoxy-carbenes via ether dehydrogenation

Intermolecular ether dehydrogenation to give cationic alkoxy-carbenes remains a challenging transformation.^{19,21} For that reason, we initially targeted the dehydrogenation of 2-(methoxymethyl)aniline as a likely precursor for an isolable alkoxy-carbene resulting from Lewis base directed α,α -dehydrogenation of the benzyl ether moiety. Activation of bis(solvent) complex **3.1** by dehydrogenation with tert-butylethylene (TBE) in the presence of 2-(methoxymethyl)aniline (**3.2**) gives the desired cationic alkoxy-carbene complex **3.3** (eq 3.1). The cationic alkoxy-carbene so obtained displays a very long M–C bond length of 1.997(8) Å, consistent with reduced back-bonding relative to known neutral iridium(III) alkoxy-carbenes, which typically show M–C bond lengths between 1.86 and 1.92 Å (Figure 3.1 and Table 3.1).^{68,18,69–71}



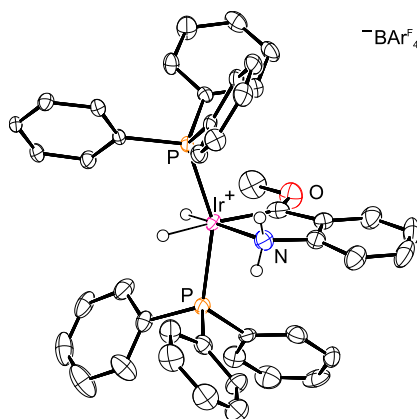


Figure 3.1. ORTEP of complex **3.3**. Ellipsoids are shown at 50% probability.

The alkoxy carbene ligand in **3.3** results from an oxidative addition– α -hydride elimination sequence that is known to be reversible in certain cases.^{19,22,68} Using acetonitrile to trap the intermediate α -alkoxyalkyl monohydride provided ¹H NMR evidence for this complex: a new doublet appeared at 4.91 ppm, which was attributed to the α -hydrogen (Figure 3.2). The appearance of this signal occurs concurrently with the disappearance of the hydride resonance at -10.33 ppm. Other tightly-binding dative ligands such as carbon monoxide, tert-butylisocyanate, and cyclohexylisocyanate showed similar resonances at 4.92, 4.78, and 4.77 ppm, respectively. In all cases, the structure of the resulting product was not able to be verified by X-ray crystallography.

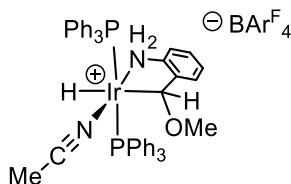


Figure 3.2. Proposed structure of **3.3** adduct with acetonitrile.

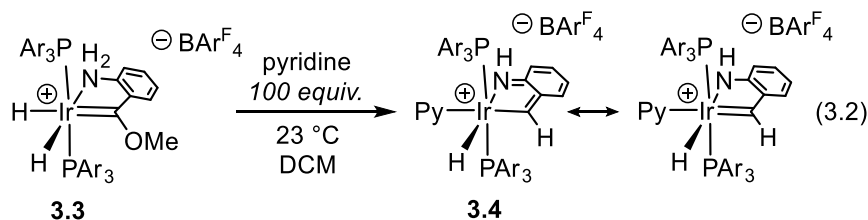


Table 3.1. Selected bond lengths from X-ray data in Å.

	Ir-N	Ir-C ₁	C ₁ -C ₂	C ₂ -C ₃	N-C ₃	C ₁ -R
3.3	2.203(5)	1.997(8)	1.486(11)	1.387(11)	1.459(9)	1.309(6)
3.4	2.132(4)	2.005(4)	1.372(6)	1.480(6)	1.301(6)	
3.5	2.102(4)	2.034(5)	1.422(8)	1.432(8)	1.327(7)	1.354(7)
3.6	2.130(5)	2.025(6)	1.382(9)	1.450(8)	1.316(7)	1.528(9)

Base-induced C-O bond cleavage

Interestingly, addition of excess pyridine to complex **3.3** gives a new monohydride complex, **3.4**. This complex displays a downfield-shifted ¹H resonance at 10.2 ppm, and its formation coincides with the appearance of a ¹H NMR signal consistent with free methanol. We were able to determine the structure of complex **3.4** by single-crystal X-ray diffraction (Figure 3.3). Elimination of methanol from **3.3** gives the corresponding formal amidoiridium benzylidene; however, a careful inspection of the bond metrics provided by the X-ray data reveals an alternate description (Table 3.1). A contraction of the exocyclic C-C bond from 1.486(11) Å in **3.3** to 1.372(6) Å in complex **3.4** is indicative of substantial double-bond character. On this basis as well as clear evidence for isolated diene-like distortion of the aryl ring, complex **3.4** can be formulated as an iridium benzylidene having significant iridium(III) azaquinone methide character. This contributing structure may also be considered as a vinylogous aminocarbene.⁷² DFT calculations (M06L/def2-SVP:(CHNO)/TZVP:(PIr)) are consistent with this description, reproducing the

observed bond metrics and suggesting a HOMO that is largely ligand-centered with metal–ligand π^* character (Figure 3.4). Accordingly, the observed M–C bond of 2.005(4) Å in **3.4** is at least 0.1 Å longer than those of known authentic Ir(III) benzylidenes.⁷³

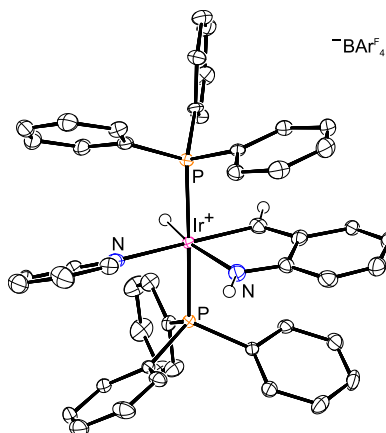


Figure 3.3. ORTEP of complex **3.4**. Ellipsoids are shown at 50% probability.

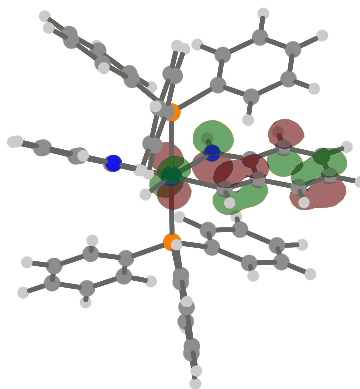


Figure 3.4. Depiction of the HOMO of **3.4** (isovalue = 0.06 e⁻/Å³).

A survey of the literature reveals only a few crystallographically characterized complexes for which an o-azaquinone methide resonance structure is appropriate. Complexes of Ir, Ru, and Fe have been prepared and in the last two cases were examined for their potential role in olefin metathesis. Synthesis of a ruthenium amidobenzylidene complex has been achieved through a metathesis route from the vinyl aniline.⁷⁴ Although the parent amido complex was not crystallized,

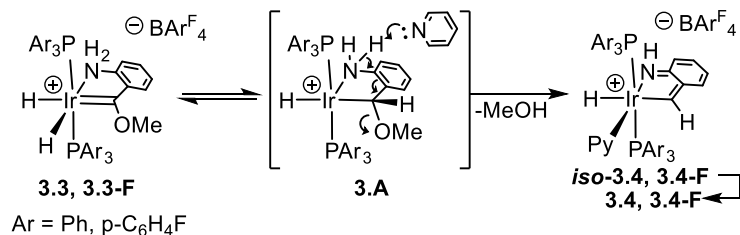
a look at N-tert-butylcarbamoyl derivatives shows modest distortion in the arene and a contracted exocyclic C–C bond on the order of 1.42 Å. Wolczanski has prepared a neutral amidoiron benzylidene by nucleophilic addition to a cationic precursor.⁶⁷ They identified the azaquinone methide resonance form as contributing some Fe(II) character to the formally Fe(IV) benzylidene, which is supported by a slightly contracted exocyclic C–C bond distance of 1.420(2) Å. By comparison, the exocyclic C–C bond in complex **3.4** is significantly shorter than in these examples, suggesting a more extreme distortion away from a classic benzylidene structure.

Two closely related diiridium o-azaquinone methides have been prepared from 2,6-dialkylanilines.⁷⁵ These complexes have bond metrical parameters similar to those of **3.4** but display methine ¹H chemical shifts near 6.5 ppm indicative of vinylic character. By comparison, the methine protons resonate at 10.2 ppm for **3.4**, suggesting a structure intermediate between benzylidene and vinylic. These observed chemical shifts are in line with an iridapyrrole previously characterized by Carmona.⁷⁶

The delocalized electronic structure of **3.4** no doubt contributes to its ease of synthesis by C–O bond cleavage in the precursor alkoxy carbene. C–O bond cleavage of alkoxy carbenes has been observed but occurs via nucleophilic dealkylation to give a metal acyl.^{77,78} In contrast, methanol elimination in **3.3** must occur by a distinct mechanism. Initial, reversible α -hydride insertion is believed to generate the α -alkoxyalkyl intermediate **3.A**.^{19,22} This species presumably undergoes a base-promoted vinylogous elimination reaction via deprotonation of the aniline (Scheme 3.1).

Both acid- and base-promoted elimination reactions of free o-aminobenzyl alcohol derivatives are known; however, the resulting free azaquinone methides are too reactive to be isolated.^{79,80} Alternatively, C–O bond cleavage could occur by α -methoxide elimination from

alkoxyalkyl intermediate **3.A**; however, this mechanism requires an open site and would be expected to suffer from inhibition by excess pyridine (vide infra).

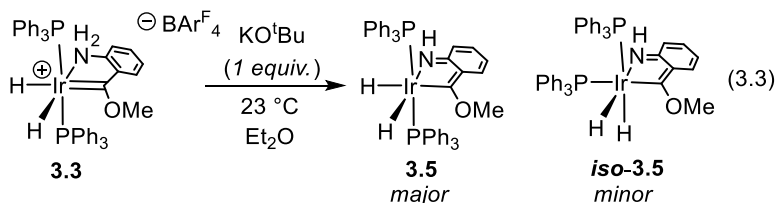


Scheme 3.1. Proposal for formation of **3.4** via pyridine-promoted elimination from α -alkoxyalkyl intermediate **3.A**.

Kinetic analysis of the formation of a related complex, **3.4-F**, reveals several features consistent with the mechanistic proposal given in Scheme 3.1. **3.4-F** is the tris(4-fluorophenyl)phosphine derivative of **3.4**. The series of tris(4-fluorophenyl)phosphine complexes was developed alongside the triphenylphosphine complexes with Dr. Yuanyuan Zhang, and are denoted here by appending -F to the compound number for the parent triphenylphosphine complex. The consumption of **3.3-F** is found to be first order in pyridine. An intermediate is observed by ^{31}P NMR; however, its appearance coincides with MeOH formation. We have tentatively assigned it as the isomeric species *iso-3.4-F*, in which the hydride is trans to the benzylidene. This species converts to **3.4-F** on standing. Even in the presence of excess pyridine, **3.4-F** appears to be stable with respect to hydride insertion and binding of a second equivalent of pyridine. Studies on the parent compound **3.3** also provide evidence for formation of the analogous intermediate *iso-3.4*. C–O bond cleavage in both cases appears to be irreversible, as addition of excess methanol to **3.4** or **3.4-F** does not result in conversion back to **3.3** or **3.3-F**, respectively. Furthermore, when **3.4** or **3.4-F** are treated with excess methanol- d_4 at room temperature, neither the metal hydride nor the vinylic proton appears to undergo H/D exchange.

Formation of a neutral iridium alkoxy-carbene

Although the hydride insertion product **3.A** is not observed experimentally, elimination via direct deprotonation of the amine ligand in complex **3.3** can be ruled out. Treatment of **3.3** with potassium tert-butoxide in the absence of pyridine does not lead to C–O bond scission; instead, it gives the neutral amido complex **3.5** as a mixture of cis (*iso-3.5*) and trans (**3.5**) phosphine isomers in a ratio of 0.19:1 (eq 3.3). **3.5** also shows some quinone-like distortion, although to a lesser extent than for **3.4** (Figure 3.5, left, and Table 3.1). Crucially, alkoxy-carbene **3.5** does not lose methanol on standing.



Although previous examples of metal benzylidenes with azaquinone methide character were prepared with olefin metathesis in mind, they appear to be less reactive than conventional benzylidenes. Wolczanski's Fe(IV) benzylidenes do not show reactivity with olefins,⁶⁷ and related ruthenium complexes are similarly inert in the absence of exogenous acid, suggesting that the reactivity of the benzylidene is modulated by the amido protonation state.⁸¹ In this context we examined reactions of **3.4** with ethylene under the assumption that the quinone-like distortion in **3.4** would lead to reactivity distinct from that of authentic iridium benzylidenes.

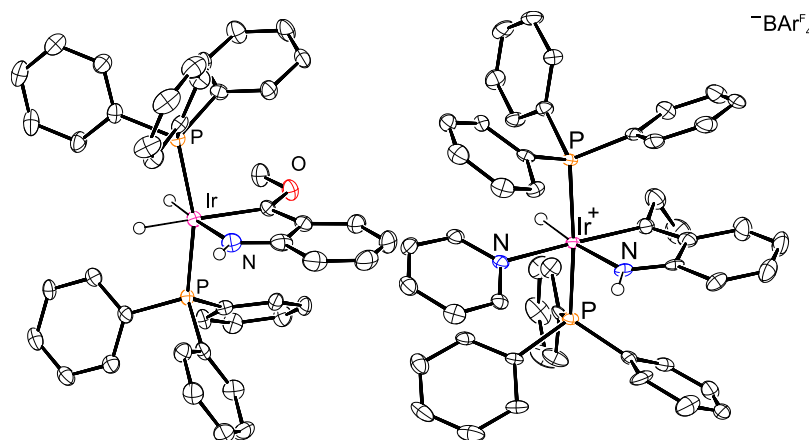
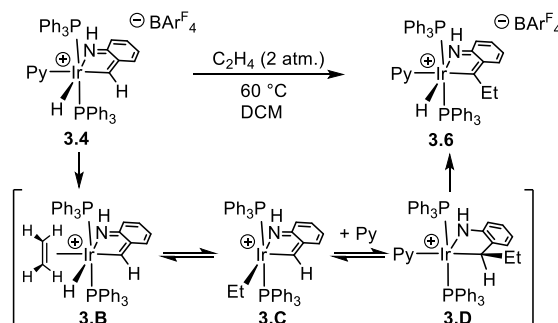


Figure 3.5. ORTEPs of complexes **3.5** (left) and **3.6** (right). Ellipsoids are shown at 50% probability.

Ethylene insertion into iridium benzylidene

Complex **3.4** reacts with ethylene to give a single new monohydride product with loss of the downfield vinylic ^1H NMR signal. We have been able to characterize this product as complex **3.6**, resulting from the formal insertion of ethylene into the vinylic C–H bond (Scheme 3.2).

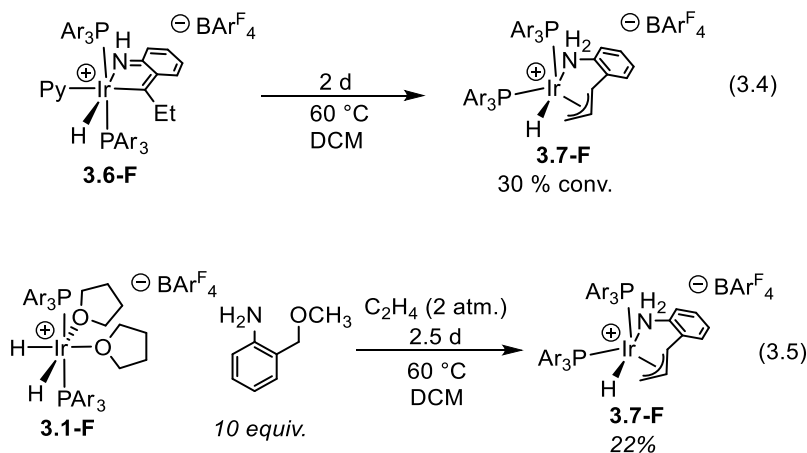


Scheme 3.2. Proposed mechanism for formation of **3.6**.

We considered three plausible mechanisms for C–C bond formation in **3.6**. Insertion of alkyl ligands into electrophilic benzylidenes is a classic reaction and has been observed for an authentic cationic iridium(III) ethylidene.⁸² Alternatively, the direct addition of electrophilic methylenes to olefins to give alkylidenes (“hydrocarbation”) has been previously demonstrated by Casey.^{83–85} A third possibility would be insertion of the azaquinone methide Ir–C bond into the

bound olefin followed by isomerization of the resulting primary alkyl to **3.6**. In our case alkylation is believed to occur via the sequence shown in Scheme 3.2. Initial 1,2-insertion of the hydride ligand into ethylene gives an iridium ethyl (**3.C**), which undergoes α -alkyl insertion (**3.D**) followed by α -hydride elimination. A similar mechanism may be operative in a related case involving olefin insertion into a cationic iridium aminocarbene prepared by Crabtree;⁸⁶ however, they favor a mechanism involving C–C bond formation via reductive elimination of an iridium ethyl and an α -aminoalkyl,⁸⁶ a route unavailable to the monohydride complex **3.4**.

Once formed, the ethylbenzylidene complex **3.6** is apparently stable for weeks in solution. However, it was noted that in the corresponding fluorinated complex, **3.6-F**, isomerization occurs upon standing. Heating over 2 days forms **3.7-F**, which was characterized as an η^3 -allyl complex (eq 3.4). The parent compound, **3.6**, was not observed to undergo a similar isomerization. While initial efforts to apply these processes to catalytic reactions of 2-(methoxymethyl)aniline were unsuccessful, **3.7-F** can be formed in low yield directly from **3.1-F** without the requirement of tert-butylethylene or pyridine. Presumably the excess ethylene and 2-(methoxymethyl)aniline serve as substitutes for these reagents, respectively (eq 3.5).



Stoichiometric reactions of iridium alkoxy-carbenes

With alkoxy-carbene complex **3.3** in hand, we sought to explore the reactivity beyond C-O bond cleavage. Reactions in which alkoxy-carbenes act as electrophiles were of particular interest. Work from the Hermida-Ramón group has shown that an iridium alkoxy-carbene complex was able to undergo aminolysis with ammonia to convert to the corresponding aminocarbene.²⁴ Coupled with reversible carbene formation from ethers, such a reaction could be used as method to directly interconvert amines and ethers.

When a solution of **3.3** in dichloromethane was treated with n-butylamine, an immediate color change was observed. This red compound was not able to be characterized, but the continued presence of a signal associated with the methoxy group indicated that aminolysis had not occurred. The color change in this reaction is likely attributable to a small amount of **3.4** being generated due to the basicity of the primary amine. Further experiments with methanol-*d*₄ were used to ascertain the susceptibility of the alkoxy-carbene in complex **3.3** to nucleophilic attack. Unfortunately, no deuterium incorporation was observed upon heating with deuterated methanol. This result, in which there is no strong thermodynamic preference for either form of the methoxy group, indicated that there was a high kinetic barrier to alkoxide exchange.

In lieu of the desired electrophilic reactivity, the ability of complex **3.3** to react with oxidants was explored. It has been reported that certain iridium alkoxy-carbene complexes undergo group transfer^{62,87} and oxygen atom transfer reactions.^{20,88} We reasoned that in the absence of electrophilic activity, reactions with oxidants or nitrene equivalents might transform the carbene bond. Following the work of the Piers group, we explored the iradepoxidation of the M-C bond in **3.3**. Using N₂O was not effective, and showed no reactivity by ³¹P NMR until heating at 50 °C slowly decomposed **3.3**. Likewise, no reaction was observed between molecular oxygen (1 atm)

and **3.3** at room temperature. Finally, catalytic oxidation of **3.2** with N-methylmorpholine N-oxide (NMO) in the presence of **3.1** at 60 °C for 5 hours did oxidize the complex; GC-MS and ³¹P NMR data both indicated the presence of triphenylphosphine oxide. This result demonstrated that NMO was perhaps too strong of an oxidant to be compatible with this system.

We also tested the reactivity with nitrene precursors, curious to see if there would be “iridaaziridination.” Reaction between **3.3** and azobenzene did not show any change by ³¹P NMR in the presence or absence of blue light. Tosyl iminoiodinane was also tested as a nitrene precursor, but caused apparent degradation of **3.3** without generating an isolable product. Taken together with the lack of electrophilicity of **3.3**, the lack of reactivity towards oxidants seems to indicate that the electronics of this system are intermediate between the nucleophilic neutral iridium (I) carbenes and the more electrophilic cationic iridium (III) complexes.

Ether-directed alkoxy-carbenes

Throughout this work, the intramolecular C-H activation that lead to alkoxy-carbene formation was amine-directed. Although this is likely a weaker interaction than what is found in previous work using phosphine directing groups²², the primary amine group is still a relatively strong directing group that leads to stable organometallic products. In the context of developing future catalytic reactions, a weaker directing group will aid in the dissociation of product, allowing the catalyst to turn over. We therefore proposed the use of an ethereal directing group for this chemistry.

Thus, we sought to synthesize compound analogous to **3.3** using 2-(methoxymethyl)anisole (**3.8**). The room temperature reaction between **3.8** and **3.1** in the presence of TBE in dichloromethane provided a relatively pure alkoxy-carbene product, **3.9**, by ³¹P NMR. The reactivity observed at room temperature is in contrast to the reactivity of **3.2**, which required

elevated temperatures for formation of the corresponding alkoxy carbene. Complex **3.9** was characterized by X-ray crystallography, which revealed a long Ir-C bond of 2.031(4) Å. This elongated Ir-C bond reflects once again the reduced backbonding observed in **3.3**.

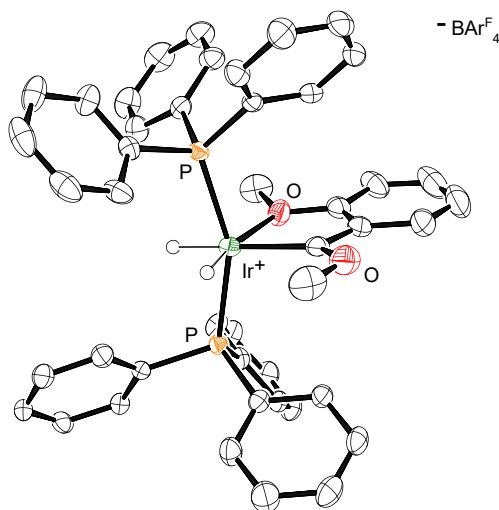


Figure 3.6. ORTEP of complex **3.9**. Ellipsoids are shown at 50% probability.

Closer comparison of the NMR spectra of both the reaction mixture and of the crystals of **3.9** showed that although **3.9** had formed, it was a minor product whose isolation was a fortunate outcome. When the reaction was repeated in benzene-*d*₆, the only crystalline product obtained was that of a bis(phosphine)iridium (I) η^6 -arene complex. The chemical shifts of this complex and of the major product in dichloromethane were quite similar, leading us to speculate that the major product in dichloromethane was the η^6 -arene of **3.8**. Further NMR experiments indicated that **3.9** could be formed by heating, but the putative arene complex persisted as a major byproduct. More distressingly, the synthesis was reproduced poorly on larger scales; when efforts were made to isolate **3.9**, the resulting crude material did not match with either known compound by ³¹P NMR. While we were not able to undertake any studies on the isolated alkoxy carbene complex, it remains an interesting potential target for future studies of Lewis base-directed alkoxy carbene formation.

Catalytic reactions

The observation of reactivity associated with a proposed α -alkoxyalkyl monohydride complex **3.A** generated interest in developing reactivity around this intermediate. One type of transformation that could be explored is directed alkane borylation.⁸⁹ Undirected borylation of primary benzylic C-H bonds has been shown to proceed through similar intermediates resulting from benzylic C-H oxidative addition.⁹⁰ The resulting borylated products are versatile intermediates which can be further cross-coupled to introduce a wide variety of functionality.⁹¹ As such, we explored the possibility of catalytic borylation of 2-(methoxymethyl)aniline (**3.2**) and 2-(methoxymethyl)anisole (**3.8**) with common borylation reagents bis(pinacolato)diboron (B_2pin_2) and pinacolborane (HBpin). These reagents are both known to generate metal boryl ligands, which can reductively eliminate with metal alkyls to release an alkyl borane.

Preliminary stoichiometric reactions between **3.3** and B_2pin_2 generated an unidentified major product by ^{31}P NMR, prompting a further investigation of the catalytic activity. The organic products of catalytic experiments using **3.1** and **3.3** were characterized by gas chromatography-mass spectrometry (GC-MS). In all experiments, tert-butylethylene was employed to dehydrogenate the iridium dihydride, forming a reduced metal complex that is able to oxidatively add the borylation reagents. In the presence of **3.3**, no borylated products were observed from the reaction between B_2pin_2 and either **3.2** or **3.8** either at 50 °C or 80 °C. Experiments with HBpin and in other solvents were similarly unsuccessful. In one experiment run in dichloromethane with HBpin, an unknown quantity of benzyl methyl ether, the product of reductive demethoxylation, was observed by GC-MS, although the significance of this observation is not clear. When 1,2-difluorobenzene or dichloromethane were employed as solvent with B_2Pin_2 , reactions heated to 50-80 °C showed only residual **3.2** and free pinacol by GC-MS. Analogous reactions with HBpin

gave similar outcomes, though without release of pinacol. In all, no borylated products were detected from any of the catalytic reactions run with HBpin or B₂pin₂.

In addition to borylation, hydroalkylation of alkynes was explored as a possible mode of catalytic reactivity of this system. Coordination of an alkyne to putative complex **3.A** would allow for migratory insertion of the alkoxyalkyl ligand into the bound alkyne.⁹² Further reductive elimination of the newly formed vinyl ligand with the remaining hydride would release the hydroalkylated product. Both **3.2** and **3.8** were tested as substrates in the presence of **3.1** and tert-butylethylene. Terminal alkynes (phenyl acetylene and 1-hexyne) provided only dimers as minor products, while an internal alkyne, 3-hexyne, did not react at all. Direct reactions between alkynes and **3.3** showed the same pattern, with 1-hexyne dimerizing, and 3-hexyne showing no reactivity.

Conclusion

In summary, a Lewis base directed approach has enabled α,α -dehydrogenation of an o-aminobenzyl ether. The resulting alkoxy-carbene dihydride undergoes an unusual base-promoted elimination reaction resulting in C–O bond scission to give a delocalized iridium benzylidene. X-ray and DFT studies demonstrate a substantial distortion toward an azaquinone methide structure. This cationic iridium azaquinone methide is found to be reactive toward ethylene in the formation of a new ethylbenzylidene. This transformation demonstrates an unusual strategy for C–C bond formation via C–O bond cleavage and supports a role for azaquinone methide-like benzylidenes as reactive species accessible from o-aminobenzyl ethers.

In addition to these demonstrated results, the reactivity of the alkoxy-carbene complex **3.3** was explored, showing a lack of expected reactivity towards electrophiles and oxidants. Neither catalytic borylation of **3.2** and **3.8** nor the hydroalkylation of alkynes with these compounds

showed the desired results. Finally, we were able to show the synthesis of an ether-directed alkoxy carbene, although further efforts will be required in order to fully characterize its reactivity.

Future Directions

More recent work from our research group has focused on the use of pincer ligands for the synthesis and reactivity of alkoxy carbenes.⁸⁷ These pincer ligands impart increased thermal stability, but their tridentate binding mode precludes the use of directing groups for intramolecular ether activation. Nevertheless, some preliminary work has been undertaken in the synthesis of a pincer ligand that is expected to generate highly electrophilic carbenes. This cationic PNP ligand has a central triazolium moiety which is expected to exhibit strong π -acidity, reducing the ability of the metal to stabilize the alkoxy carbene through backbonding.⁹³ This should give a more electrophilic alkoxy carbene, although no carbene complexes of this ligand have yet been synthesized.

The formal conversion of a C-O bond to a C-C is certainly intriguing, but the low yield for the one-pot conversion of **3.1-F** to **3.7-F** demonstrates the difficulty in translating this reaction to a catalytic manifold. Even a high-yielding conversion of **3.1** to **3.6** would not address the issue of turnover- there is no obvious mechanism by which the ligand will be released from the metal center.

The reactivity of the 2-(methoxymethyl)anisole-derived carbene is one of the more intriguing directions to pursue moving forward. The reliable isolation of the alkoxy carbene remains challenging, but the successful crystallization indicates that isolation is not an unattainable goal. With **3.9** in hand, stoichiometric experiments can be conducted in pursuit of catalytic reactivity. Importantly, the lack of acidic protons on the directing group compared to **3.3** will allow

the use of stronger, more basic nucleophiles to react directly with the alkoxy carbene. While the lack of observed stability of **3.9** will make such a study relatively challenging, it may also contribute to more robust reactivity and more facile catalytic turnover.

Experimental Section

General Considerations. All syntheses and manipulations were carried out using standard vacuum, Schlenk, cannula, or glovebox techniques under N₂ unless otherwise specified. Tetrahydrofuran, dichloromethane, pentane, and diethyl ether were degassed with argon and dried over activated alumina using a solvent purification system. The following chemicals were purchased from commercial vendors and used as received: IrCl₃·3H₂O, tri(4-fluorophenyl)phosphine, triphenylphosphine, pyridine, hydrogen gas, and ethylene gas (≥ 99.5%).

Spectroscopy. ¹H, ¹³C and ³¹P NMR spectra were recorded on Bruker NMR spectrometers at ambient temperature unless otherwise noted. ¹H and ¹³C chemical shifts are referenced to residual solvent signals; ³¹P chemical shifts are referenced to an external H₃PO₄ standard. ¹³C assignments were made with the assistance of 2D methods.

X-ray Crystallography. X-ray crystallographic data were collected on a Rigaku Oxford Diffraction Supernova diffractometer. Crystal samples were handled under immersion oil and quickly transferred to a cold nitrogen stream.

Elemental Analysis. Elemental analyses of complexes **3.1**, **3.3**, **3.4**, **3.5**, and **3.6** are of the bulk samples for which yields are reported. No additional purification operations are carried out prior to packaging for analysis, but samples are dried under vacuum for *ca.* 2 days to remove residual or co-crystallized solvent. Elemental analyses were performed at the University of Rochester CENTC Elemental Analysis Facility.

Preparation of [(PPh₃)₂IrH₂(THF)₂]BAr^F₄ (3.1**).** A 20 mL vial was charged with [(PPh₃)₂Ir(COD)]BAr^F₄ (0.4288 g, 0.25 mmol) and 4 mL of tetrahydrofuran then sealed with a

PTFE-lined septum cap. The solution was cooled to 0 °C and H₂ was bubbled through the solution while stirring for 15 minutes, causing a color change from red to pale yellow. After 15 minutes, the solution was diluted with 12 mL of dry pentane using a syringe. The vial was brought into an inert atmosphere glove box and its contents transferred to a 40 mL vial. The solution was evaporated under vacuum to yield a yellow residue. This material was treated with 8 mL of pentane which was evaporated under vacuum to give a pale yellow foam. This process was repeated 5 times. The solid was dried under vacuum to give the product as an off-white solid. Yield: 0.3602 g (82%). Single crystals of **3.1** were obtained by vapor diffusion of pentane into a 1:1 pentane:ether solution of **3.1** at -25 °C. Elemental Analysis for C₇₆H₆₀BF₂₄IrO₂P₂: C, 52.88; H, 3.50. Found C, 52.95; H, 3.51.

¹H NMR (500 MHz, 23 °C, CD₂Cl₂): δ -28.32 (br, 2H, Ir-*H*), 1.41 (br, 8H, THF), 3.38 (br, 8H, THF), 7.44-7.57 (m, 30 H), 7.58 (br, 4H, C-*H* of BAr^F₄), 7.75 (br, 8H, C-*H* of BAr^F₄)

³¹P{¹H} NMR (202 MHz, 23 °C, CD₂Cl₂): δ 26.39 (s).

¹³C{¹H} NMR (125 MHz, 23 °C, CD₂Cl₂): δ 25.85 (br, CH₂-O of THF), 72.63 (br, C-H of THF), 117.90 (m, C-H of BAr^F₄), 125.03 (q, ¹J_{CF} = 273.5 Hz, CF₃ of BAr^F₄), 129.19 (q, ²J_{CF} = 31.3 Hz, C of BAr^F₄), 129.43 (t, ³J_{CP} = 4.8 Hz, C-H of PPh₃), 131.75 (C-H of PPh₃), 132.27 (t, ¹J_{CP} = 27.0 Hz, C of PPh₃), 134.02 (t, ²J_{CP} = 6.1 Hz, C-H of PPh₃) 135.23 (C-H of BAr^F₄), 162.20 (q, ¹J_{CB} = 49.5 Hz, B-C of BAr^F₄).

Preparation of complex 3.3. A 20 mL glass vial was charged with [(PPh₃)₂Ir(THF)₂H₂]BAr^F₄ (0.338 g, 0.196 mmol) and 2-(methoxymethyl)aniline (0.027 g, 0.20 mmol, 1 equiv.) in 10 mL dichloromethane. After stirring for thirty minutes, the volatiles were removed under reduced pressure. The oily residue was redissolved in 4 mL diethyl ether and dried

under reduced pressure twice to ensure complete removal of THF resulting from the precursor. The resulting residue was then dissolved in 10 mL dichloromethane and treated with tert-butylethylene (0.166 g, 1.96 mmol, 10 equiv.) and this solution was heated for 3 hours at 60 °C. Removal of the volatiles under reduced pressure gave a residue which was crystallized by dissolution in 3 mL of a 1:1 solution of diethyl ether and pentane followed by storage at -35 °C to give the product as a yellow crystalline solid. Yield: 0.268 g (80%). Elemental Analysis for $C_{76}H_{53}BF_{24}IrNOP_2$: C, 53.16; H, 3.11; N, 0.82. Found: C, 53.48; H, 3.20; N, 0.78.

1H NMR (600 MHz, 23 °C, CD_2Cl_2): δ -19.07 (td, $^2J_{HP} = 24.5$ Hz, $^2J_{HH} = 4.3$ Hz, 2H, Ir-*H*), -10.33 (td, $^2J_{HP} = 32.4$ Hz, $^2J_{HH} = 4.6$ Hz, 1H, Ir-*H*), 3.60 (s, 3H, CH_3), 4.04 (s, 2H, NH_2), 6.89 (d, $^3J_{HH} = 7.9$ Hz, 1H, N- C_6H_4), 7.32 (m, 13H, C-*H* of PPh_3 & N- C_6H_4), 7.38 (t, $^3J_{HH} = 7.5$ Hz, 12H, C-*H* of PPh_3), 7.45 (t, $^3J_{HH} = 7.2$ Hz, 6H, C-*H* of PPh_3), 7.48 (d, $^3J_{HH} = 6.3$ Hz, 1H, N- C_6H_4), 7.55 (s, 4H, C-*H* of BAr^F_4), 7.66 (d, $^3J_{HH} = 7.8$ Hz, 1H, N- C_6H_4), 7.73 (m, 8H, C-*H* of BAr^F_4).

$^{31}P\{^1H\}$ NMR (121 MHz, 23 °C, CD_2Cl_2): δ 20.57 (s).

$^{13}C\{^1H\}$ NMR (126 MHz, 23 °C, CD_2Cl_2): δ 70.53 (OCH_3), 117.88 (m, C-*H* of BAr^F_4), 123.37 (C-*H* of $-C_6H_4-$), 125.01 (q, $^1J_{CF} = 272.6$ Hz, CF_3 of BAr^F_4), 126.38 (C-*H* of $-C_6H_4-$), 129.27 (q, $^2J_{CF} = 31.5$ Hz, C- CF_3 of BAr^F_4), 129.28 (t, $^3J_{CP} = 5.4$ Hz, C-*H* of PPh_3), 129.53 (C-*H* of $-C_6H_4-$), 131.61 (C-*H* of PPh_3), 132.90 (t, $^1J_{CP} = 28.5$ Hz, C of Ar), 133.40 (t, $^2J_{CP} = 6.4$ Hz, C-*H* of PPh_3), 135.21 (C-*H* of BAr^F_4), 135.47 (C-*H* of $-C_6H_4-$), 150.02 (C of Ar), 150.76 (C of Ar), 162.17 (q, $^1J_{CB} = 49.8$ Hz, B-*C* of BAr^F_4), 285.95 (Ir=C).

Preparation of complex 3.4. A 20 mL glass vial was charged with **3.3** (0.098 g, 0.057 mmol) and 3 mL of dichloromethane followed by pyridine (0.657 g, 5.7 mmol, 100 equiv.). The resulting solution was stirred at room temperature for 18 hours during which time the color

changed from yellow to reddish-orange. The volatiles were then removed under vacuum. Dissolution of the residue in 2 mL diethyl ether followed by evaporation twice gave the crude product free from excess pyridine. This residue was purified by storage of a saturated dichloromethane solution at -35 °C to give the product as reddish-orange crystals. Yield: 0.095 g, (94%). Elemental Analysis for $C_{80}H_{54}BF_{24}IrN_2P_2$: C, 54.46; H, 3.09; N, 1.59. Found: C, 54.66; H, 2.97; N, 1.64.

1H NMR (600 MHz, 23 °C, CD_2Cl_2): δ -14.22 (t, $^2J_{HP} = 15.6$ Hz, 1H, Ir-H), 5.92-5.95 (m, 2H, N- C_6H_4 -), 6.11 (d, $^3J_{HH} = 8.5$ Hz, 1H, N- C_6H_4 -), 6.32 (dd, $^3J_{HH} = 8.6$ Hz, $^3J_{HH} = 6.5$ Hz, 1H, N- C_6H_4 -), 6.63 (t, $^3J_{HH} = 6.8$ Hz, 2H, pyridine), 7.19 (t, $^3J_{HH} = 7.7$ Hz, 12H, C-H of PPh_3), 7.28 (m, 18H, C-H of PPh_3), 7.33 (t, $^3J_{HH} = 7.7$ Hz, 1H, pyridine), 7.56 (s, 4H, C-H of BAr^F_4), 7.74 (m, 9H, NH & C-H of BAr^F_4), 8.18 (d, $^3J_{HH} = 5.3$ Hz, 2H, pyridine), 10.15 (s, 1H, Ir-CH).

$^{31}P\{^1H\}$ NMR (121 MHz, 23 °C, CD_2Cl_2): δ 18.92 (s).

$^{13}C\{^1H\}$ NMR (151 MHz, 23 °C, CD_2Cl_2): δ 115.83 (C-H of $-C_6H_4-$), 117.88 (m, C-H of BAr^F_4), 119.50 (C-H of $-C_6H_4-$), 125.01 (q, $^1J_{CF} = 272.5$ Hz, CF_3 of BAr^F_4), 126.45 (C-H of pyridine), 128.46 (t, $^3J_{CP} = 5.5$ Hz, C-H of PPh_3), 128.60 (t, $^1J_{CP} = 28.1$ Hz, C-P of Ar), 129.29 (q, $^2J_{CF} = 31.7$ Hz, C- CF_3 of BAr^F_4), 130.97 (C-H of PPh_3), 132.14 (C-H of $-C_6H_4-$), 133.76 (t, $^2J_{CP} = 5.6$ Hz, C-H of PPh_3), 135.22 (C-H of BAr^F_4), 137.18 (C-H of pyridine), 138.35 (C-H of $-C_6H_4-$), 148.69 (C of Ar), 156.03 (C-H of pyridine), 162.17 (q, $^1J_{CB} = 49.8$ Hz, B-C of BAr^F_4), 176.66 (C of Ar), 200.49 (t, $^2J_{CP} = 7.4$ Hz, -CH-Ir).

Preparation of complex 3.5. A 20 mL vial was charged with **3.3** (0.147 g, 0.085 mmol), 3 mL of diethyl ether, followed by solid potassium *tert*-butoxide (0.0095 g, 0.085 mmol). The reaction mixture was stirred for 30 minutes at room temperature, during which time the color of

the solution changed from yellow to red and a precipitate formed. The supernatant was separated by filtration and the precipitate was washed with two 0.5 mL portions of diethyl ether. The combined organic extracts were evaporated to dryness and redissolved in 2 mL of THF. 4 mL of pentane was carefully layered on top of the THF solution and the mixture stored at -35 °C for 18 hours, giving the product mixture as red crystals. Yield: 0.069 g (89%). This method gives crystals suitable for X-ray diffraction. The product is formed as a mixture of two isomers **3.5** and *iso-3.5* in a ratio of 1:0.19. The isomers were inseparable by fractional crystallization. Elemental Analysis for C₄₄H₄₀IrNOP₂: C, 61.96; H, 4.73; N, 1.64. Found: C, 61.68; H, 4.79; N 1.49.

¹H NMR of **3.5** (600 MHz, 23 °C, CD₂Cl₂): δ -16.75 (td, ²J_{HP} = 18.3 Hz, ²J_{HH} = 2.8 Hz, 1H, Ir-*H*), -11.25 (td, ²J_{HP} = 22.1 Hz, ²J_{HH} = 3.8 Hz, 1H, Ir-*H*), 3.37 (s, 3H, -OCH₃), 5.41 (br, 1H, N-*H*), 5.84 (dd, ³J_{HH} = 7.9 Hz, ³J_{HH} = 6.8 Hz, 1H, N-C₆H₄-), 6.06 (d, ³J_{HH} = 8.6 Hz, 1H, N-C₆H₄-), 6.51 (dd, ³J_{HH} = 7.5 Hz, ³J_{HH} = 7.4 Hz, 1H, N-C₆H₄-), 6.87 (d, ³J_{HH} = 8.3 Hz, 1H, N-C₆H₄-), 7.31 (m, 18H, -C₆H₅), 7.46 (apparent q, 6.2 Hz, 12H, -C₆H₅).

³¹P{¹H} NMR of **3.5** (121 MHz, 23 °C, CD₂Cl₂): δ 17.21 (s).

¹³C{¹H} NMR (151 MHz, 23 °C, CD₂Cl₂): δ 67.27 (-OCH₃), 109.20 (N-C₆H₄-), 117.72 (N-C₆H₄-), 124.08 (N-C₆H₄-), 127.88 (t, ³J_{CP} = 4.8 Hz, C-H of PPh₃), 129.76 (C-H of PPh₃), 133.64 (C of Ar), 133.88 (N-C₆H₄-), 134.14 (t, ²J_{CP} = 6.3 Hz, C-H of PPh₃) 136.72 (t, ¹J_{CP} = 27.2, P-C of PPh₃), 175.26 (C of Ar), 266.65 (Ir=C).

¹H NMR of *iso-3.5* (600 MHz, 23 °C, CD₂Cl₂): δ -16.10 (m, 1H, Ir-*H*), -12.03 (dd, ²J_{HP} = 98.5 Hz, ²J_{HP} = 22.5 Hz, 1H, Ir-*H*), 3.77 (s, 3H, -OCH₃), 5.89 (br, 1H, N-*H*), 5.97 (dd, ³J_{HH} = 7.4 Hz, ³J_{HH} = 7.2 Hz, 1H, N-C₆H₄-), 6.43 (d, ³J_{HH} = 8.7 Hz, 1H, N-C₆H₄-), 6.63 (dd, ³J_{HH} = 7.7 Hz, ³J_{HH} = 7.3

Hz, 1H, N-C₆H₄-), 6.94 (m, 6H, -C₆H₅), 7.02 (m, 6H, -C₆H₅), 7.13 (d, ³J_{HH} = 8.3 Hz, 1H, N-C₆H₄-), 7.19 (m, 12H, -C₆H₅), 7.37 (m, 6H, -C₆H₅).

³¹P{¹H} NMR of *iso*-**3.5** (121 MHz, 23 °C, CD₂Cl₂): δ 6.92 (d, ²J_{PP} = 20.0 Hz), 8.95 (d, ²J_{PP} = 20.0 Hz).

Preparation of complex 3.6. A 50 mL heavy-walled glass vessel was charged with **3.4** (0.080 g, 0.045 mmol), 3 mL of dichloromethane and a stir bar. The vessel was degassed on a vacuum manifold by a freeze-pump-thaw cycle, and was then charged with two atmospheres of ethylene. The vessel was sealed and heated at 60 °C for 10 hours, during which time the solution changed color from reddish-orange to purple. (Safety note: The heating of pressurized, sealed glass vessels should only be done carefully in an unoccupied fume hood behind a polycarbonate blast shield.) After cooling, the volatiles were removed under vacuum to give a crude residue which was extracted with 3 mL diethyl ether and evaporated to dryness again. The crude purple solid was dissolved in 0.3 mL of a 1:1 solution of diethyl ether and pentane which was transferred into an open 4 mL vial. This vial was placed in an empty 20 mL vial that was sealed and stored at -35 °C. The solution crystallized on standing over 2 days at -35 °C to give the product as purple crystals. Yield: 0.060 g (74%). This method gives crystals suitable for X-ray diffraction. Elemental Analysis for C₈₂H₅₈BF₂₄IrN₂P₂: C, 54.95; H, 3.26; N, 1.56. Found: C, 54.78; H, 3.08; N, 1.66.

¹H NMR (500 MHz, 23 °C, CD₂Cl₂): δ -13.86 (t, ²J_{HP} = 15.4 Hz, 1H, Ir-H), 0.58 (t, ³J_{HH} = 7.6 Hz, 3H, -CH₃), 2.87 (q, ³J_{HH} = 7.6 Hz, 2H, -CH₂-), 6.03 (dd, ³J_{HH} = 8.6 Hz, ³J_{HH} = 6.2 Hz, 1H, N-C₆H₄-), 6.28 (d, ³J_{HH} = 8.9 Hz, 1H, N-C₆H₄-), 6.48 (d, ³J_{HH} = 8.4 Hz, 1H, N-C₆H₄-), 6.49 (br, 1H, NH), 6.63 (t, ³J_{HH} = 7.3 Hz, 1H, N-C₆H₄-), 7.16-7.30 (m, 32H, C-H of pyridine & PPh₃), 7.45 (br, 1 H, pyridine), 7.57 (s, 4H, C-H of BAr^F₄), 7.74 (s, 8H, C-H of BAr^F₄), 8.02 (d, ³J_{HH} = 4.5 Hz, 2H, pyridine).

$^{31}\text{P}\{^1\text{H}\}$ NMR (121 MHz, 23 °C, CD_2Cl_2): δ 13.18 (s).

$^{13}\text{C}\{^1\text{H}\}$ NMR (126 MHz, 23 °C, CD_2Cl_2) δ 16.23 (-CH₃), 38.97 (-CH₂-), 114.57 (C-H of -C₆H₄-), 117.89 (m, C-H of BAr^F₄), 120.80 (C-H of -C₆H₄-), 125.02 (q, $^1J_{\text{CF}} = 272.6$ Hz, CF₃ of BAr^F₄), 126.10 (C-H of -C₆H₄-), 126.28 (C-H of pyridine), 128.52 (t, $^3J_{\text{CP}} = 4.9$ Hz, C-H of PPh₃), 128.76 (t, $^1J_{\text{CP}} = 27.2$ Hz, C-P of PPh₃), 129.29 (q, $^2J_{\text{CF}} = 31.7$ Hz, C-CF₃ of BAr^F₄), 131.04 (C-H of PPh₃), 133.89 (t, $^2J_{\text{CP}} = 5.0$ Hz, C-H of PPh₃), 135.22 (C-H of BAr^F₄), 137.10 (C-H of pyridine), 137.94 (C-H of -C₆H₄-), 144.75 (C of Ar), 162.19 (q, $^1J_{\text{CB}} = 49.6$ Hz, B-C of BAr^F₄), 178.18 (C of Ar), 231.53 (Ir=C). The $^{13}\text{C}\{^1\text{H}\}$ resonance corresponding to the CH-N group of the bound pyridine is not observed due to broadening.

IV. SYNTHESIS OF SCS-PINCER LIGANDS FOR A LACTATE RACEMASE MODEL COMPLEX

Background and Introduction

Lactate racemase in Lactobacillus plantarum

Vancomycin is a powerful antibiotic which is active towards a broad range of gram-positive bacteria⁹⁴. It is often considered the drug of choice against antibiotic resistant infections such as methicillin-resistant *Staphylococcus aureus* (MRSA).⁹⁵ The mechanism of action for vancomycin is through disruption of the peptidoglycan cell wall of these organisms.⁹⁶ This cellular feature is formed through the crosslinking of layers of the polymer by peptide chains, which results in a rigid structure. Vancomycin acts by binding to this crosslink, specifically to the C-terminal D-Ala-D-Ala sequence.⁹⁶ The now-disrupted peptidoglycan is more porous, leaving the bacterium inside more susceptible to osmotic effects and cell lysis.⁹⁷

Lactobacillus is one of the very few genera of gram-positive bacteria with resistance to vancomycin.⁹⁸ This resistance is conferred by the incorporation of D-lactate at the C-terminus in place of the terminal alanine residue. The resulting D-Ala-D-Lac sequence has much lower affinity for vancomycin,⁹⁹ reducing the extent to which it permeabilizes the cell. In *Lactobacillus plantarum*, both enantiomers of lactate are produced by separate lactate dehydrogenases (LDH). Knockout experiments show that mutants lacking both LDHs become sensitive to vancomycin.⁹⁹ Interestingly, when the gene responsible for the production of D-LDH was knocked out, there was still a roughly 1:1 mixture of D-lactate and L-lactate. This result was attributed to the presence of a lactate racemase enzyme, which can provide the cell with the necessary enantiomer of lactate when

only the L-form is available. As such, lactate racemase plays an important role in maintaining vancomycin resistance in these organisms in the absence of D-lactate.

Lactate racemase active site

In 2015, the structure of the enzyme active site was characterized, revealing a unique cofactor (Figure 4.1).¹⁰⁰ The nickel is coordinated in a distorted square planar geometry: one coordination site is occupied by histidine, the two *cis* sites are occupied by the sulfur atoms of thioamide and thioacid groups, and the site *trans* to histidine is bound to nickel through C4 of a dihydropyridine ring.

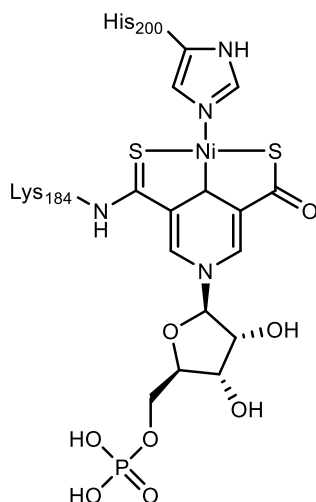


Figure 4.1. Active site of lactate racemase.

This structure is unique in that it is one of just nine known nickel-dependent enzymes and includes the only Ni-C bond between a metal center and cofactor.^{101,102} The only protein cofactor previously known to bind nickel is coenzyme F₄₃₀, which binds nickel in a reduced tetrapyrrole derivative.^{103,104} The metal center in lactate racemase is bound by a meridional tridentate ligand, which is more commonly described as a pincer ligand. While metal pincer complexes have been employed in synthetic inorganic chemistry quite effectively,^{105,106} this is the first, and thus far only, example of a pincer ligand binding mode for a transition metal in a biological system.^{100,102}

In addition to characterizing the active site, Hausinger and coworkers showed that the dihydropyridine ring is derived from nicotinic acid.¹⁰⁰ This structure is similar to the reducing agent NADH, hinting at a possible mechanism for the enzyme. Deprotonation of the alcohol group of lactate is hypothesized to trigger the abstraction of a hydride by the cofactor, oxidizing the lactate to pyruvate and generating the dihydropyridine form of the cofactor (Figure 4.2a). Subsequent reduction with this hydride in a non-stereospecific manner releases a racemized lactate and leaves the pyridinium form of the cofactor (Figure 4.2b).

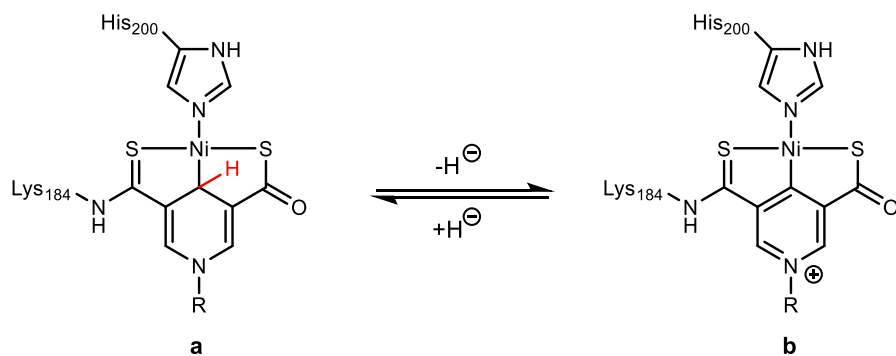


Figure 4.2. Structure of (a) reduced and (b) oxidized form of lactate racemase cofactor.

In order to gain a better understanding of the mechanism of this enzyme and its role in vancomycin resistance, as well as to potentially harness the reactivity of this new class of bifunctional ligand, the construction of a model complex was undertaken. This project began in March 2016, at which point no model complexes had been published. The model that was proposed (Figure 4.3) was designed with the intent to be as structurally faithful to the biological system as possible. The proposed complex retains all the ligands from the primary coordination sphere. The lysine residue is substituted by an analogous butyl chain in the thioamide moiety. The thioacid is retained, as is the dihydropyridine core. Addition of methyl groups at C₂ and C₆ are incorporated as part of the synthesis but are not anticipated to have a large impact on the metal center. Finally,

the ribose phosphate moiety is replaced by a phenyl group in order to reduce the potential electrophilicity of the pyridinium ion.

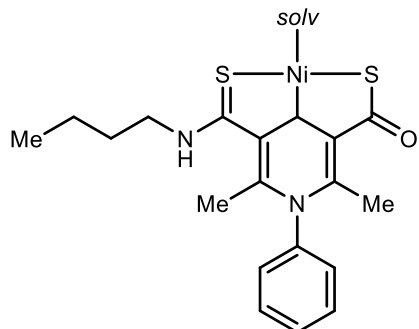


Figure 4.3. Proposed model complex of lactate racemase (**4.9**).

Since 2016, a pair of model complexes have been published which show modest activity towards alcohol dehydrogenation¹⁰⁷ and lactate racemization.¹⁰⁸ These complexes have symmetric pincer ligands, and attempt to prioritize the replication of the enzyme function over its structure (Figure 4.4). Even when reproducing the alcohol racemization activity of lactate racemase, final enantiomeric excess (ee) remained at 66%, with a turnover number of 3 and turnover frequency of $> 0.1 \text{ h}^{-1}$. Neither model faithfully mimics the net charge on the complex or the unsymmetrical structure. There remains a dearth of literature surrounding the synthesis of both structural models and of highly active functional models. The work described herein attempts to address this problem through the synthesis of a structural mimic of the lactate racemase active site.

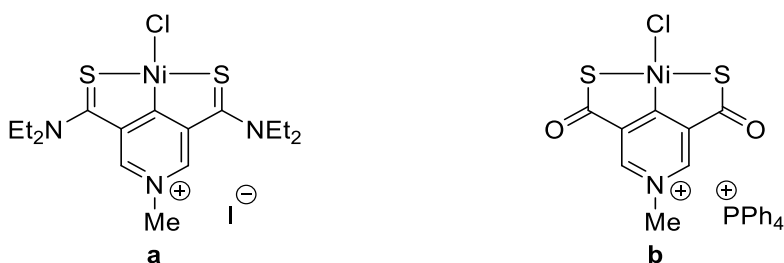
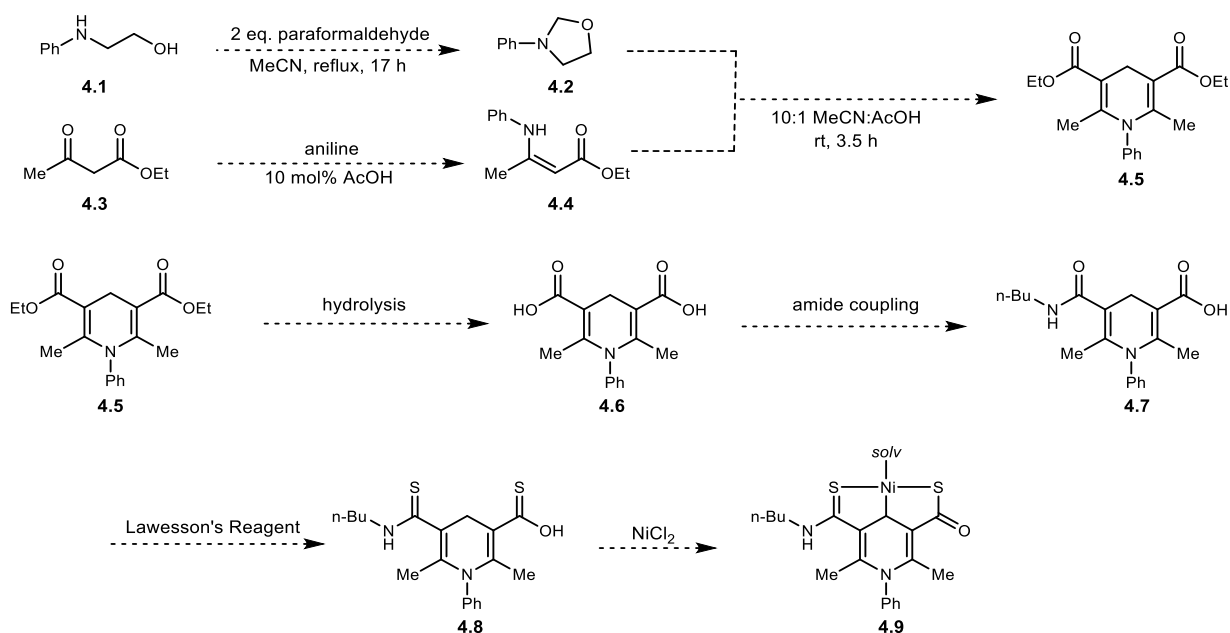


Figure 4.4. Published model complexes of lactate racemase as of 2021: (a) Shi et. al., 2017 (b) Xu et. al., 2019.

Synthesis of a Lactate Racemase Model Complex

Ligand synthesis

The proposed synthesis of the model complex is presented in Scheme 4.1. The synthesis of a previously characterized Hantzsch ester (**4.5**) is accomplished over 3 convergent steps.¹⁰⁹ From there, hydrolysis of the ester moieties would yield the corresponding dicarboxylic acid (**4.6**). Desymmetrization of **4.6** would be accomplished by amide coupling using 1 equiv. of amine. Subsequent thionation of **4.7** with Lawesson's reagent is proposed to convert both the amide and acid groups to the corresponding thioamide and thioacid groups, respectively. Finally, metalation of this ligand (**4.8**) will yield the proposed model complex (**4.9**).



Scheme 4.1. Proposed synthesis of model complex **4.9**.

The synthesis of Hantzsch ester **4.5** was achieved beginning from commercially available 2-(phenylamino)ethanol (**4.1**) and ethyl acetoacetate (**4.3**). **4.1** was cyclized with paraformaldehyde in refluxing acetonitrile to yield N-phenyloxazolidine (**4.2**) in good yield.^{110,111}

Condensation of aniline with **4.3** in acetic acid yielded the desired enamine (**4.4**).¹¹² Finally, the Hantzsch ester (**4.5**) was synthesized according to a literature procedure.¹⁰⁹

Initial attempts to hydrolyze **4.5** with potassium, sodium, and lithium hydroxides failed to generate the desired diacid **4.6**. Using Olah conditions for ester cleavage with trimethylsilyl chloride and sodium iodide¹¹³ was equally ineffective; however, these conditions were proposed to be more effective on a methyl ester. Using the same synthetic route, the methyl derivative, **4.12**, was synthesized. These conditions once again failed to cleave the methyl ester groups. Surprisingly, LiOH effectively produced a hydrolysis product, **4.13** (Scheme 4.2). Furthermore, only one of the two ester groups was hydrolyzed, even using six equivalents of hydroxide. The single hydrolysis event yielded an unsymmetrical product, a feature of the eventual desired product. The sluggish reactivity towards hydrolysis in this product was attributed to extensive delocalization of the π system (Figure 4.5). The use of lithium ion to increase the electrophilicity at one site is hypothesized to have an activating effect which enables the first hydrolysis event. However, upon cleavage, the resulting carboxylate anion is delocalized into the π system, further reducing the electrophilicity of the remaining ester group. This is proposed to be the reason for the unsymmetric product recovered from this hydrolysis step.

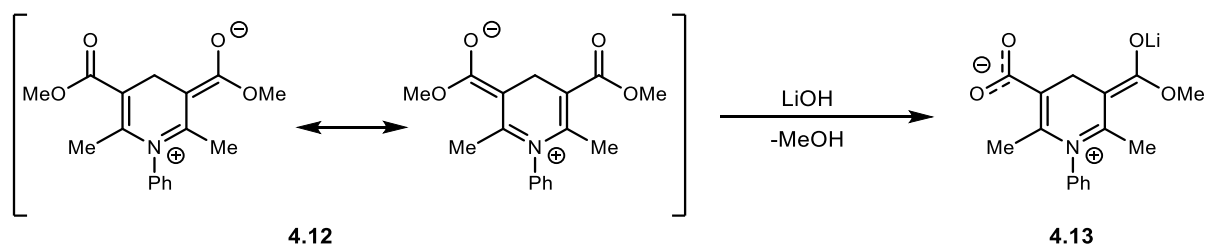


Figure 4.5. Proposed mechanism of unsymmetric hydrolysis of **4.12**.

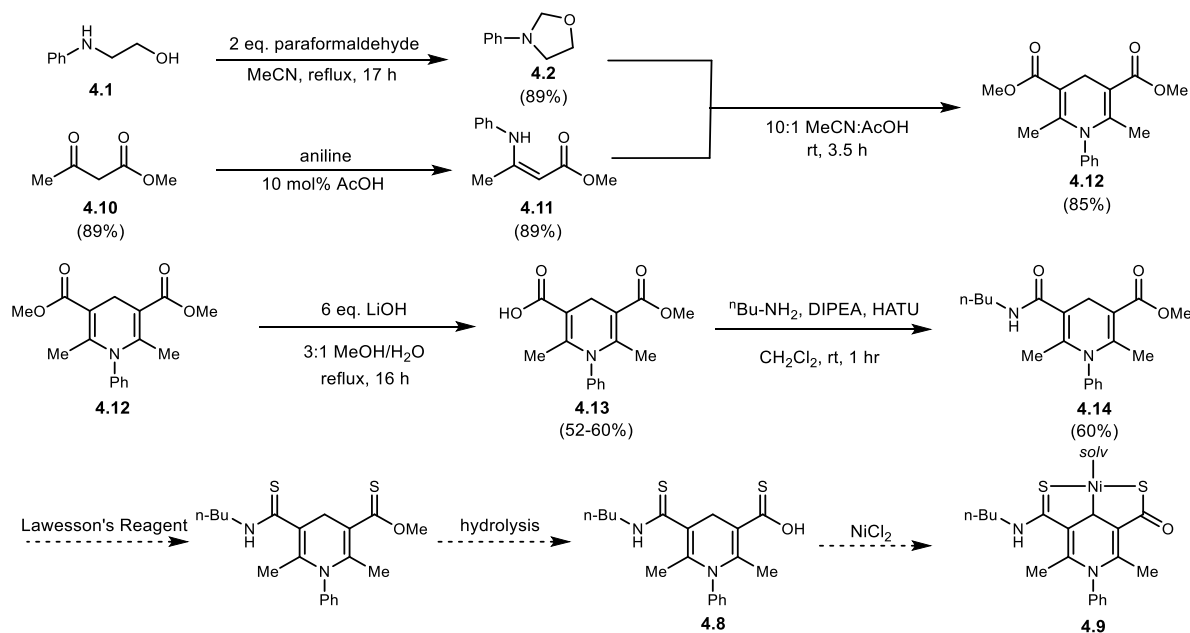
Although both acid groups were not cleaved, the asymmetry that was introduced into the molecule was considered an opportunity to proceed with a reliable route to desymmetrize the

ligand. Initial attempts were undertaken to convert the ester group to an amide using butyl amine, but no reactivity of the ester group was observed. Efforts were shifted to amide coupling reactions at the acid group. Common activating reagents such as ethylchloroformate and carbodiimide reagents (DCC, EDC) generally effected the conversion of starting material, but the desired product was not detected. When using HATU, the acid group was converted to the corresponding butyl amide (**4.14**).

Compound **4.14** represented a crossroads from which the amide and ester groups could be converted to the corresponding thionoester and thioamide or from which dealkylation of the ester could reveal the acid group prior to thionation. Dealkylation conditions including aluminum tribromide,¹¹⁴ trimethylsilyl chloride/sodium iodide, and lithium hydroxide were examined. These reactions generated mixtures of products that included unconverted starting material, but in no case was the desired product detected. This result was not totally unexpected—the lack of reactivity could be attributed to the same electronic effects that were hypothesized to be causing problems with the original dihydropyridine diester compounds **4.5** and **4.12**. Electron density from the amide nitrogen lone pair can delocalize into the C-O bond of the amide, which again pushes more of the pyridinyl nitrogen lone pair density onto the ester carbonyl system.

In the interest of conserving material, thionation conditions were tested on **4.12**. Lawesson's reagent¹¹⁵, P₄S₁₀, and elemental sulfur were each employed. In the latter two cases, only decomposition of **4.12** was observed. When using Lawesson's reagent, thionation did not occur, but isomerization from the 1,4-dihydropyridine to the 1,2-dihydropyridine was detected by ¹H NMR. Indeed, it has been previously observed by Vigante et. al. that unsubstituted 3,5-diethoxycarbonyl-1,4-dihydropyridines do not undergo thionation with Lawesson's reagent, which was attributed to their ability to be oxidized and low stability.¹¹⁶ Instead, they were able to thionate

the pyridine, and subsequently reduce to the corresponding dihydropyridine. Since either the pyridine or dihydropyridine form of the ligand would be a faithful model complex, a new synthetic route that centers on pyridine derivatives was developed. A summary of the final progress of the original route can be seen in Scheme 4.2.



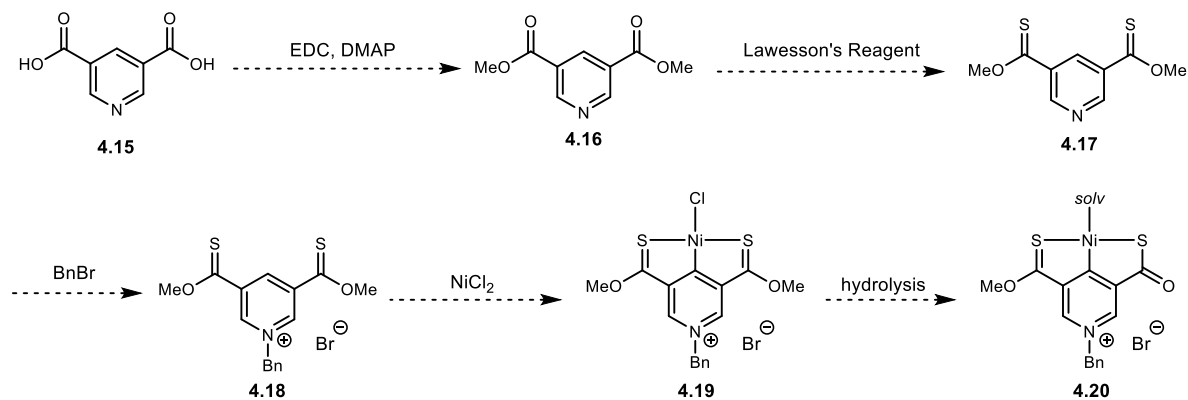
Scheme 4.2. Progress towards the synthesis of model complex 4.9.

Second-generation ligand synthesis

Given the hypothesis that the dihydropyridine was contributing to reduced electrophilicity, an alternate synthesis to obtain a modified model complex was devised. This complex maintains the SCS binding motif of the previous model, and of the cofactor, but the synthesis relies on the use of a pyridine ring in place of the dihydropyridine. The thioester is proposed to replace the thioamide due to the ease of synthesis, and the thioacid moiety is retained. The methyl groups at the C₂ and C₆ positions of the ring are not present in this model, matching the cofactor. The aromaticity of the ring throughout the synthesis was expected to reduce the conjugation with the carbonyl systems, allowing for more facile chemical manipulations. Finally, the pyridine is

unsubstituted at nitrogen, but in order to display the bifunctional capability of the cofactor, the pyridine must be alkylated to give the redox-active pyridinium ion.

The proposed synthesis (Scheme 4.3) begins with commercially available 3,5-pyridine dicarboxylic acid (**4.15**), the esterification of which will yield the corresponding dimethyl ester (**4.16**). Thionation of the ester groups generates the dithionoester (**4.17**). Alkylation of this compound with benzyl bromide will yield complex **4.18**, which can be metalated with a nickel (II) salt to provide complex **4.19**. Hydrolysis of one thionoester group affords complex **4.20**.



Scheme 4.3. Proposed synthesis of model complex **4.20**.

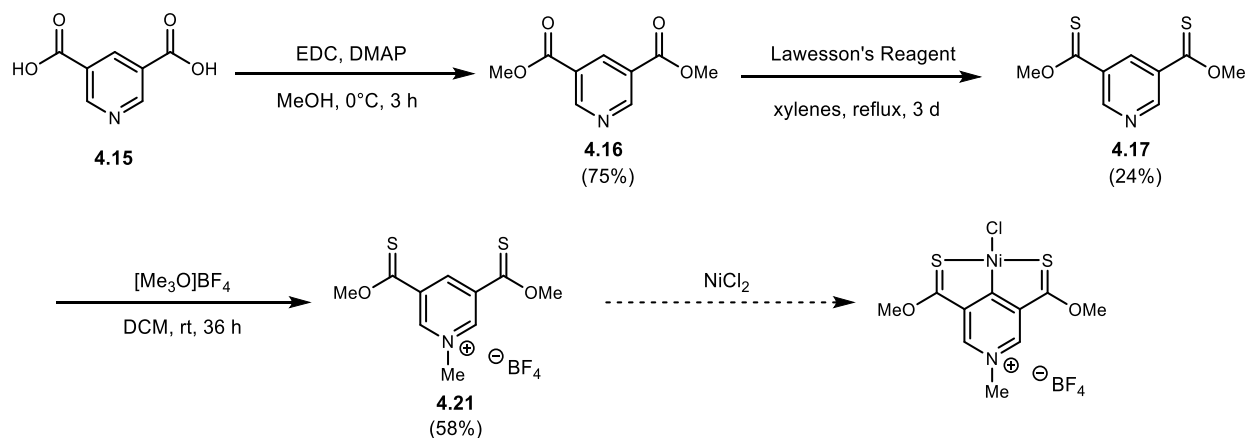
Initial Steglich esterification of 3,5-pyridine dicarboxylic acid (**4.15**) proceeded smoothly to afford the dimethyl ester derivative (**4.16**) according to a literature procedure.¹¹⁷ Thionation of **4.16** with Lawesson's reagent provided the desired dithionoester in low yield.¹¹⁶ Optimization of the conditions improved yields slightly, but increased temperatures and reaction times continued to return a mixture of starting material, and an intermediate product containing one thionoester and one ester group.

In order to match the bifunctional capability of the cofactor, alkylation of the pyridinyl nitrogen will be required to stabilize the lone pair in the reduced dihydropyridine form. Benzylation using benzyl bromide produced only trace amounts of the benzylated product. Methyl

iodide gave similarly low yields under a variety of conditions. This was presumably due to the relatively poor nucleophilicity of the pyridyl nitrogen, which is deactivated by a pair of electron-withdrawing substituents. Moving to a more powerful methylating reagent proved to be fruitful, as Meerwein's salt (trimethyloxonium tetrafluoroborate) was able to successfully methylate **4.17** in decent yield to afford **4.21**.

Metalation of second generation ligand

Both **4.17** and **4.21** represent potential ligands for nickel and both were subjected to metalation conditions. Metalation of **4.17** caused a color change and broadening of ^1H NMR signals typically associated with paramagnetic species in solution. When **4.21** was used as the ligand, nickel salts did not generate the desired complex, under various conditions. Nickel perchlorate and nickel nitrate were heated with **4.21** in acetonitrile, but no coordination was observed by ^1H NMR. Nickel chloride and bromide proved to be incompatible using toluene and ethanol as the solvents, returning only degradation products after heating. The metalation of palladium salts were also tested due to their increased activity towards aryl C-H activation.¹¹⁸ Palladium chloride showed little reactivity at low temperatures, and ligand degradation upon heating. The addition of base, or the use of acetate as the palladium counterion, generated new signals by ^1H NMR, but indicated the loss of the pyridinium methyl group.

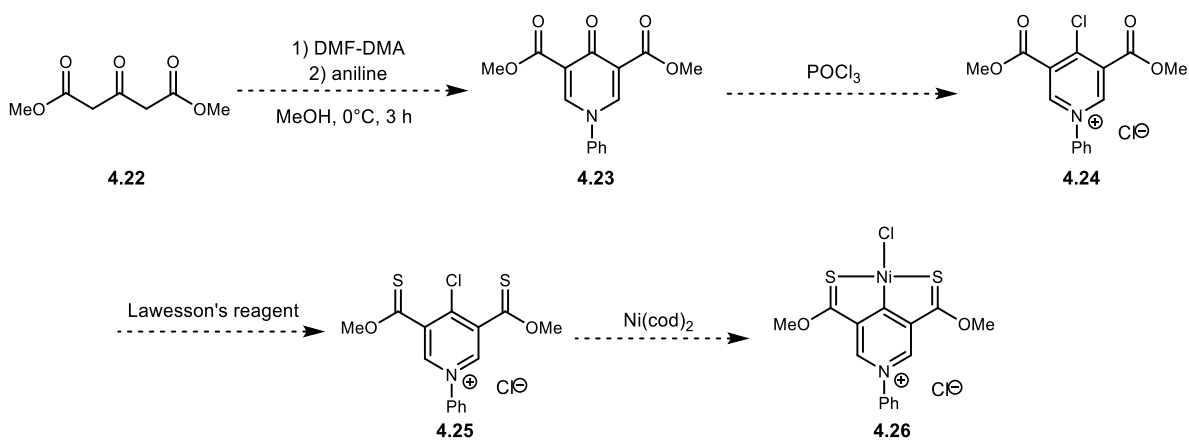


Scheme 4.4. Progress towards the synthesis of model complex **4.20**.

The difficulty metalating the C₄-H bond revealed an issue that would likely have plagued the first generation ligand as well: the challenging nature of the desired C-H activation with nickel. While not impossible, it represents a difficult transformation at a late stage, particularly using a nickel (II) precursor. Future iterations of this ligand can be made more amenable to metalation by introducing an aryl halide to facilitate Ni-C bond formation by oxidative addition.

Third-generation ligand synthesis

The difficulty in metalating **4.21** prompted the design of a ligand bearing a C-Cl bond. Further, the N-methyl group appeared to be a liability and was replaced by a phenyl group in the new ligand design. Scheme 4.5 outlines the proposed synthesis. The first step has literature precedent for the ethyl derivative and should be applicable to the methyl derivative. Chlorination with POCl₃ aromatizes the dihydropyridine ring of **4.23** to the 4-chloropyridinium. Thionation of the ester groups yields the corresponding dithionoester **4.25**. This ligand can be metalated with Ni(cod)₂ to form complex **4.26**.



Scheme 4.5. Proposed synthesis of model complex **4.26**.

Following a slightly modified literature procedure, **4.23** was able to be synthesized in moderate yield. Chlorination with POCl_3 showed inconclusive results which did not scale up well. When allowed to react with neat thionyl chloride, however, the chlorination proceeded smoothly in excellent yield to afford **4.24**.

Thionation of **4.24** with Lawesson's reagent was carried out in a microwave reactor.¹¹⁹ After 30 min at 100 °C, ^1H NMR of the crude product showed an upfield shift for the protons at C_2 and C_6 . This contrasts with the successful thionation of **4.16**, which had shown a modest downfield shift to the analogous protons in **4.17**. When examined by mass spectrometry, this reaction mixture showed the formation of a species with $m/z = 304$ (Figure 4.6). This could correspond with an $[\text{M}]^+$ ion of a cationic derivative which has lost chlorine and replaced two oxygen atoms with sulfur (Figure 4.6b) or an $[\text{M}+\text{H}]^+$ ion of a neutral derivative which has lost chlorine and gained one sulfur (Figure 4.6c). Based on the NMR evidence that the esters were not converted to thionoesters, it was hypothesized that the dihydropyridine is the product of the thionation reactions. This product would result from nucleophilic thionation and dearomatization, followed by loss of chloride. Thionation of all three carbonyl groups of **4.23** was proposed to avoid

losing the chloride, but treatment of **4.23** with Lawesson's reagent in xylenes caused degradation of the starting material.

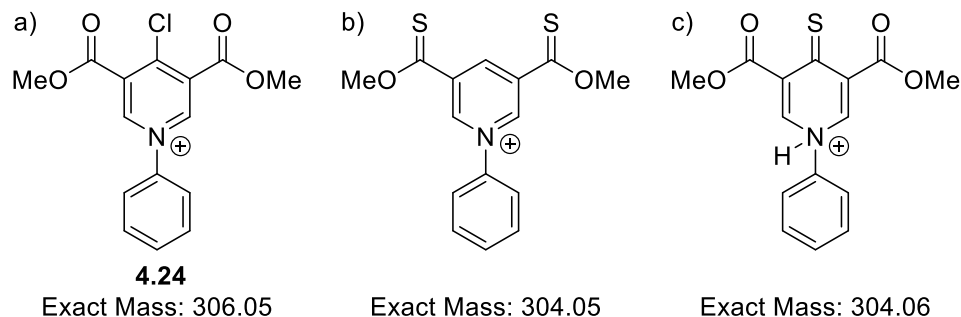
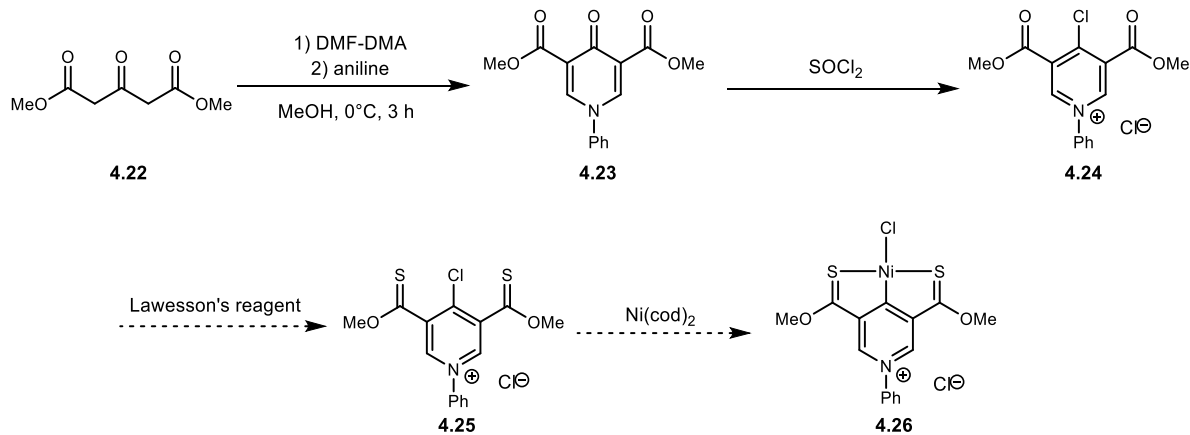


Figure 4.6. Plausible products of thionation of **4.24**.

Metalation of third generation ligand

Attempts at metalation of the **4.24** intermediate did not prove fruitful. Reaction with Ni(cod)₂ led to significant broadening of signals in the ¹H NMR spectrum attributed to paramagnetism of the sample. A reaction with palladium tetrakis(triphenylphosphine) in dichloromethane resulted in deposition of crystals of palladium bis(triphenylphosphine) dichloride. Even a successful metalation of **4.24** with a Pd (0) precursor would have provided a complex with only a passing resemblance to the active site of lactate racemase. The overarching weakness of this route was the N-aryl moiety, which was installed in the first step of the synthesis to provide a chemically inert group which provides stabilization of the dihydropyridine form. Unfortunately, this also made the aryl chloride susceptible to electrophilic attack. The lack of reactivity with **4.24** showed that further work on this route was unlikely to provide a desired product.



Scheme 4.6. Progress towards the synthesis of model complex **4.26**.

Conclusion

Each of three routes that were undertaken during this project had advantages and disadvantages when compared to each other. The first-generation ligand had the strongest structural similarities to the active site and was the only route in which a desymmetrized product was synthesized. However, the electronics of the dihydropyridine seemed to cause problems with substitution of the carbonyl groups and prevented some of the desired transformations that were expected to be more straightforward. The desymmetrization of **4.12**, while fortuitous, was an early indication of the atypical behavior observed around those carbonyl groups.

The second-generation route seemed to address some of the electronic pitfalls of the first-generation route. The published EDC coupling of **4.15** was an affirmation that these acid groups would display more typical behavior, and the thionation with Lawesson's reagent was successful, albeit in low yield. The failure of both **4.17** and **4.21** to undergo metalation was a signal that insertion across a C-H bond was not the most straightforward C-M bond formation. Overall, despite the ultimate failure to generate a metal complex from this ligand, the improvement in the predictability of the ligand behavior towards common reagents provided strong evidence for the

hypothesis around the electronics of the dihydropyridines employed in the first-generation ligand synthesis.

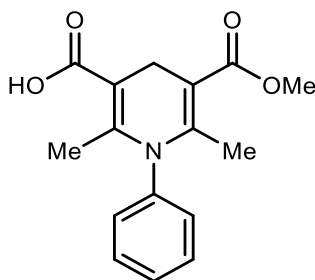
Finally, the third-generation route was designed to facilitate oxidative addition by incorporating a C-Cl bond at C₄. The chloride was able to be incorporated, but the N-aryl pyridinium group became a liability during the thionation conditions by promoting putative dechlorination. While **4.25** would be expected to metalate more readily than the analogous compounds such as **4.17** and **4.21**, the route that was followed did not allow access to **4.25**. That **4.24** did not metalate certainly argues against this point, but it is reasonable to expect that low valent nickel and palladium precursors would bind preferentially to the softer sulfur sites in **4.25**. Although this route did not provide the desired metal complex, it did successfully demonstrate the redox activity of the pyridinium/dihydropyridine functional group pair, a key feature of the proposed mechanism of the enzyme active site.

In 2017, the Hu group published a model complex¹⁰⁷ that effected stoichiometric dehydrogenation of benzyl alcohol. The synthesis of this complex was similar to the second-generation route beginning with a 4-chloropyridine. Further, the thionation step came before the alkylation of the pyridyl nitrogen, preventing the dechlorination that was observed in the third-generation synthesis. The successful synthesis validates the approach taken herein, while also highlighting how important the order of transformations is in these systems.

The aromatization of **4.23** and subsequent dearomatization of **4.24** shows that there is some ability of this ligand to switch between the two oxidation states. It is plausible that this type of ligand can catalyze the racemization of alcohols, or other reactions which rely on a similar hydrogen borrowing scheme. A limited number of pincer complexes bearing what has been termed a “reverse pyridine” motif have been reported.^{107,108,120–123} Thus far, only one such complex has

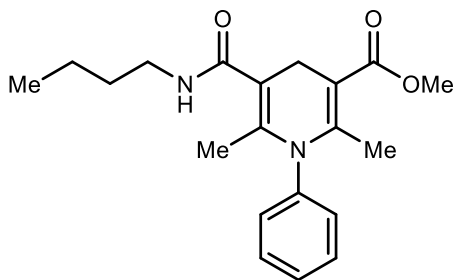
exhibited catalytic activity based on bifunctional hydride transfer, racemizing lactate.¹⁰⁸ The attention brought about by the characterization of the lactate racemase active site is quantifiable—four of the six reports of these complexes have come since 2016, including two that are model complexes. As methods to synthesize this type of complex mature, it is fair to expect that a further increase in both the quantity and the utility of this class of complex will be seen in the literature.

Experimental Section



Preparation of 5-(methoxycarbonyl)-2,6-dimethyl-1-phenyl-1,4-dihydropyridine-3-carboxylic acid (4.13). A 250 mL round bottom flask was charged with Hantzsch ester **4.12** (520 mg, 1.73 mmol, 1.0 equiv.) and lithium hydroxide (244 mg, 10.19 mmol, 6.0 equiv.) in 72 mL of a 3:1 mixture of methanol/water. The flask was heated at 85 °C for 18 hours. The solvent was subsequently removed by rotary evaporation, and the residue was redissolved in water. The solution was acidified to a pH of approximately 1, resulting in the precipitation of the product. The product was filtered, dissolved in dichloromethane, and dried with Na₂SO₄. The solvent was removed by rotary evaporation and the product was dried under vacuum. Yield: 281 mg (57%).

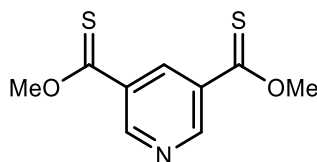
¹H NMR (400 MHz, 23 °C, *d*₆-DMSO): δ 1.84 (s, 3H, -CH₃), 1.85 (s, 3H, -CH₃), 3.26 (s, 2H, CH₂), 3.62 (s, 3H, -OCH₃), 7.31-7.33 (m, 2H, -C₆H₅), 7.44-7.51 (m, 3H, -C₆H₅), 12.00 (bs, 1H, -COOH).



Preparation of methyl 5-(butylcarbamoyl)-2,6-dimethyl-1-phenyl-1,4-dihydropyridine-3-carboxylate (4.14). A 500 mL flask was charged with **4.13** (281 mg, 0.97

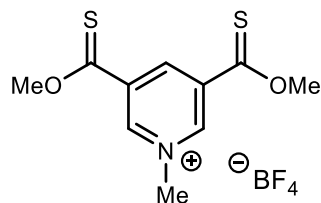
mmol, 1.0 equiv.), n-butylamine (78 mg, 1.07 mmol, 1.1 equiv.), diisopropylethylamine (277 mg, 2.14 mmol, 2.2 equiv.), and HATU (371 mg, 0.97 mmol, 1.0 equiv.) in 150 mL dichloromethane. The reaction mixture was stirred for 2 hours and quenched with a saturated solution of sodium bicarbonate. The aqueous layer was extracted with dichloromethane three times. The combined organic layers were dried with Na₂SO₄ and evaporated by rotary evaporation. The crude product was purified by column chromatography to afford the title compound. Yield: 200. mg (60%).

¹H NMR (400 MHz, 23 °C, CDCl₃): δ 0.94 (t, 3H, ³J_{HH} = 7.3 Hz, CH₃ of butyl), 1.37 (m, 2H, ³J_{HH} = 7.7 Hz, -CH₂- of butyl), 1.53 (m, 2H, ³J_{HH} = 7.3 Hz, -CH₂- of butyl), 1.73 (s, 3H, CH₃ of dihydropyridine), 1.93 (s, 3H, CH₃ of dihydropyridine), 3.32 (m, 2H, ³J_{HH} = 7.5 Hz, -CH₂- of butyl), 3.35 (s, 2H, CH₂ of dihydropyridine), 3.71 (s, 3H, OCH₃), 5.54 (s, 1H, NH), 7.12-7.16 (m, 2H, -C₆H₅), 7.36-7.43 (m, 3H, -C₆H₅).



Preparation of dimethyl pyridine-3,5-bis(carbothioate) (4.17). A 500 mL round bottom flask was charged with dimethyl pyridine-3,5-bis(carboxylate) (9.52 g, 48.8 mmol, 1.00 equiv.) and Lawesson's reagent (24.3 g, 60.1 mmol, 1.23 equiv.) in 250 mL dry xylenes. The mixture was heated to reflux for 3 days. The solvent was removed by rotary evaporation, and the resulting brown oil was flushed through a plug of silica. The resulting yellow oil was further purified by column chromatography to yield a yellow solid. Yield: 2.667 g (24%).

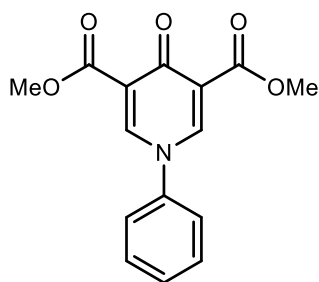
¹H NMR (400 MHz, 23 °C, CDCl₃): δ 4.35 (s, 6H, -OCH₃), 9.07 (t, ⁴J_{HH} = 2.2 Hz, 1H, C-H of pyridine), 9.46 (d, ⁴J_{HH} = 2.2 Hz, 2H, C-H of pyridine).



Preparation of 3,5-bis(methoxycarbonothioyl)-1-methylpyridinium tetrafluoroborate (4.21). A 100 mL round bottom flask was charged with dithionoester (200. mg, 0.88 mmol, 1.0 equiv.) and trimethyl oxonium tetrafluoroborate (147 mg, 0.99 mmol, 1.12 equiv.) in 35 mL of dichloromethane. The reaction was stirred at room temperature for 36 hours, at which point the solvent was removed by rotary evaporation. The resulting oil was dissolved in a minimal amount of dichloromethane, and product was crystallized by the slow addition of diethyl ether. The crystals were filtered and dried under vacuum. Yield: 168 mg (58%).

^1H NMR (400 MHz, 23 °C, CD_2Cl_2): δ 4.43 (s, 6H, $-\text{OCH}_3$), 4.61 (s, 3H, $\text{N}-\text{CH}_3$), 9.46 (d, $^4J_{\text{HH}} = 1.6$ Hz, 2H, C-*H* of pyridine), 9.67 (t, $^4J_{\text{HH}} = 1.6$ Hz, 1H, C-*H* of pyridine).

$^{13}\text{C}\{^1\text{H}\}$ NMR (101 MHz, 23 °C, CD_2Cl_2): δ 50.3, 61.3, 136.9, 143.1, 146.7, 201.9.

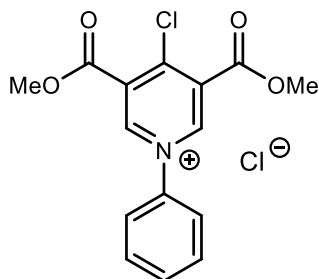


Preparation of dimethyl 4-oxo-1-phenyl-1,4-dihydropyridine-3,5-dicarboxylate (4.23). A 250 mL round bottom flask was charged with dimethyl-1,3-acetonedicarboxylate (7.239 g, 41.6 mmol, 1.00 equiv.) and dimethylformamide dimethylacetal (20.04 g, 168.2 mmol, 4.04 equiv.) in 36 mL of 100% ethanol. The reaction was heated to reflux for 3 hours. After cooling,

the solvent was removed by rotary evaporation. The remaining material was dissolved in 80 mL of methanol. Aniline (5.81 g, 62.4 mmol, 1.5 equiv.) was added and the reaction mixture was heated to reflux for an additional 3 hours. Approximately 25% of the solvent was removed by rotary evaporation and the remaining solution was stored overnight at -20 °C overnight to induce crystallization. The crystals were filtered and dried under vacuum. Yield: 7.216 g (60%).

^1H NMR (400 MHz, 23 °C, d_6 -DMSO): δ 3.75 (s, 6H, -OCH₃), 7.50-7.54 (m, 1H, -C₆H₅), 7.57-7.60 (m, 2H, -C₆H₅), 7.66-7.68 (m, 2H, -C₆H₅), 8.43 (s, 2H, C=CH).

^1H NMR (400 MHz, 23 °C, d_6 -DMSO): δ 51.8, 122.2, 123.4, 128.9, 129.9, 142.2, 143.8, 164.3, 170.0.



Preparation of 4-chloro-3,5-bis(methoxycarbonyl)-1-phenylpyridinium chloride (4.24). A 20 mL scintillation vial was charged with 4-oxoDHP (1.187 g, 4.13 mmol, 1.00 equiv.) and 7 mL thionyl chloride (11.5 g, 96.5 mmol, 24.0 equiv.) and stirred for 16 hours with an exit bubbler. Excess thionyl chloride was removed by vacuum through a trap containing an aqueous solution of sodium bicarbonate. Trace amounts of remaining thionyl chloride were removed by trituration with dichloromethane. Yield: 1.41 g (100%).

^1H NMR (400 MHz, 23 °C, CD₂Cl₂): δ 4.08 (s, 6H, -OCH₃), 7.75-7.77 (m, 3H, -C₆H₅), 8.06-8.08 (m, 2H, -C₆H₅), 9.56 (s, 2H, C-H of pyridinium).

V. REFERENCES

- 1 J. W. Walton and L. A. Wilkinson, In *Organometallic Chemistry: Volume 42*; The Royal Society of Chemistry, 2019; Vol. 42, pp 125–171.
- 2 E. P. Kundig and Bottcher, A., *Transition metal arene π -complexes in organic synthesis and catalysis*, Springer-Verlag, Berlin, New York, 2004.
- 3 M. Rosillo, G. Domínguez and J. Pérez-Castells, *Chem. Soc. Rev.*, 2007, **36**, 1589–1604.
- 4 D. R. Buckle, S. J. Collier and M. D. McLaws, in *Encyclopedia of Reagents for Organic Synthesis*, American Cancer Society, 2005.
- 5 R. H. Crabtree, *The Organometallic Chemistry of the Transition Metals*, John Wiley & Sons, Inc., Hoboken, New Jersey, 6th edn.
- 6 Y.-P. Li, Z.-Q. Li and S.-F. Zhu, *Tetrahedron Lett.*, 2018, **59**, 2307–2316.
- 7 A. G. Sergeev and J. F. Hartwig, *Science*, 2011, **332**, 439–443.
- 8 N. I. Saper and J. F. Hartwig, *J. Am. Chem. Soc.*, 2017, **139**, 17667–17676.
- 9 M. Utsunomiya and J. F. Hartwig, *J. Am. Chem. Soc.*, 2004, **126**, 2702–2703.
- 10 J. Takaya and J. F. Hartwig, *J. Am. Chem. Soc.*, 2005, **127**, 5756–5757.
- 11 S. Takemoto, E. Shibata, M. Nakajima, Y. Yumoto, M. Shimamoto and H. Matsuzaka, *J. Am. Chem. Soc.*, 2016, **138**, 14836–14839.
- 12 H. Amii and K. Uneyama, *Chem. Rev.*, 2009, **109**, 2119–2183.
- 13 S. J. Blanksby and G. B. Ellison, *Acc. Chem. Res.*, 2003, **36**, 255–263.
- 14 V. A. Pistritto, M. E. Schutzbach-Horton and D. A. Nicewicz, *J. Am. Chem. Soc.*, 2020, **142**, 17187–17194.
- 15 K. H. Dötz and J. Stendel, *Chem. Rev.*, 2009, **109**, 3227–3274.
- 16 K. Miki, S. Uemura and K. Ohe, *Chem. Lett.*, 2005, **34**, 1068–1073.
- 17 H. Le Bozec, K. Ouzzine and P. H. Dixneuf, *Organometallics*, 1991, **10**, 2768–2772.
- 18 O. Boutry, E. Gutierrez, A. Monge, M. C. Nicasio, P. J. Perez and E. Carmona, *J. Am. Chem. Soc.*, 1992, **114**, 7288–7290.
- 19 H. F. Luecke, B. A. Arndtsen, P. Burger and R. G. Bergman, *J. Am. Chem. Soc.*, 1996, **118**, 2517–2518.
- 20 M. T. Whited and R. H. Grubbs, *J. Am. Chem. Soc.*, 2008, **130**, 5874–5875.
- 21 J. Meiners, A. Friedrich, E. Herdtweck and S. Schneider, *Organometallics*, 2009, **28**, 6331–6338.
- 22 Y. Zhang and N. D. Schley, *Chem. Commun.*, 2017, **53**, 2130–2133.
- 23 U. Klabunde and E. Otto. Fischer, *J. Am. Chem. Soc.*, 1967, **89**, 7141–7142.
- 24 M. Talavera, S. Bolaño, J. Bravo, J. Castro, S. García-Fontán and J. M. Hermida-Ramón, *Organometallics*, 2013, **32**, 4402–4408.
- 25 Sk. R. Amin and A. Sarkar, *Organometallics*, 1995, **14**, 547–550.
- 26 H. Wang, R. P. Hsung and W. D. Wulff, *Tetrahedron Lett.*, 1998, **39**, 1849–1852.
- 27 J. F. Hartwig, *J. Am. Chem. Soc.*, 2016, **138**, 2–24.
- 28 S. Murai, F. Kakiuchi, S. Sekine, Y. Tanaka, A. Kamatani, M. Sonoda and N. Chatani, *Nature*, 1993, **366**, 529–531.
- 29 L. A. P. Kane-Maguire, E. D. Honig and D. A. Sweigart, *Chem. Rev.*, 1984, **84**, 525–543.
- 30 F. C. Pigge, R. Dhanya and D. C. Swenson, *Organometallics*, 2009, **28**, 3869–3875.
- 31 M. E. O'Reilly, S. I. Johnson, R. J. Nielsen, W. A. Goddard and T. B. Gunnoe, *Organometallics*, 2016, **35**, 2053–2056.
- 32 R. M. Moriarty, U. S. Gill and Y. Y. Ku, *J. Organomet. Chem.*, 1988, **350**, 157–190.

- 33 D. Astruc, *Tetrahedron*, 1983, **39**, 4027–4095.
- 34 A. J. Pearson, P. Y. Zhu, W. J. Youngs, J. D. Bradshaw and D. B. McConville, *J. Am. Chem. Soc.*, 1993, **115**, 10376–10377.
- 35 R. M. Moriarty and U. S. Gill, *Organometallics*, 1986, **5**, 253–256.
- 36 F. Hossner and M. Voyle, *J. Organomet. Chem.*, 1988, **347**, 365–371.
- 37 R. P. Houghton, M. Voyle and R. Price, *J. Chem. Soc., Perkin Trans. 1*, 1984, **0**, 925–931.
- 38 A. I. Konovalov, E. O. Gorbacheva, F. M. Miloserdov and V. V. Grushin, *Chem. Commun.*, 2015, **51**, 13527–13530.
- 39 Q.-K. Kang, Y. Lin, Y. Li and H. Shi, *J. Am. Chem. Soc.*, 2020, **142**, 3706–3711.
- 40 M. Otsuka, H. Yokoyama, K. Endo and T. Shibata, *Synlett*, 2010, **2010**, 2601–2606.
- 41 M. Otsuka, K. Endo and T. Shibata, *Chem. Commun.*, 2009, **46**, 336–338.
- 42 J. W. Walton and J. M. J. Williams, *Chem. Commun.*, 2015, **51**, 2786–2789.
- 43 M. F. Semmelhack, A. Chlenov and D. M. Ho, *J. Am. Chem. Soc.*, 2005, **127**, 7759–7773.
- 44 E. L. Muetterties, J. R. Bleeke and A. C. Sievert, *J. Organomet. Chem.*, 1979, **178**, 197–216.
- 45 W. Tian, A new process for the synthesis of morpholinylbenzenes, WO2001087865A1, 2001.
- 46 G. R. Brown, A. J. Foubister and P. D. Ratcliffe, *Tetrahedron Lett.*, 1999, **40**, 1219–1222.
- 47 A. C. Sievert and E. L. Muetterties, *Inorg. Chem.*, 1981, **20**, 489–501.
- 48 T. G. Traylor, K. Stewart and M. Goldberg, *J. Am. Chem. Soc.*, 1984, **106**, 4445–4454.
- 49 T. G. Traylor and K. Stewart, *Organometallics*, 1984, **3**, 325–327.
- 50 M. L. H. Green, D. S. Joyner and J. M. Wallis, *J. Chem. Soc., Dalton Trans.*, 1987, 2823–2830.
- 51 S. Zhang, J. K. Shen, F. Basolo, T. D. Ju, R. F. Lang, G. Kiss and C. D. Hoff, *Organometallics*, 1994, **13**, 3692–3702.
- 52 S. Boggs, V. I. Elitzin, K. Gudmundsson, M. T. Martin and M. J. Sharp, *Org. Process Res. Dev.*, 2009, **13**, 781–785.
- 53 A. W. Kruger, M. J. Rozema, A. Chu-Kung, J. Gandarilla, A. R. Haight, B. J. Kotecki, S. M. Richter, A. M. Schwartz and Z. Wang, *Org. Process Res. Dev.*, 2009, **13**, 1419–1425.
- 54 A. J. Blacker, G. Moran-Malagon, L. Powell, W. Reynolds, R. Stones and M. R. Chapman, *Org. Process Res. Dev.*, 2018, **22**, 1086–1091.
- 55 X. Liu, C. Xu, M. Wang and Q. Liu, *Chem. Rev.*, 2015, **115**, 683–730.
- 56 L. Banfi, E. Narisano, R. Riva and D. S. Matteson, in *Encyclopedia of Reagents for Organic Synthesis*, American Cancer Society, 2007.
- 57 T. Knauber, F. Arikani, G.-V. Rösenthaller and L. J. Gooßen, *Chem. Eur. J.*, 2011, **17**, 2689–2697.
- 58 V. V. Levin, A. D. Dilman, P. A. Belyakov, M. I. Struchkova and V. A. Tartakovskiy, *Tetrahedron Lett.*, 2011, **52**, 281–284.
- 59 J. A. Pike and J. W. Walton, *Chem. Commun.*, 2017, **53**, 9858–9861.
- 60 O. Singh Sisodia, A. N. Sahay, D. S. Pandey, U. C. Agarwala, N. K. Jha, P. Sharma, A. Toscano and A. Cabrera, *J. Organomet. Chem.*, 1998, **560**, 35–40.
- 61 M. A. Bennett and A. K. Smith, *J. Chem. Soc., Dalton Trans.*, 1974, 233–241.
- 62 M. T. Whited and R. H. Grubbs, *J. Am. Chem. Soc.*, 2008, **130**, 16476–16477.
- 63 M. T. Whited and R. H. Grubbs, *Organometallics*, 2009, **28**, 161–166.
- 64 M. T. Whited and R. H. Grubbs, *Acc. Chem. Res.*, 2009, **42**, 1607–1616.
- 65 S. Conejero, M. Paneque, M. L. Poveda, L. L. Santos and E. Carmona, *Acc. Chem. Res.*, 2010, **43**, 572–580.
- 66 S. M. Chapp and N. D. Schley, *Organometallics*, 2017, **36**, 4355–4358.

- 67 B. M. Lindley, B. P. Jacobs, S. N. MacMillan and P. T. Wolczanski, *Chem. Commun.*, 2016, **52**, 3891–3894.
- 68 J. E. V. Valpuesta, E. Álvarez, J. López-Serrano, C. Maya and E. Carmona, *Chem. Eur. J.*, 2012, **18**, 13149–13159.
- 69 L. L. Santos, K. Mereiter, M. Paneque, C. Slugovc and E. Carmona, *New J. Chem.*, 2003, **27**, 107–113.
- 70 E. Álvarez, M. Paneque, A. G. Petronilho, M. L. Poveda, L. L. Santos, E. Carmona and K. Mereiter, *Organometallics*, 2007, **26**, 1231–1240.
- 71 P. Lara, M. Paneque, M. L. Poveda, L. L. Santos, J. E. V. Valpuesta, E. Carmona, S. Moncho, G. Ujaque, A. Lledós, E. Álvarez and K. Mereiter, *Chem. Eur. J.*, **15**, 9034–9045.
- 72 M. Barbasiewicz, A. Szadkowska, A. Makal, K. Jarzemska, K. Woźniak and K. Grela, *Chem. Eur. J.*, 2008, **14**, 9330–9337.
- 73 J. Campos and E. Carmona, *Organometallics*, 2015, **34**, 2212–2221.
- 74 C. Pietraszuk, S. Rogalski, B. Powała, M. Miętkiewski, M. Kubicki, G. Spólnik, W. Danikiewicz, K. Woźniak, A. Pazio, A. Szadkowska, A. Kozłowska and K. Grela, *Chem. Eur. J.*, 2012, **18**, 6465–6469.
- 75 Y. Sato, Y. Kayaki and T. Ikariya, *Chem. Lett.*, 2014, **44**, 188–190.
- 76 Y. Alvarado, P. J. Daff, P. J. Pérez, M. L. Poveda, R. Sánchez-Delgado and E. Carmona, *Organometallics*, 1996, **15**, 2192–2194.
- 77 J. M. O'Connor, Lin. Pu and A. L. Rheingold, *Organometallics*, 1988, **7**, 2060–2062.
- 78 L. M. Toomey and J. D. Atwood, *Organometallics*, 1997, **16**, 490–493.
- 79 A. S. Caillé, L. Trimble, C. Berthelette and C. K. Lau, *Synlett*, 1996, **1996**, 669–671.
- 80 K. Wojciechowski, *Eur. J. Org. Chem.*, 2001, **2001**, 3587–3605.
- 81 S. Rogalski, P. Žak, P. Pawluć, M. Kubicki and C. Pietraszuk, *J. Organomet. Chem.*, 2018, **859**, 1–9.
- 82 F. M. Alías, M. L. Poveda, M. Sellin and E. Carmona, *J. Am. Chem. Soc.*, 1998, **120**, 5816–5817.
- 83 C. P. Casey and P. J. Fagan, *J. Am. Chem. Soc.*, 1982, **104**, 4950–4951.
- 84 C. P. Casey, M. W. Meszaros, P. J. Fagan, R. K. Bly, S. R. Marder and E. A. Austin, *J. Am. Chem. Soc.*, 1986, **108**, 4043–4053.
- 85 C. P. Casey, M. W. Meszaros, P. J. Fagan, R. K. Bly and R. E. Colborn, *J. Am. Chem. Soc.*, 1986, **108**, 4053–4059.
- 86 X. Li, L. N. Appelhans, J. W. Faller and R. H. Crabtree, *Organometallics*, 2004, **23**, 3378–3387.
- 87 S. M. Chapp and N. D. Schley, *Inorg. Chem.*, 2020, **59**, 7143–7149.
- 88 L. E. Doyle, W. E. Piers and J. Borau-Garcia, *J. Am. Chem. Soc.*, 2015, **137**, 2187–2190.
- 89 A. Ros, R. Fernández and J. M. Lassaletta, *Chem. Soc. Rev.*, 2014, **43**, 3229–3243.
- 90 M. A. Larsen, C. V. Wilson and J. F. Hartwig, *J. Am. Chem. Soc.*, 2015, **137**, 8633–8643.
- 91 L. Xu, G. Wang, S. Zhang, H. Wang, L. Wang, L. Liu, J. Jiao and P. Li, *Tetrahedron*, 2017, **73**, 7123–7157.
- 92 B. Liu, T. Zhou, B. Li, S. Xu, H. Song and B. Wang, *Angew. Chem. Int. Ed.*, 2014, **53**, 4191–4195.
- 93 Y. Tulchinsky, M. A. Iron, M. Botoshansky and M. Gandelman, *Nat. Chem.*, 2011, **3**, 525–531.
- 94 M. P. Wilhelm, *Mayo Clin. Proc.*, 1991, **66**, 1165–1170.
- 95 S. T. Micek, *Clin. Infect. Dis.*, 2007, **45**, S184–S190.

- 96 G. D. Wright and C. T. Walsh, *Acc. Chem. Res.*, 1992, **25**, 468–473.
- 97 C. T. Walsh, *Science*, 1993, **261**, 308–309.
- 98 P. Goffin, M. Deghorain, J.-L. Mainardi, I. Tytgat, M.-C. Champomier-Vergès, M. Kleerebezem and P. Hols, *J. Bacteriol.*, 2005, **187**, 6750–6761.
- 99 T. Ferain, J. N. Hobbs, J. Richardson, N. Bernard, D. Garmyn, P. Hols, N. E. Allen and J. Delcour, *J. Bacteriol.*, 1996, **178**, 5431–5437.
- 100 B. Desguin, T. Zhang, P. Soumillion, P. Hols, J. Hu and R. P. Hausinger, *Science*, 2015, **349**, 66–69.
- 101 J. L. Boer, S. B. Mulrooney and R. P. Hausinger, *Arch. Biochem. Biophys.*, 2014, **544**, 142–152.
- 102 M. Alfano and C. Cavazza, *Protein Sci.*, 2020, **29**, 1071–1089.
- 103 G. Diekert, R. Jaenchen and R. K. Thauer, *FEBS Letters*, 1980, **119**, 118–120.
- 104 K. Zheng, P. D. Ngo, V. L. Owens, X. Yang and S. O. Mansoorabadi, *Science*, 2016, **354**, 339–342.
- 105 A. Mukherjee and D. Milstein, *ACS Catal.*, 2018, **8**, 11435–11469.
- 106 M. Vogt and R. Langer, *Eur. J. Inorg. Chem.*, 2020, **2020**, 3885–3898.
- 107 T. Xu, M. D. Wodrich, R. Scopelliti, C. Corminboeuf and X. Hu, *PNAS*, 2017, **114**, 1242–1245.
- 108 R. Shi, M. D. Wodrich, H.-J. Pan, F. F. Tirani and X. Hu, *Angew. Chem. Int. Ed.*, 2019, **58**, 16869–16872.
- 109 H. Singh and K. Singh, *Tetrahedron*, 1989, **45**, 3967–3974.
- 110 P. Quinodoz, B. Drouillat, K. Wright, J. Marrot and F. Couty, *J. Org. Chem.*, 2016, **81**, 2899–2910.
- 111 M. Joucla and J. Mortier, *Bull. Soc. Chim. Fr.*, 1988, 579–583.
- 112 M. Zhao, F. Wang and X. Li, *Org. Lett.*, 2012, **14**, 1412–1415.
- 113 G. A. Olah, S. C. Narang, B. G. B. Gupta and R. Malhotra, *J. Org. Chem.*, 1979, **44**, 1247–1251.
- 114 M. Node, K. Nishide, M. Sai, K. Fuji and E. Fujita, *J. Org. Chem.*, 1981, **46**, 1991–1993.
- 115 T. Ozturk, E. Ertas and O. Mert, *Chem. Rev.*, 2007, **107**, 5210–5278.
- 116 B. A. Vigante, Y. Y. Ozols, B. S. Chekavichus and G. Y. Dubur, *Chem. Heterocycl. Compd.*, **24**, 1017–1023.
- 117 A.-M. Fuller, D. A. Leigh, P. J. Lusby, I. D. H. Oswald, S. Parsons and D. B. Walker, *Angew. Chem. Int. Ed.*, 2004, **43**, 3914–3918.
- 118 J. Yamaguchi, K. Muto and K. Itami, *Eur. J. Org. Chem.*, 2013, **2013**, 19–30.
- 119 Y. Rao, X. Li, P. Nagorny, J. Hayashida and S. J. Danishefsky, *Tetrahedron Lett.*, 2009, **50**, 6684–6686.
- 120 A. Weisman, M. Gozin, H.-B. Kraatz and D. Milstein, *Inorg. Chem.*, 1996, **35**, 1792–1797.
- 121 H. Meguro, T. Koizumi, T. Yamamoto and T. Kanbara, *J. Organomet. Chem.*, 2008, **693**, 1109–1116.
- 122 E. H. Yen Wong, Y.-X. Jia, Y. Li, S. A. Pullarkat and P.-H. Leung, *J. Organomet. Chem.*, 2018, **862**, 22–27.
- 123 N. A. Swisher and R. H. Grubbs, *Organometallics*, 2020, **39**, 2479–2485.

Experimental Methods

General procedure for catalytic reactions. A 4 mL vial was charged with Ru(cod)(methallyl)₂ (6.3 mg, 0.020 mmol), DPPPent (12.5 mg, 0.028 mmol) and 1,4-dioxane (0.4 mL). Trifluoromethanesulfonic acid (3.5 μ L, 0.040 mmol) was then added to the stirred mixture. To this solution was added fluorobenzene (187 μ L, 2.00 mmol), morpholine (35 μ L, 0.40 mmol), triethylamine (56 μ L, 0.40 mmol), and triethylsilane (64 μ L, 0.40 mmol). The reaction mixture was heated at 100 °C in an oil bath for 24 hours, at which point the vessel was removed from the oil bath and allowed to cool to room temperature. A portion of dodecane (3.0 μ L, 0.013 mmol) was then added as an internal standard for analysis by flame ionization gas chromatography.

Note on product quantitation: GC-FID allows for detection of product bound to ruthenium. For instance, analysis of 1 equiv. complex **2.2** by GC-FID leads to detection of 0.90 eq. N-phenyl morpholine, presumably due to liberation of the arene in the GC inlet (300 °C).

Safety note: Glass etching by liberated fluoride ions in conventional (non-catalyzed) S_NAr reactions has been reported, which has led to issues on scale-up. Additionally, these experiments have the potential to generate HF, therefore care should be taken in all cases to minimize risk from fluoride ion or HF to laboratory equipment and personnel.

Quantification of precipitate in additive-free catalytic reaction. A catalytic reaction was set up according to the general procedure, omitting triethylamine and triethylsilane additives. A yellow precipitate deposited during the reaction. After 24 hours, the vessel was removed from the oil bath and allowed to cool to room temperature. The reaction was returned to the glove box and filtered. The filtered solid was washed with dioxane (0.5 mL) and was then dissolved in a

mixture of DMF/ CDCl_3 (1.5:1) containing trimethylphosphate ($20\ \mu\text{L}$, $0.170\ \text{mmol}$) as an internal standard. The quantity of **2.2** was quantified by ^{31}P NMR.

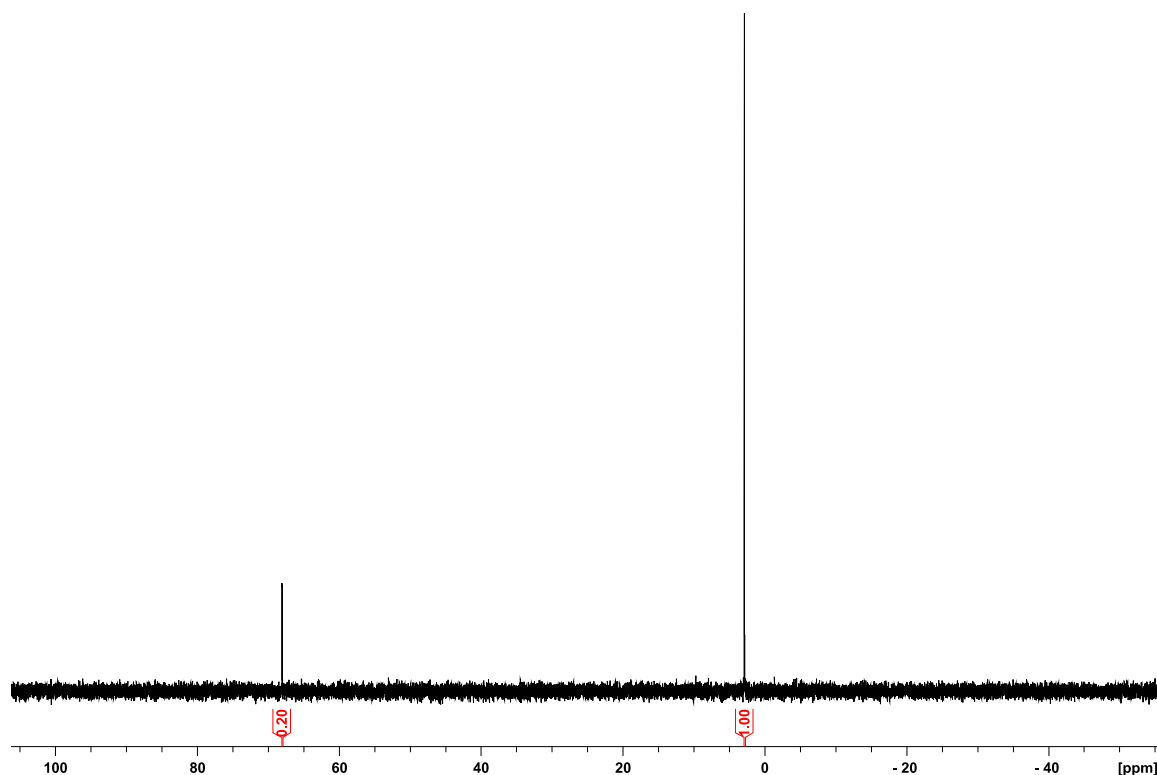


Figure A1. ^{31}P NMR of **2.2** (67.7 ppm) after precipitation at the end of a catalytic reaction.

Kinetic analysis of formation of 2.2 from 2.1 (Figure 2.3). In a nitrogen-filled glove box, a screw-cap NMR tube was charged with complex **2.1** ($0.0050\ \text{g}$, $6.36\ \mu\text{mol}$) in a solution of $0.1\ \text{mL}$ of DMF (for solubility), followed by $0.4\ \text{mL}$ of dioxane. A sealed capillary containing a C_6D_6 solution of $\text{P}(\text{OMe})_3$ was added as a standard. Immediately prior to kinetic analysis, a portion of morpholine ($5.5\ \mu\text{L}$, $64\ \mu\text{mol}$) was added via a syringe through the septum cap. The sample was mixed by inversion and then analyzed by ^{31}P NMR every 60 seconds. The experiment was conducted in triplicate.

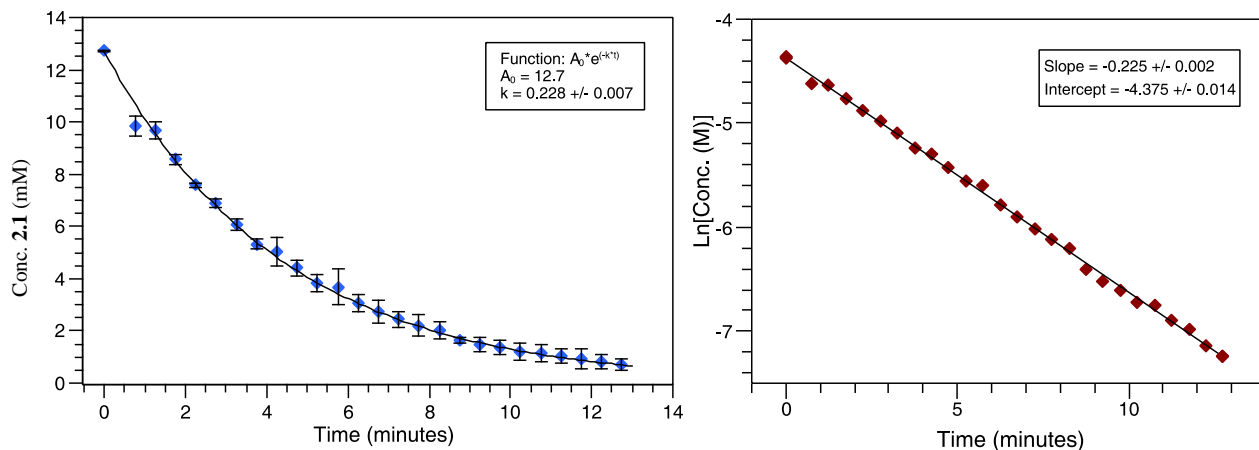


Figure A2. Consumption of **2.1** over time.

Determination of equilibrium constant of arene exchange. In a nitrogen-filled glove box, a screw-cap NMR tube was charged with 500 μL of a saturated solution of **2.1** in fluorobenzene, followed by N-phenylmorpholine (2.5 μmol as stock solution in fluorobenzene). The temperature of the NMR spectrometer was raised to 373 K, and the sample monitored by ^{31}P until a stable equilibrium was reached (< 15 min). This equilibrium ratio was stable on cooling, suggesting a moderate kinetic barrier to arene exchange. Relative concentrations of **2.1** and **2.2** were measured both at 373K and at *ca.* 323K. Both measurements gave results consistent with one another but the lower temperature measurement gave an improved signal-to-noise ratio. Finally, the sample was cooled to room temperature and trimethylphosphate (2.0 μL , 17 μmol) was added as an internal standard to aid in quantifying absolute concentrations.

Kinetic analysis of arene displacement in **2.2 by fluorobenzene to give **2.1** (Table 2.3).** In a nitrogen-filled glove box, a screw-cap NMR tube was charged with complex **2.2** (0.0038 g, 4.5 μmol) in a solution of 0.3 mL of 1,2-dichloroethane, followed by 0.3 mL of fluorobenzene. A sealed capillary containing a C_6D_6 solution of PPh_3 was added as a standard. The NMR spectrometer sample bore was preheated to the temperature required for kinetic analysis and the

sample was then analyzed by ^{31}P NMR. Initial rate constants were obtained using kinetic data in the range from $[\mathbf{2.2}] = 7.5 \text{ mM}$ to $[\mathbf{2.2}] = 6.0 \text{ mM}$.

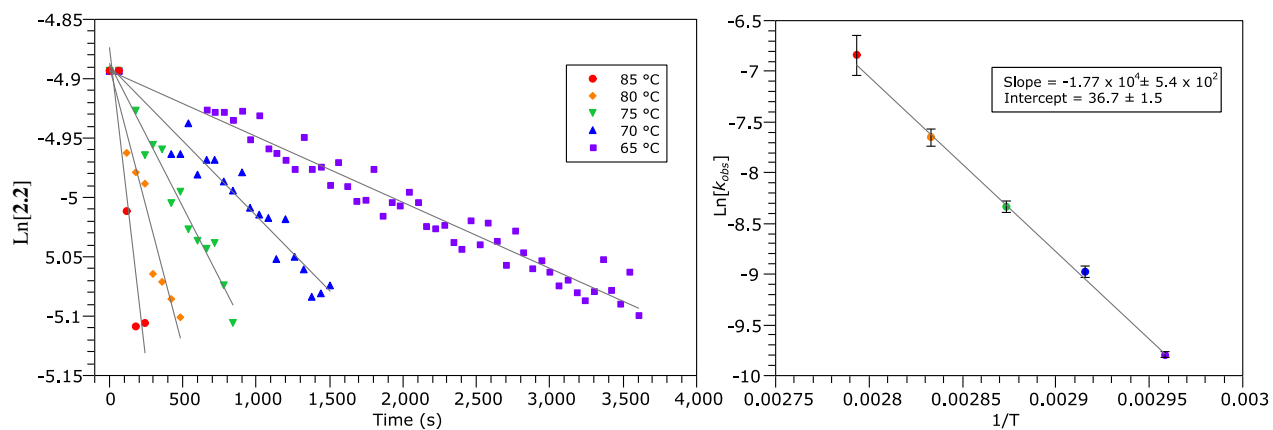
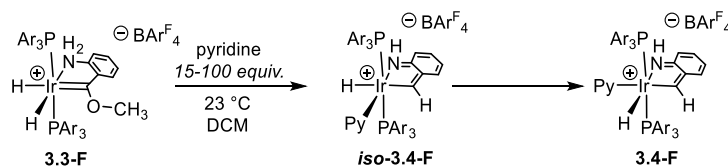


Figure A3. Temperature dependence of arene exchange in **2.2**

VII. APPENDIX B – SUPPLEMENTAL INFORMATION FOR CHAPTER III



Kinetic analysis of the formation of 3.4-F

In a nitrogen-filled glove box, a screw-cap NMR tube was charged with complex **3.3-F** (0.010 g, 5.48 μmol) in a solution of 0.5 ml of CD_2Cl_2 . A sealed capillary containing a CD_2Cl_2 solution of $\text{P}(\text{OMe})_3$ was added as a standard. Immediately prior to kinetic analysis, a portion of pyridine (15, 20, 30, 50, and 100 equivalents) was added via a syringe through the septum cap. The sample was mixed by inversion and then analyzed by ^{31}P NMR to monitor **3.3-F** consumption. Pseudo first-order rate constants of **3.3-F** consumption were calculated by taking the slope of a $\text{Ln}[\text{3.3-F}]$ vs time plot. These rate data were plotted as $\text{Ln}[\text{rate}]$ vs $\text{Ln}[\text{pyridine}]$ and fit to give a line with slope equal to the reaction order in pyridine.

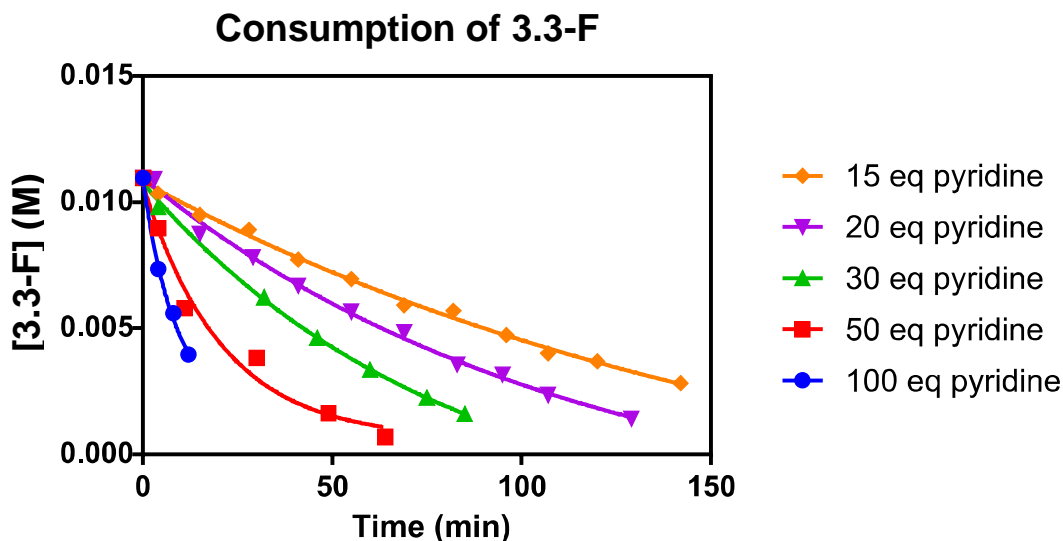


Figure B1. Consumption of **3.3-F** as a function of pyridine concentration.

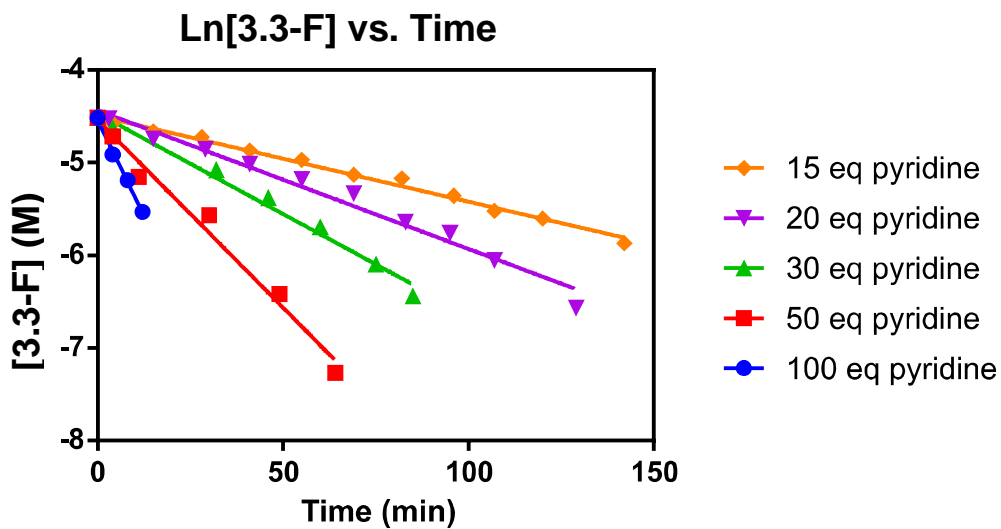


Figure B2. Natural log of 3.3-F as a function of pyridine concentration.

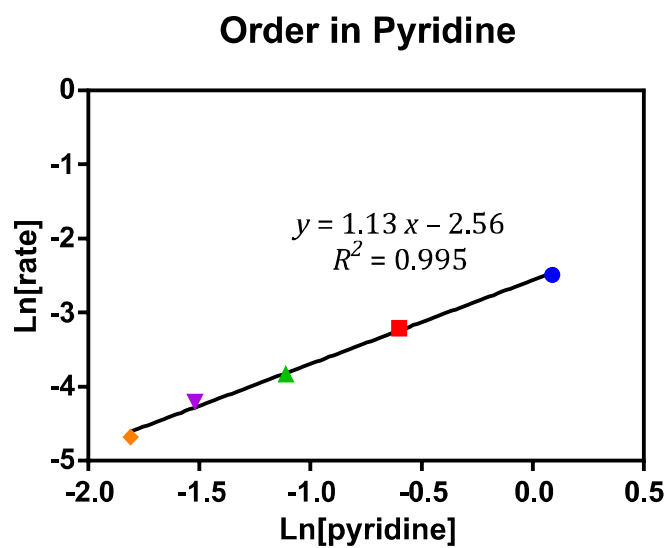


Figure B3. Ln-Ln plot giving the order in pyridine for the consumption of 3.3-F.

VIII. APPENDIX C – SUPPLEMENTAL INFORMATION FOR CHAPTER IV

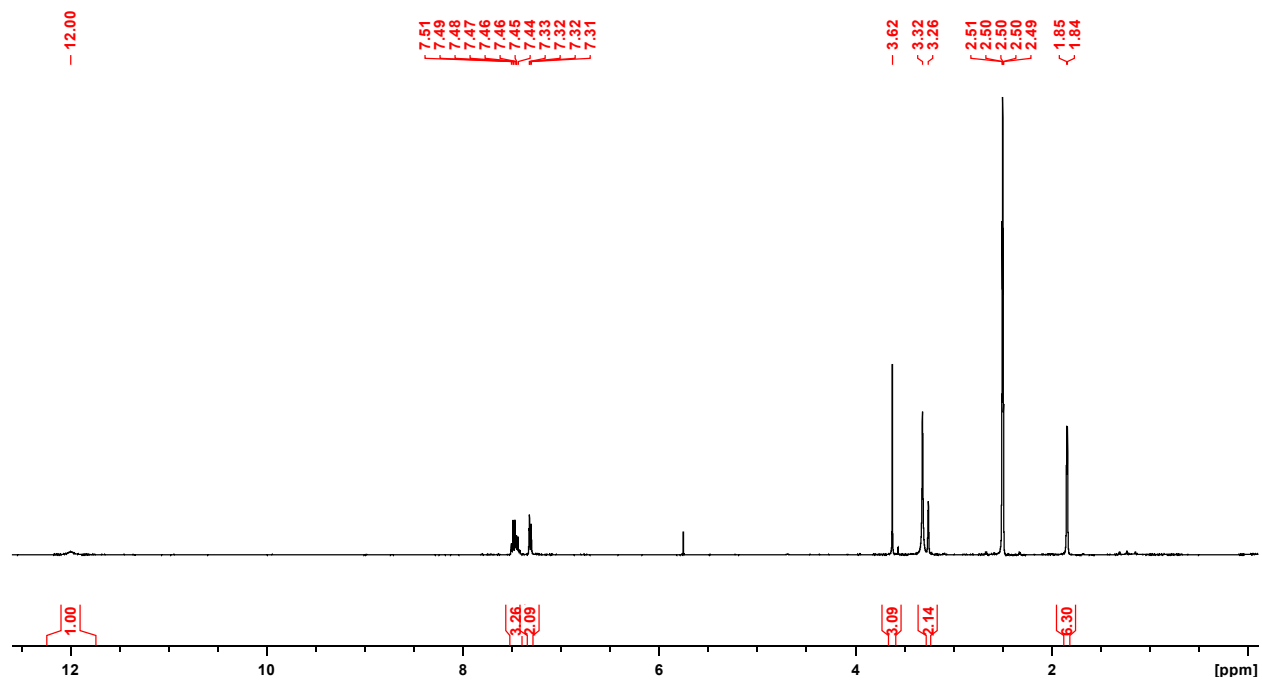


Figure C1. ^1H NMR of 4.13 (400 MHz, d_6 -DMSO).

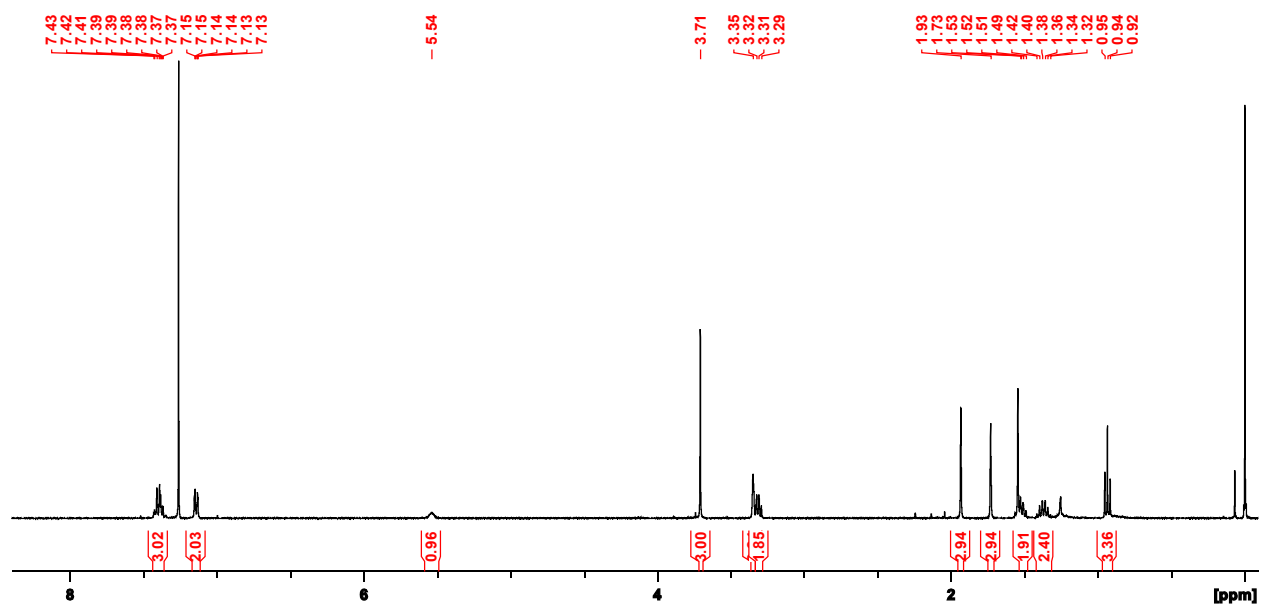


Figure C2. ^1H NMR of 4.14 (400 MHz, CDCl_3).

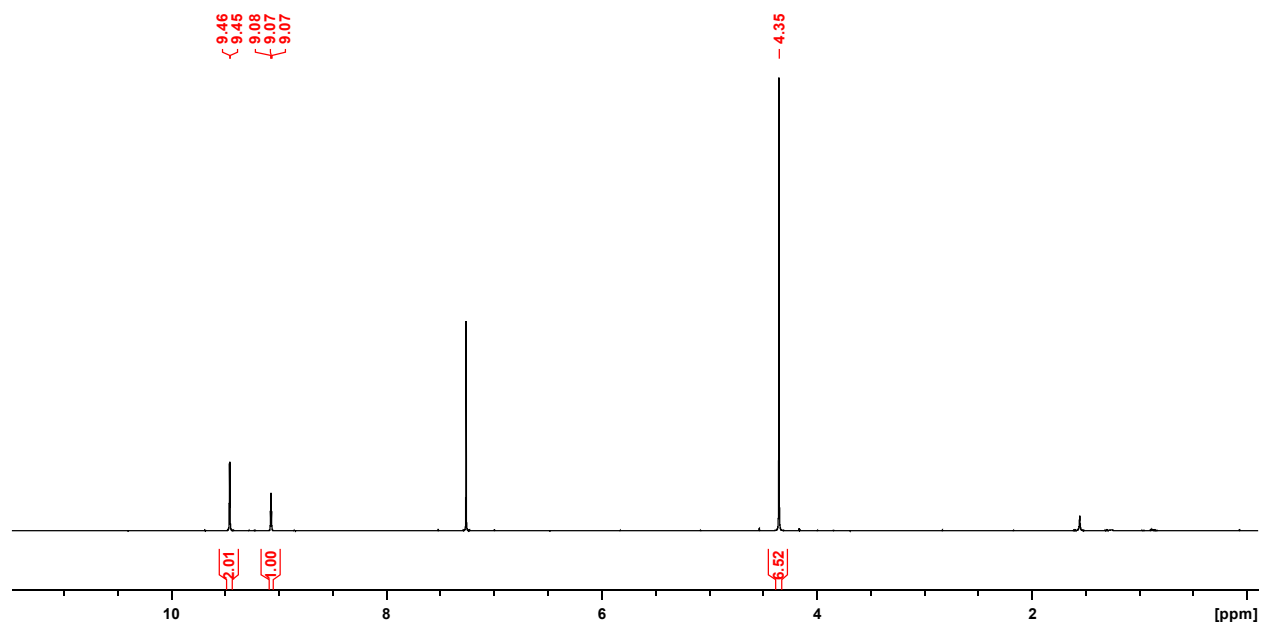


Figure C3. ^1H NMR of **4.17** (400 MHz, CDCl_3).

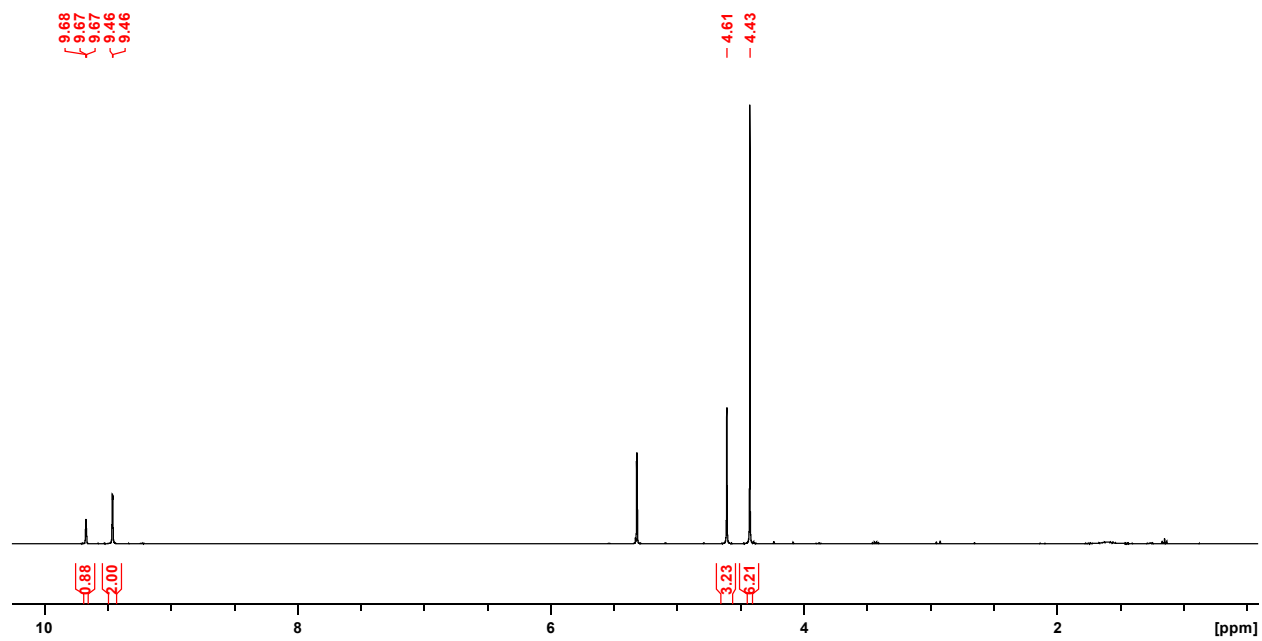


Figure C4. ^1H NMR of **4.21** (400 MHz, CD_2Cl_2).

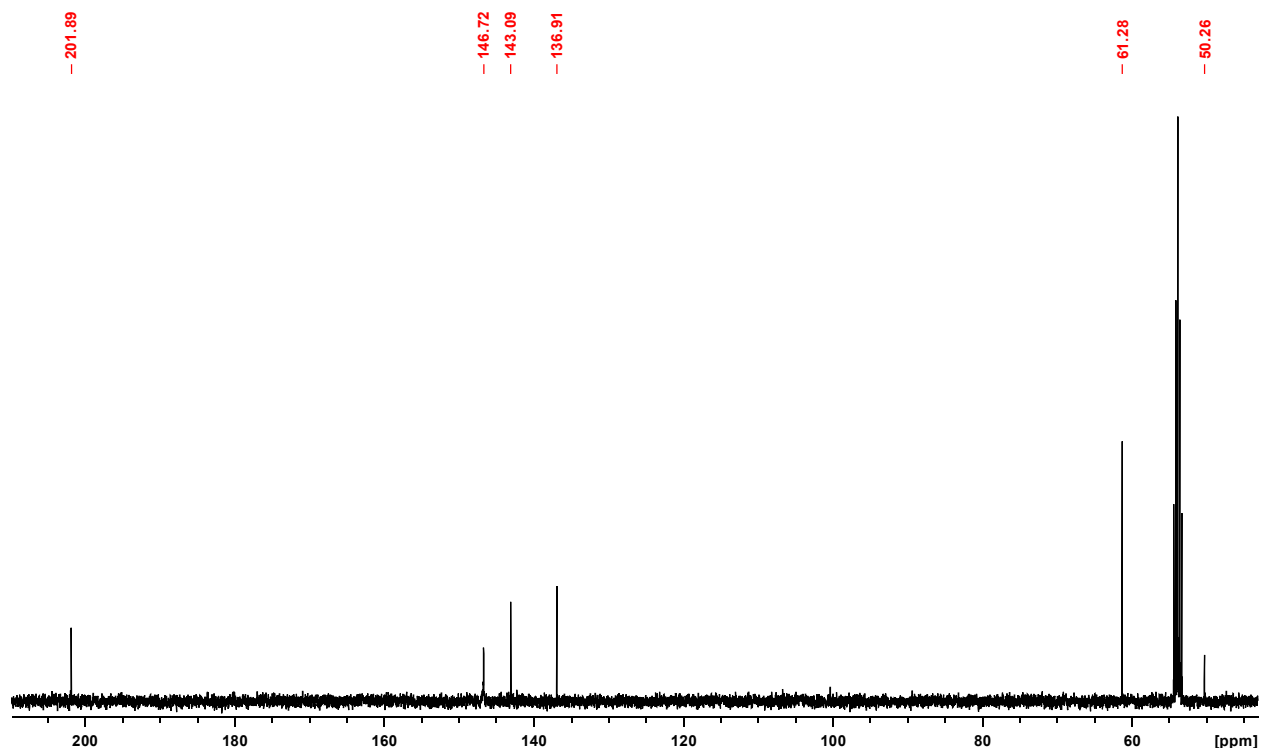


Figure C5. $^{13}\text{C}\{^1\text{H}\}$ NMR of **4.21** (101 MHz, CD_2Cl_2).

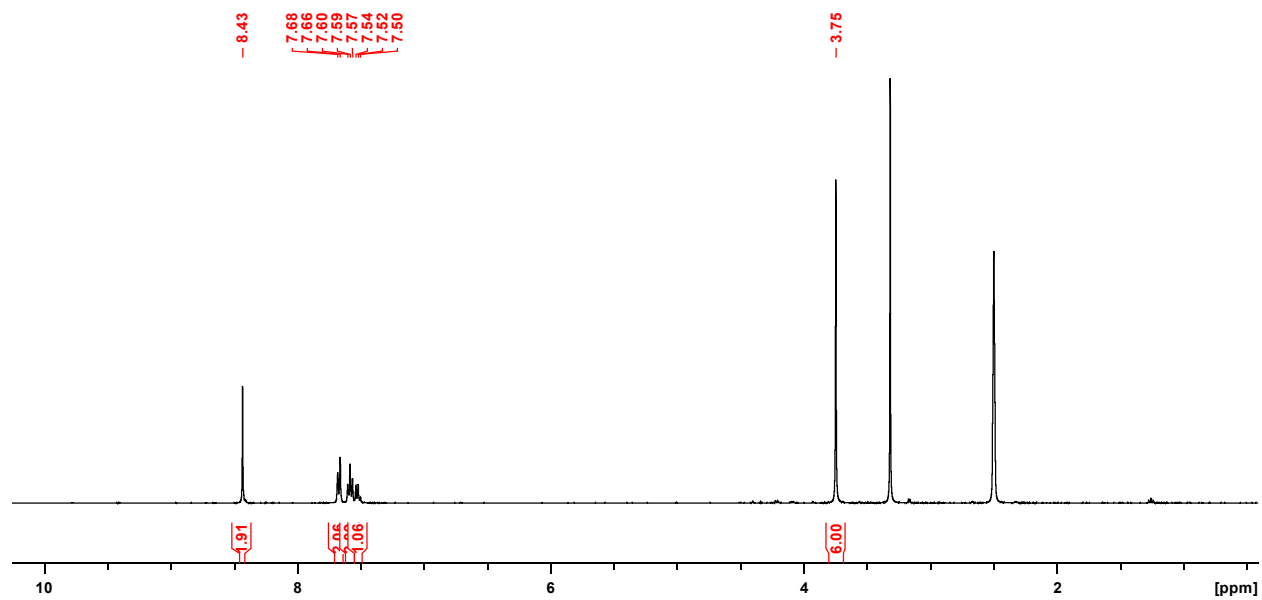


Figure C6. ^1H NMR of **4.23** (400 MHz d_6 -DMSO).

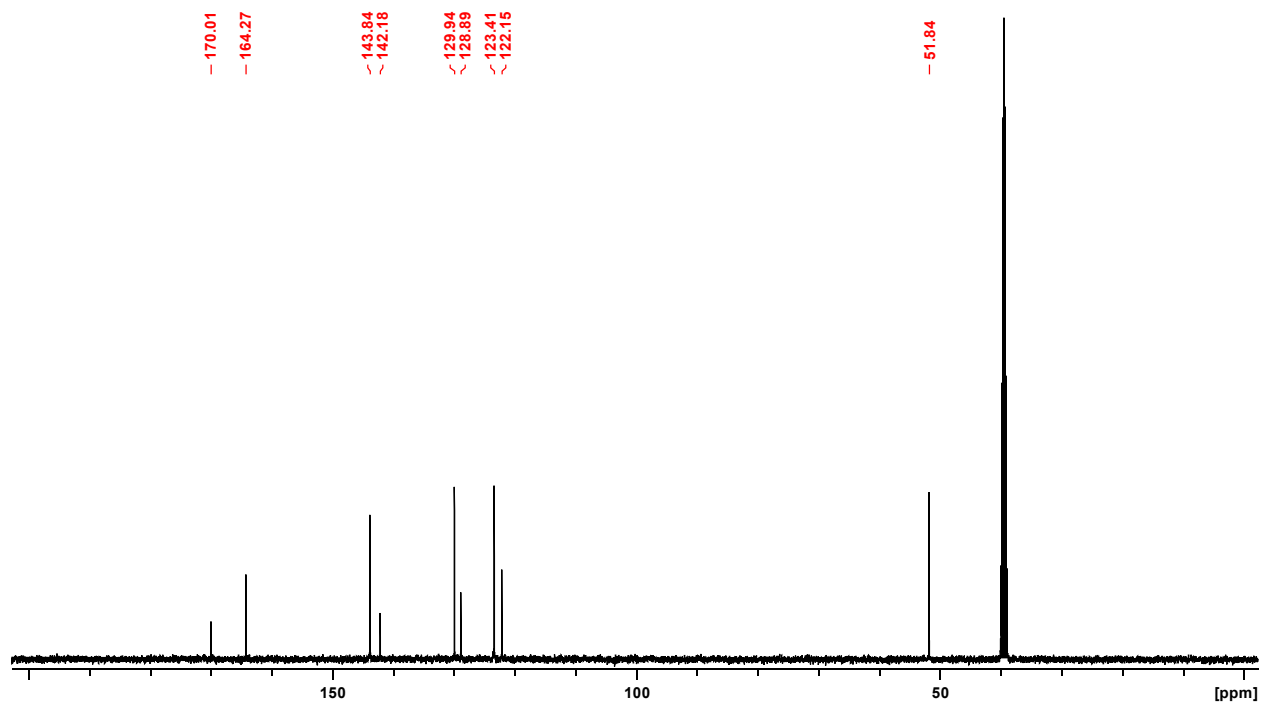


Figure C7. $^{13}\text{C}\{^1\text{H}\}$ NMR of 4.23 (101 MHz d_6 -DMSO).

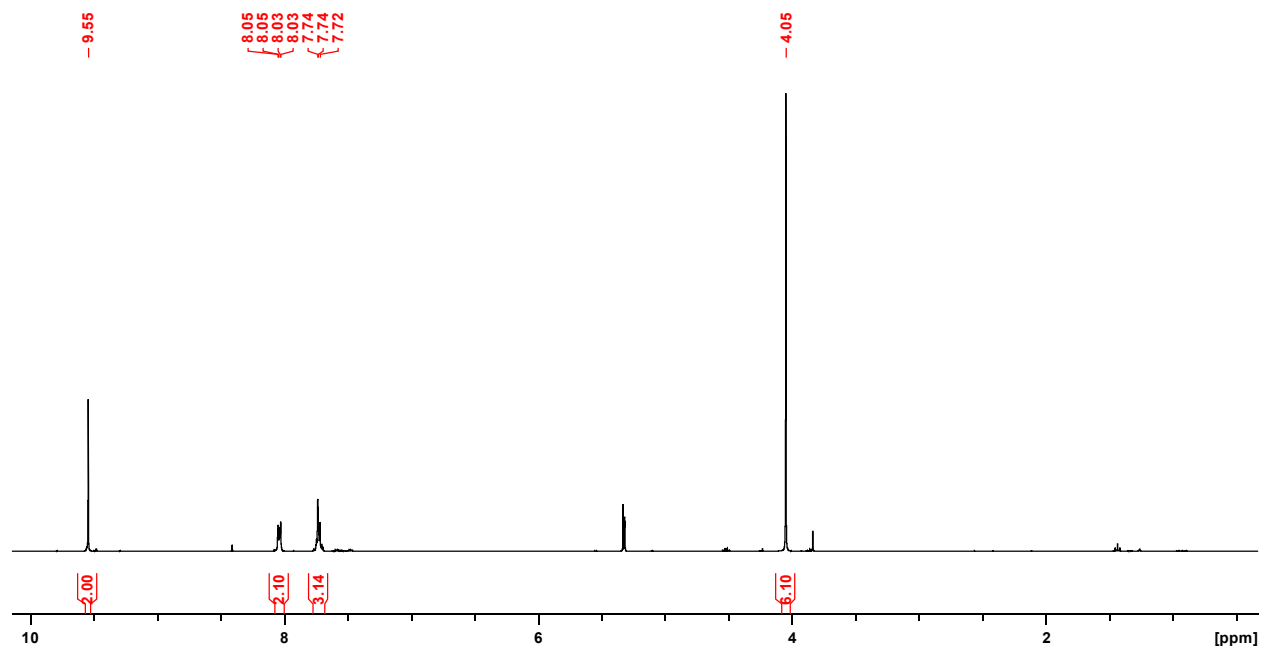


Figure C8. ^1H NMR of 4.24 (400 MHz, d_6 -DMSO).